REGULATION OF TAZ (WWTR1) BY PROTEIN-PROTEIN INTERACTIONS IN STRIATED MUSCLE

STEPHANIE SANSONE

A THESIS SUBMITTED TO
THE FACULTY OF GRADUATE STUDIES
IN PARTIAL FULFILLMENT OF THE REQUIREMENTS
FOR THE DEGREE OF

MASTER OF SCIENCE

GRADUATE PROGRAM IN BIOLOGY
YORK UNIVERSITY
TORONTO, ONTARIO

DECEMBER 2025

Abstract

Tissue growth depends on cellular proliferation, survival, and differentiation. Hippo signaling controls these processes by regulating transcriptional co-activators Yap/Taz. Taz function is context-dependent, including repression of myogenic differentiation. Taz does not bind DNA; its activity is determined by interacting partners. To discover functional regulators of Taz, nuclear FLAG-affinity purification and LC-MS/MS were performed in HEK293T, identifying 57 interactors (33 unique; 24 ≥3-fold enriched). Among these, transcription factor Yin-Yang1 (YY1) was prioritized. Biochemical analyses revealed YY1 binds Taz at/near its Tead-binding domain, with Tead1 enhancing this interaction. YY1 repressed Taz-mediated transcription on a Tead-responsive reporter. In proliferating myoblasts, YY1 increased phospho-Taz (Ser89), its Hippo-inactivated form. Taz formed LLPS-driven nuclear condensates, during which YY1 was excluded from the nucleus. During differentiation, YY1-mediated stabilization of phospho-Taz (Ser89) was not observed, and Taz and YY1 co-operatively repressed myogenic gene expression. Collectively, these findings identify YY1 as a regulator of Taz function in striated muscle.

Acknowledgements

I would first like to thank my supervisor, Dr. John McDermott, for his constant support, patience, and guidance. I entered your lab with virtually no wet-lab experience, yet you welcomed me, encouraged my curiosity, and provided the environment I needed to grow. Your mentorship has shaped me into a scientist I never imagined I could become. It is because of you that I now know this is the path I want to pursue for the rest of my life. I am deeply grateful; I could not have asked for a better supervisor. I would also like to thank Dr. Tetsuaki Miyake, for always being willing to answer questions, and for the thoughtful conversations that helped me not only in science, but the life of a scientist. I hope to lead a similar career as yours. It was the greatest honour working with you and hearing your stories. Your guidance has meant more to me than I can express. To Catherine Chan, thank you for your kindness, generosity, and unwavering support in and out of the lab. You are truly the heart of the lab, and I will miss you greatly. To my lab mates: Anastasia, thank you for training me with patience and care, and for being a wonderful friend. It was the busiest time of your life, and still, you always supported me. Fatima, thank for always listening to me, and for your calm presence during challenging experiments. You always brought me a sense of relief. Sophia, thank you for your friendship and encouragement. Dr. Xiao Dong (XD), thank you for helping me get pups for cardiomyocyte isolation, no matter how busy you were. To my partner, Micheal, thank you for your endless patience, love, and waiting up when I stayed at the lab late at night. Finally, to my family, thank you for your encouragement and for supporting my goals, even when it required sacrifices from you as well. I am profoundly grateful to all of you. I would also like to acknowledge the Vivaria animal facility for maintaining the breeder rats, and Dr. Maxime Rossato at the YSci Core Mass Spectrometry Facility for performing the mass spectrometry analysis.

Table of Contents

List of Tables

List of Figures

Chapter I: Literature Review

Chapter II: Regulation of Taz by protein-protein interactions in striated muscle

List of Abbreviations

α-actin – alpha-actin
ACC – Animal Care Committee
AIP4 – atrophin-1 interacting protein
Akt – Akt serine/threonine kinase
Amot – Angiomotin
AmotL1 – Angiomotin-like 1
AmotL2 – Angiomotin-like 2
ATCC – American Type Culture Collection
α-tubulin – alpha-tubulin
axl *– AXL receptor tyrosine kinase*
β-actin – beta actin
β-catenin – beta catenin
birc5 *– baculoviral IAP repeat-containing 5*
BMP – bone morphogenetic protein
β-TrCP – Beta-transducin repeat containing protein
C2C12 – mouse myoblast cell line
CCDC85C – coiled-coil domain-containing protein 85C
CDK9 – cyclin-dependent kinase 9
Cdx2 – caudal-type homeobox protein 2
c-myc *– cellular myelocytomatosis*
ctgf *– connective tissue growth factor*
CK1 – casein kinase 1
CO_2 – carbon dioxide
cTnT – cardiac troponin-T
cyr61 – cysteine-rich angiogenic inducer 61
DAPI - 4',6-diamidino-2-phenylindole
DE – definitive endoderm
DIAP1 – *Drosophila* inhibitor of apoptosis-1
DM – differentiation media
Dm *– Drosophila melanogaster*
DMEM - Dulbecco's modified Eagle's medium
DSHB – Developmental Studies Hybridoma Bank
DTT – Dithiothreitol
E – embryonic day
E-cadherin – epithelial cadherin
ECM – extracellular matrix
ERM - Ezrin/radixin/moesin
Ex – Expanded
eYFP – enhanced yellow fluorescent protein
Ezh2 – Enhancer of zeste homolog 2
F-actin – filamentous actin
FBS – fetal bovine serum
FGF – fibroblast growth factor

G-actin – globular actin
Gata4/6 – GATA-binding factor 4/6
GCKs – germinal center kinases
GFP – green fluorescent protein
gli2 *– GLI family zinc finger 2*
GM – growth media
GSK-3β - glycogen synthase kinase 3β
HA – hemagglutinin
Hand1/2 – heart and neural crest derivatives expressed 1/2
HEK293T – human embryonic kidney cell line
HGF/SF – hepatocyte growth factor/scatter factor
Hpo – Hippo
HRP – horseradish peroxidase
HXRXXS – histidine-x-arginine-x-x-serine motif
ICM – inner cell mass
IDR – intrinsically disordered region
IF – immunofluorescence
IGF1 – insulin-growth factor 1
IP – immunoprecipitation
Lats1/2 – large tumor suppressor kinase 1/2
LC/MS-MS – liquid chromatography-tandem mass spectrometry
kDa – kilodaltons
Mats – Mob as tumor suppressor
MCAT – muscle CAT element
MCK – muscle creatine kinase
Mef2 – myocyte enhancer factor 2
Mob1α/β – Mps one binder kinase activator 1
MS – mass spectrometry
Mst1/2 – mammalian Sterile20-like protein kinases 1 and 2
mTOR – mammalian target of rapamycin
MuSCs – muscle satellite cells
Myf5 – myogenic factor 5
MyHC – myosin heavy chain
MyoD – myoblast differentiation protein 1
MyoG – myogenin
N-cadherin – neural cadherin
NDR – nuclear Dbf-2-related family
NF2 – Neurofibromatosis type 2
NH_4HCO_3 – ammonium bicarbonate
Nkx2.5 – NK2 Homeobox 5
NP-40 – Nonidet P-40
Oct3/4 – octamere-binding transcription factor ¾
Pax3/7 – paired-homeobox transcription actors 3/7
PBS – phosphate-buffered saline
PCM – primary rat neonatal cardiomyocytes
PDZ – post-synaptic density, discs large, zonula occludens-1

PE – primitive endoderm
PEI – polyethyleneimine
PI3K – phosphatidylinositol 3-kinase
PPXY – proline-proline-x-tyrosine motif
PVDF – polyvinylidene fluoride
qPCR – quantitative polymerase chain reaction
REPO - Recruit POlycomb motif
Rest – RE1-silencing transcription factor
Rho – Ras homologous
RPM – revolutions per minute
SARAH - Salvador/Ras-association domain family
Sav – Salvador
Sav1 – Salvador homolog 1
Sd – Scalloped
SDS – sodium dodecyl sulfate
SDS-PAGE – sodium dodecyl sulfate polyacrylamide gel electrophoresis
$SCF^{\beta\text{-}TrCP}$ - SKP1-CUL1-F-box E3 ubiquitin ligase
SH3 – Src homology 3
SMA – S100B and MOB Association domain
Smad2/3 – mothers against decapentaplegic homolog 2/3
Smad7 – mothers against decapentaplegic homolog 7
Taz – transcriptional co-activator with PDZ-binding motif
TBS – tris-buffered saline
TBS-T – tris-buffered saline with 0.1% Tween-20
TE – trophoectoderm
TEAD – TEA-domain containing family of transcription factors
TEF-1 – transcriptional enhancer factor-1
TGF-β - transforming growth factor-beta
WB – western blot
Wnt – Wingless integration site
Wts – Warts
WW-domain – tryptophan-rich domain
WWTR1 – WW-domain containing transcription regulator protein 1
Yap – Yes-associated protein
Yki – Yorkie
YY1 – Yin-Yang 1
ZO-1 - zonula occludens-1
ZO-2 - zonula occludens-2

Chapter I: Literature Review

I. Overview of Striated Muscle Biology

Muscle tissue supports a wide range of physiological activities including locomotion, oxygen and nutrient delivery, and digestion. Muscle is broadly classified into two categories: striated muscle and smooth muscle, based on differences in their characteristic appearance (1-3). Striated muscle, which encompasses skeletal and cardiac muscle, displays a striped or *striated* pattern when viewed under the microscope. Individual muscle fibers are composed of myofibrils, which consist of repeating sarcomeres. As illustrated in Figure 1, a sarcomere is the fundamental unit of muscle contraction, defined by the anisotropic (A) band composed of thick myofilaments (myosin) and the light isotropic (I) band composed of thin myofilaments (actin), responsible for the striated appearance of skeletal and cardiac muscle (1-3). Smooth muscle, in contrast, lacks this ordered sarcomeric structure, and therefore does not exhibit visible striations. Instead, contractile proteins myosin and actin are organized in a disordered pattern arranged in a net-like sheet (4).

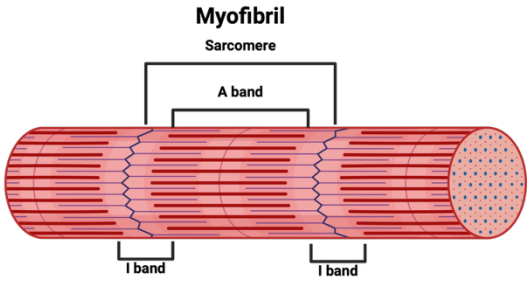

Figure 1. **Schematic of striated muscle myofibril.** Myofibrils are composed of repeating sarcomeres, the fundamental contractile unit of striated muscle. Each sarcomere contains thick (myosin) filaments that form the anisotropic (A) band, and thin (actin) filaments that form the isotropic (I) band. The alternating A and I bands produce the characteristic striped appearance of skeletal and cardiac muscle. *Created in Biorender.com.*

Skeletal and cardiac muscle are foundational to human physiology, each fulfilling distinct roles necessary for survival. Skeletal muscle constitutes approximately 40% of total body mass on average; about 38.4% in men and 30.6% in women (5, 6). Beyond generating voluntary movement, skeletal muscle is multifaceted, contributing to posture, respiration, energy metabolism, and overall physical activity (1, 5). Its importance to health and well-being is underscored by the fact that skeletal muscle atrophy, the loss of muscle fibers, compromises the body's resilience to stress and disease, adversely affecting survival and recovery outcomes across a wide range of illnesses (5).

Skeletal muscle is highly dynamic and exhibits a remarkable capacity for regeneration and repair in response to injury associated with exercise or daily activity (1). Muscle stem cells or satellite cells (MuSCs), are activated upon damage, proliferate, and differentiate to renew or replace injured myofibers (7). However, aging and chronic degenerative diseases, such as muscular dystrophy and cancers, can lead to progressive skeletal muscle dysfunction and atrophy (8). In these conditions, the MuSC population becomes progressively depleted due to repeated activation, resulting in diminished muscle regeneration, and increased fibrosis (9).

Cardiac muscle constitutes far less body mass compared to skeletal muscle, weighing approximately 270 g on average (10). It is composed of specialized contractile muscle cells, cardiomyocytes, which are arranged in a branched network connected through intercalated discs. These cell-cell junctions facilitate the synchronous electromechanical contraction of the heart. In contrast to the multi-nucleated morphology of skeletal myofibers, human cardiomyocytes are mono-or bi-nucleated (1, 11).

Unlike skeletal muscle, which performs multiple roles within the body, cardiac muscle serves a singular purpose. Cardiac muscle continuously pumps blood throughout the body to deliver oxygen and nutrients to all organs and tissues (1). Importantly, post-natal cardiomyocytes have a limited capacity for regeneration, and therefore injury to the heart results in replacement of damaged tissue with fibrotic scarring, ultimately leading to diminished cardiac function over time (12). A schematic representation of the structural differences between skeletal and cardiac muscle is shown in Figure 2.

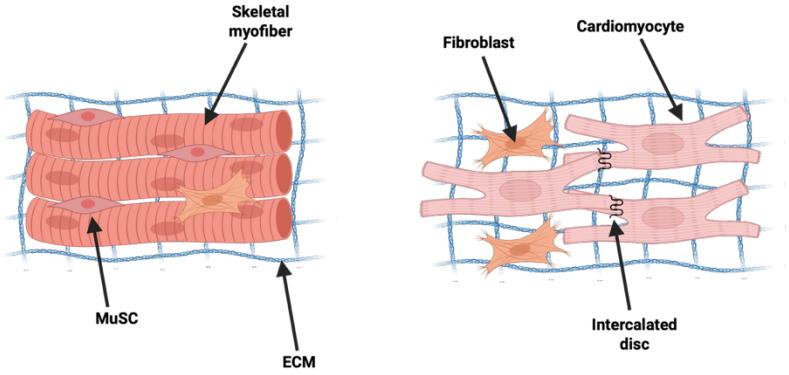

Figure 2. **Schematic of structural differences between the two types of striated muscle.** Skeletal and cardiac muscle are two types of striated muscle. Skeletal myofibers are multi-nucleated and contain a reserve of muscle satellite cells (MuSCs) responsible for regeneration and repair. Cardiac muscle cells, cardiomyocytes, are mono-nucleated and form a branched network connected together by intercalated discs to allow for synchronous electromechanical contraction necessary for pumping blood throughout the body. MuSC, muscle satellite cell; ECM, extracellular matrix. *Created in Biorender.com.*

II. Striated Muscle Development and Regeneration

a. Embryogenesis

Embryogenesis is a complex developmental process that is tightly regulated by co-ordinated transcriptional networks. Embryonic development begins around embryonic day 1.5 (E1.5) in mice and around E3 in humans (13). During the pre-implantation phase, the zygote

undergoes multiple rounds of cleavage. At the 8-cell stage, octamer-binding factor 3/4 (Oct3/4) and caudal-type homeobox protein 2 (Cdx2) are co-expressed in all blastomeres (14).

By the fourth cleavage, the 16-cell morula is formed, at which point the first cell fate decision occurs (13, 15). The morula blastomeres asymmetrically divide into smaller inner cells and larger outer cells, which will ultimately generate two distinct lineages within the blastocyst: the inner cell mass (ICM) that forms the embryo proper, and the trophoectoderm (TE) which contributes to the placenta in order to provide nutrients to the developing embryo. These cellular lineages emerge through location-specific, reciprocal negative regulation of Oct3/4 and Cdx2 (15). Outer cells upregulate Cdx2 and repress Oct3/4, committing to the TE lineage, while inner cells maintain Oct3/4 expression and suppress Cdx2, specifying the ICM (15).

Once the ICM and TE cells have been established, the blastocyst forms and cells of the ICM further commit to the epiblast or primitive endoderm (PE) lineages through the differential expression of homeobox transcription factor, Nanog, and GATA-binding factor 6 (Gata6) (15). Nanog promotes the pluripotency of cells that will form the epiblast, which ultimately gives rise to the embryo proper (16), whereas Gata6 drives the differentiation of ICM cells to the PE lineage (17).

The late blastocyst contains three distinct cell populations: 1) the TE, which mediates implantation and contributes to extra-embryonic tissues including the placenta, 2) the PE, which forms the yolk sac, and 3) the epiblast, which gives rise to the tissues of the embryo proper (15). Around E6 in mice and E14 in humans, the epiblast undergoes gastrulation (15, 18), a defining stage in embryogenesis which proceeds with the formation of the primitive streak. The three

germ layers are formed during gastrulation: ectoderm, mesoderm, and definitive endoderm (DE) (15, 19).

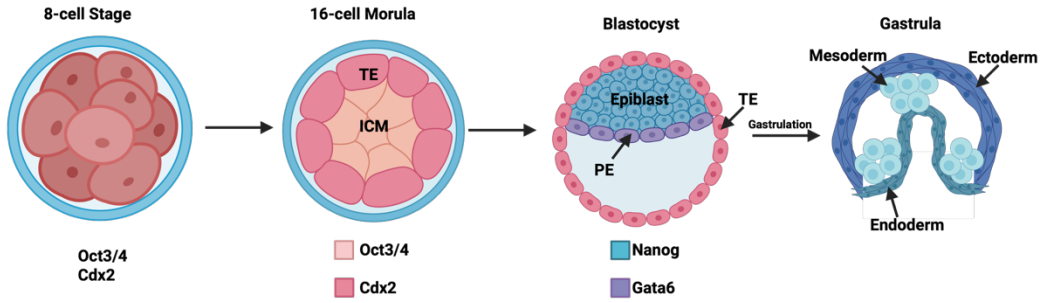

Figure 3. **Schematic of early embryonic development.** Oct3/4 and Cdx2 are co-expressed in all blastomeres at the 8-cell stage. After cell division, the embryo forms the 16-cell morula, where the first lineage decision occurs: outer cells upregulate Cdx2 and commit to the trophoectoderm (TE) lineage, while inner cells maintain Oct3/4 expression and form the inner cell mass (ICM). During the blastocyst stage, cells of the ICM further commit into the epiblast through an upregulation of Nanog, or primitive endoderm (PE) by expressing Gata6. By the late blastocyst stage, three distinct cell lineages are present: TE, PE, and epiblast. The epiblast subsequently undergoes gastrulation, generating the three germ layers: ectoderm, mesoderm, and endoderm. TE, trophoectoderm; ICM; inner cell mass; PE, primitive endoderm. *Created in Biorender.com.*

Mesoderm formation involves an EMT, whereby epiblast cells migrate through the primitive streak to form a new cell layer. This process is driven by BMP signaling from the extra-embryonic ectoderm, in conjunction with Nodal-Smad2/3 and Wnt signaling pathways within the epiblast (15, 20-22). The timing and position at which cells move through the primitive streak determine their fate (19): cells migrating through the middle of the streak generate the lateral plate mesoderm, while those migrating anterior to the streak form the paraxial mesoderm (19). Eventually, the lateral plate mesoderm will give rise to cardiac muscle, whereas the paraxial mesoderm will give rise to skeletal muscle (23).

b. Skeletal Myogenesis and Regeneration

Myogenesis, the development of skeletal muscle, proceeds through a coordinated series of stages, including stem cell maintenance, lineage specification, commitment, proliferation, and terminal differentiation. This progression is regulated through the successive activation of paired-homeobox transcription factors 3/7 (Pax3/7), and the four basic helix-loop-helix muscle regulatory factors (MRFs): Myogenic factor-5 (Myf5), Myoblast determination protein 1 (MyoD), Myogenin (MyoG), and Muscle regulatory factor-4 (Mrf4). Identified in the 1980s, these highly conserved transcription factors contain a basic domain that mediates DNA binding, and a helix-loop-helix motif that enables heterodimerization with E proteins. These protein complexes bind to E-box motifs (CANNTG) present in many myogenic-specific promoters (24-26). The MRFs are essential for committing progenitor cells to a skeletal muscle fate and coordinating the muscle-specific transcriptional programs that underlie skeletal muscle formation (27-31).

MRFs function cooperatively with myocyte enhancer factor 2 (Mef2) to facilitate proper muscle development (25). MRFs activate the expression of Mef2, while also upregulating their own transcription (32). In turn, Mef2 directly binds to MRF gene promoters to enhance their expression (33), creating a positive-feedback loop that ultimately enhances MRF function in the commitment and differentiation of skeletal muscle.

Pre-natal muscle development begins with somitogenesis, during which the paraxial mesoderm progressively condenses along the anterior-posterior axis of the embryo to form somites, which are mesenchymal cellular structures encased in epithelial shells (34). Somites are formed bilaterally alongside the neural tube in an anterior to posterior direction. Somitogenesis is regulated by morphogen gradients of Notch, Wnt, fibroblast growth factor (FGF), and retinoic

acid (RA) (25). High Wnt and FGF signaling in the caudal region of the embryo maintains cells of the paraxial mesoderm in an unsegmented, mesenchymal state.

In the newly formed somites, increased RA signaling establishes dorsoventral polarity (35). The ventral part of each somite receives Wnt, Sonic hedgehog (Shh), and BMP signaling, which together induce EMT to form the sclerotome; these cells migrate to generate the vertebrae and ribs (36, 37). In contrast, the dorsal part of the somite develops into the dermomyotome (25). The dermomyotome gives rise to nearly all skeletal muscle (with the exception of head muscles) as well as dermal tissues. Dermomyotomal progenitors express Pax3/7, along with low levels of Myf5. Pax3 plays a key role in embryonic myogenesis by promoting the expression of Myf5, the first MRF to be expressed in myogenesis (25, 37, 38).

Myf5-positive cells located at the dorsomedial lip (DML) and ventrolateral lip (VLL) of the dermomyotome undergo EMT and delaminate beneath the dermomyotome to form the myotome (25, 36). Myotomal cells are characterized by an upregulation of MyoD and downregulation of Pax3 (25). Wnt and Shh decrease BMP signaling in the DML by upregulating Noggin. The cross-talk between these developmental networks has been shown to be required for the upregulation of Myf5 and MyoD, thereby committing dermomyotomal cells to the myotome (25, 39, 40). Consistent with this, depletion of *noggin* resulted in impaired myotome formation in mouse embryos (41).

Myotomal cells, now termed myoblasts, express high levels of Myf5 and MyoD, both of which commit cells to a myogenic fate. Functional redundancy between Myf5 and MyoD has been well documented, whereby *myf5*-deficient mice exhibited delayed myogenesis until MyoD expression, at which time muscle development proceeded normally (42). Similarly, sustained Myf5 expression has been shown to compensate for loss of *myod* (43). The essential roles of

these MRFs in early pre-natal myogenesis is emphasized by *myf5:myod* double knockdown studies, in which there is a complete lack of MyoG expression and absence of skeletal muscle development (44). This finding highlights the importance of Myf5 and MyoD in facilitating skeletal muscle development in the embryo.

Epaxial myotomal progenitors give rise to deep back muscles (45), whereas hypaxial myotomal progenitors migrate to form ventral trunk and limb muscles (25). Pax3 plays a critical role in this process by upregulating c-Met. C-Met is a tyrosine kinase receptor that responds to its ligand hepatocyte growth factor/scatter factor (HGF/SF) to drive the delamination and migration of hypaxial myotomal cells to the developing limb bud (46, 47). Once at the limb site, these hypaxial progenitors proliferate and begin to express Myf5 and MyoD, committing them to the skeletal muscle lineage (36, 37, 48). Therefore, Myf5 and MyoD are essential determinants of myogenic lineage commitment and maintenance of myogenic progenitor populations. Myoblasts expressing Myf5 and MyoD subsequently proliferate and progress into the differentiation program through the upregulation of MyoG and MRF4, the latter of which is expressed at highest levels in mature muscle (49).

Some Pax3/7-expressing dermomyotomal cells do not commit to the myogenic lineage. Instead, they proliferate and become MuSCs. These MuSCs express Pax7 which plays a dominant role in post-natal muscle regeneration. Consistent with this, *pax7*-deficient mice exhibit lack of a functional MuSC population or a failure of MuSCs to proliferate, as well as post-natal muscle weakness (50), reflecting impaired regenerative potential. MuSCs reside in close proximity to differentiated myofibers, positioned underneath the extracellular matrix (ECM) of the basal lamina (36, 51). This microenvironment, known as the “stem cell niche”, maintains the MuSCs in a quiescent (G_0), non-proliferative state. Quiescence is primarily

controlled by the Notch signaling pathway, which ultimately activates downstream target genes *hey1* and *heyL* (7). Notch signaling is important for maintaining the MuSC pool, as *hey1* and *heyL* deletion results in spontaneous activation and subsequent depletion of the MuSC population (7, 52).

The MuSC population is heterogenous, with approximately 90% expressing Myf5 and are thus committed to the myogenic lineage. The remaining 10% are Myf5-negative to retain the ability to undergo self-renewal to replenish the MuSC pool. These Myf5-negative MuSCs divide either symmetrically or asymmetrically (53). Symmetrical cell division occurs when a Myf5-positive MuSC gives rise to two identical, committed cells or when a Myf5-negative MuSC gives rise to two identical, uncommitted cells. In contrast, asymmetrical division gives rise to a committed, Myf5-positive cell and an uncommitted, Myf5-negative cell that replenishes the MuSC population (54). Quiescent MuSCs are characterized by Pax7 expression and may be either Myf5-positive or Myf5-negative, reflecting their potential to both self-renew and initiate myogenic commitment (55).

Muscle injury releases mitogens that signal MuSCs to activate (7, 55). In response, MuSCs exit the quiescent G_0 phase and enter a primed G_{ALERT} state before re-entry into the cell-cycle (7). This transition is triggered by HGF which has been implicated in promoting the G_{ALERT} phase by activating the Akt (Akt serine/threonine kinase)/mTOR (mammalian target of rapamycin) pathway (7, 56). Activated MuSCs migrate to the site of injury, which is facilitated by c-Met, similar to pre-natal myogenesis. At the damaged tissue, MuSCs re-enter the cell-cycle and proliferate (55). Additional growth factors regulate MuSC activation and proliferation; for example, insulin-growth factor 1 (IGF1) relieves cell cycle inhibition and promotes cell-cycle entry (7, 57). Proliferating MuSCs that are Myf5-positive, now termed myoblasts, commit to the

myogenic lineage and contribute to the formation of new muscle fibers. In contrast, those that are Myf5-negative undergo symmetric or asymmetric cell division to self-renew and maintain the MuSC population.

After proliferation, myoblasts exit the cell cycle through the upregulation of different cell-cycle inhibitors including $p21^{Cip1}$ (7, 58). This transition is accompanied by the downregulation of Pax7 and Myf5, and upregulation of MyoG and Mrf4, which will drive terminal differentiation and fusion into multinucleated myotubes (7, 55).

Fusion is triggered by cell-cell contact and requires the muscle-specific membrane proteins Myomaker and Myomixer, whose expression is induced by MyoD and further enhanced by MyoG (55, 59). Following fusion, myotubes undergo maturation to form functional myofibers, characterized by the expression of contractile proteins such as myosin heavy chain (MyHC), while MyoD levels decrease. The maturation process is regulated by IGF1 signaling through the Akt/mTOR pathway (60). Fully mature myofibers are innervated, enabling excitation-contraction coupling, and establish metabolic machinery, all of which are necessary for proper muscle function (55). A schematic of embryonic and adult myogenesis is shown below in Figure 4.

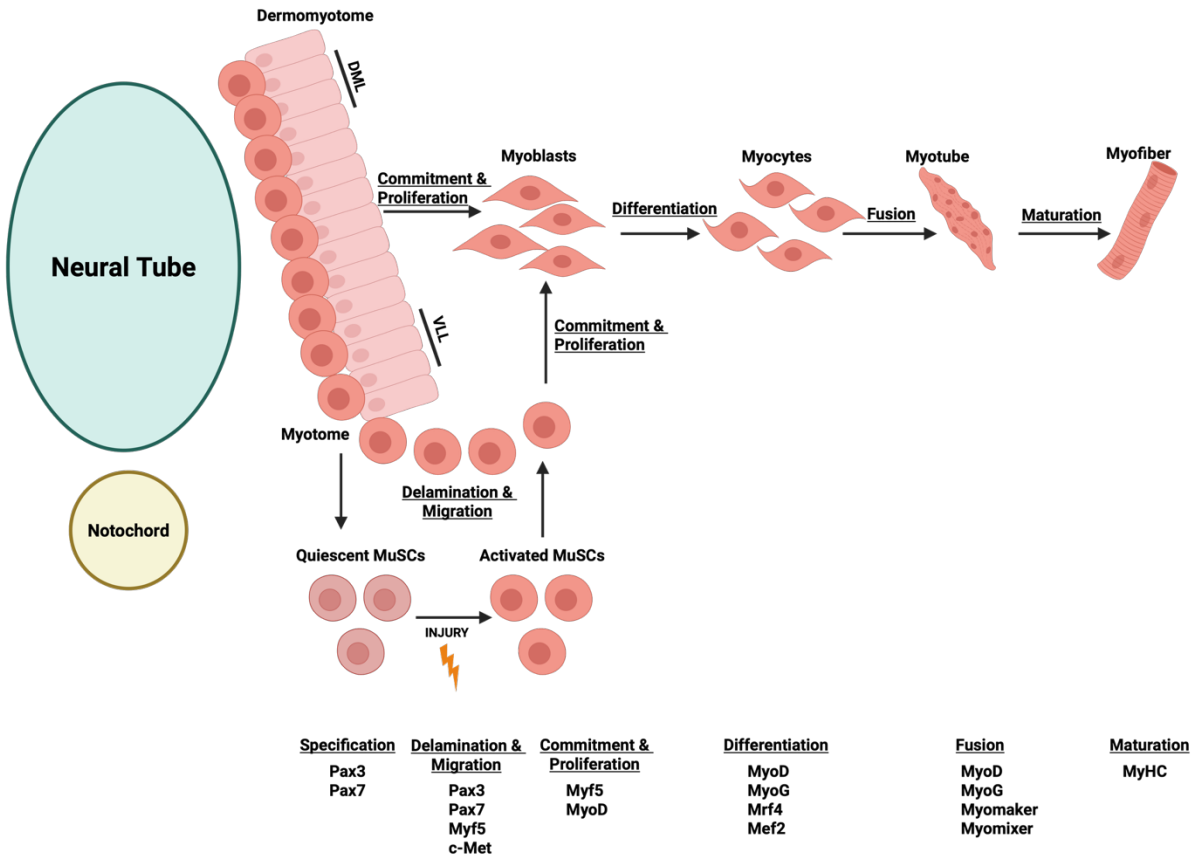

Figure 4. **Schematic of pre-natal and post-natal skeletal myogenesis.** Dermomyotomal cells express Pax3/7. Cells at the dorsomedial (DML) and ventrolateral lips (VLL) that upregulate Myf5 delaminate to form the myotome. Myotomal cells subsequently express MyoD, committing to the myogenic lineage and generating myoblasts. Some Pax3/7-positive dermomyotomal cells will not form the myotome and instead give rise to muscle satellite cells (MuSCs) required for muscle regeneration. MuSCs remain quiescent until activated by muscle injury. Embryonic myotomal cells destined for the limb, and activated MuSCs, will migrate to their respective differentiation sites through c-Met expression. At this stage, embryonic and adult myogenesis converge: myoblasts express high levels of Myf5 and MyoD, fully committing to the myogenic lineage. They proliferate, then undergo differentiation through the induction of MyoG and Mrf4. Differentiated myocytes fuse by expressing Myomaker and Myomixer to form multinucleated myotubes, which mature into fully functional myofibers characterized by the expression of contractile proteins such as MyHC. *Created in Biorender.com.*

c. Cardiogenesis

The heart is the first organ to fully form and become functional during embryogenesis thus necessitating its flawless construction. During gastrulation, the first cells to migrate through

the middle of the primitive streak will give rise to the lateral plate mesoderm, which will ultimately give rise to cardiac muscle (19). Around day 18 of human development, the lateral plate mesoderm separates into the somatopleuric and splanchnopleuric layers. The splanchnopleuric mesoderm contains myocardial progenitors that migrate to form bilateral primary heart fields, in the shape of a crescent, on both sides of the neural tube (61, 62).

Cardiac lineage specification is regulated by a myriad of signaling pathways, similar to skeletal myogenesis. BMP signaling from the neighbouring endoderm induces cardiogenic commitment within the splanchnopleuric mesoderm (62, 63). *NK2 Homeobox 5* (*Nkx2.5)* is the first cardiac-specific gene to be activated, and its expression commits the cells to the cardiogenic lineage (62, 64). Nkx2.5 cooperates with GATA transcription factors to activate cardiac-specific genes such as cardiac atrial natriuretic factor, alpha-actin (α-actin), and Mef2c (65-67). Furthermore, basic helix-loop-helix transcription factors Hand1/2 are expressed in the developing left and right ventricles, respectively. Nkx2.5 appears to regulate Hand1 expression, as *nkx2.5*-deficient mice exhibit loss of Hand1 and severe ventricular deformities (68). Moreover, Mef2c expression is also dependent on Nkx2.5 activity. Mef2c has been shown to be vital to cardiac development, as disruption of *mef2c* prevents the progression of cardiac development, impaired specification of the right ventricle, and reduced expression of cardiac-specific genes such as Hand2 (66, 69). Collectively, Nkx2.5 and GATA factors function as central regulators of transcriptional programs that direct cardiomyocyte specification and differentiation to ultimately form a functional heart.

Once specified, cardiomyocytes migrate to the ventral midline of the embryo to form a beating linear heart tube. The linear heart tube is comprised of myocardial and endocardial layers that are separated by an ECM called cardiac jelly (62, 66). Along its anterior-posterior axis,

individual cardiac chambers of the heart tube are specified to give rise to the aortic sac, outflow tract, pulmonary and systemic ventricles, and the atria (62). During vertebrate cardiogenesis, the linear heart tube elongates and undergoes subsequent looping to the right side of the embryo. Looping is a critical developmental process that is required to establish the correct orientation of the pulmonary and systemic ventricles (61, 62).

The primary heart field gives rise to the atria and ventricles, which are the main structures of the heart, whereas the secondary heart field gives rise to the outflow tract. The cells of the secondary heart field undergo EMT to contribute myocardial cells to the outflow tract. Chambers within the linear heart tube are defined by constriction points that separate the sinus venosus, common atrial chamber, atrio-ventricular canal, ventricular chamber, and outflow tract (66). Subsequently, myocardial trabeculations form within the atria and ventricles, and cardiac cushions develop through the migration of endocardial cells from the atrio-ventricular canal and outflow tract into the cardiac jelly (61, 66).

Cardiac septation proceeds as the right atrio-ventricular canal and right ventricle expand to the right, and the left and right atrio-ventricular canals are separated. Now, incoming blood can pass directly into the right atrium to the right ventricle. The myocardial ventricular septum grows between approximately 4 to 9 weeks of human embryogenesis, dividing the left and right ventricles (61). Atrial septation remains incomplete until after birth to permit shunting of oxygenated placental blood from the right to the left atrium *in utero* (61).

Finally, cardiac maturation is the last step of heart development. During embryogenesis, cardiac growth depends primarily on cardiomyocyte proliferation. However, shortly after birth, cardiomyocytes exit the cell cycle and lose their regenerative capacity. Thus, post-natal cardiac growth occurs predominantly through hypertrophy, whereby existing cardiomyocytes increase in size rather than number (61). A brief overview of cardiogenesis is shown below in Figure 5.

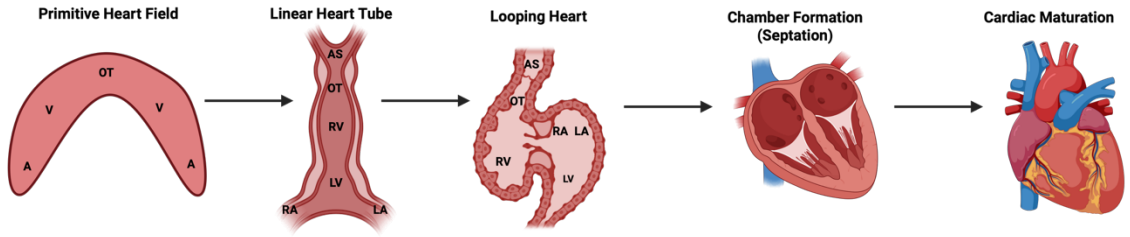

Figure 5. **Schematic of cardiac development.** Myocardial progenitors from the splanchnopleuric mesoderm form bilateral primary heart fields, then fuse at the ventral midline of the embryo to generate the beating linear heart tube. The tube then undergoes rightward looping and chamber septation, followed by proliferative and hypertrophic growth to form the mature heart. *Created in Biorender.com.*

III. Hippo Signaling Pathway

a. Discovery of Hippo Signaling

Organogenesis and regeneration are fundamental to overall tissue functionality and homeostasis within the body. Over the past three decades, regulation of organ development and size has gained considerable attention. Proper organ development depends on the precise co-ordination of cellular proliferation, survival, and differentiation. Hippo signaling is essential to maintaining organ size by controlling these interconnected biological processes. Due to its central role in organ size control, Hippo dysregulation is implicated in abnormal or disrupted tissue growth, contributing to a range of diseases, including cancer and tissue degeneration (70).

The discovery of the Hippo pathway originated in *Drosophila melanogaster (Dm*) through genetic screens designed to identify genes that regulate organ growth. Over the following decade, four core components of the pathway were characterized: Warts (Wts), Salvador (Sav), Hippo (Hpo), and Mob as tumor suppressor (Mats). The genes that encoded these proteins were shown to be key developmental regulators of tissue growth by coordinating cellular proliferation and apoptosis. The first of these, *wts*, was defined as a tumor suppressor gene encoding a serine/threonine kinase from the nuclear Dbf-2-related (NDR) family, that restricts cell growth and proliferation. Loss-of-function mutations in the *wts* gene led to dysregulated cell division and hypertrophic phenotypes of epithelial cells within developing imaginal discs, resulting in tumor formation on adult integumentary structures such as the leg, wing, and foot (71, 72).

Subsequent work in the early 2000s identified *sav* as a gene that promotes cell cycle exit and cell death (73, 74). As key regulators of both proliferation and apoptosis, Wts and Sav were shown by Tapon and colleagues (73) to interact through their respective proline-proline-x-tyrosine (PPXY) motif (where x is any amino acid) and tryptophan-rich (WW) domain. The authors proposed that these proteins operate together within a specific signaling pathway governing these developmental processes. The following year, *hpo* was identified as encoding a serine/threonine kinase in the Sterile-20 family that acts within this same pathway to restrict growth and promote apoptosis, thereby expanding the molecular network that ultimately controls organ development (75-77). Multiple independent research groups (75-77) further demonstrated that Hpo directly binds to the coiled-coil domain of Sav through its C-terminus to phosphorylate it. Sav acts as a scaffolding protein to facilitate the interaction between Hpo and Wts, allowing Hpo to phosphorylate Wts at its N-terminus and activate the growth-regulatory cascade. The

mats gene was last to be identified to encode a Mob superfamily protein as part of the core components working in this pathway. Mats was shown to physically interact with Wts to potentiate its catalytic activity (78). This activation is mediated by Hpo, which binds and phosphorylates Mats, increasing its affinity to Wts and enhancing Wts kinase activity (78, 79).

Consistent with their role as central regulators of proliferation and cell death, loss of *wts, sav, hpo,* and *mats* in eye imaginal disc cells led to elevated expression of the cell-cycle activator, Cyclin E, as well as anti-apoptotic factor, *Drosophila* inhibitor of apoptosis-1 (DIAP1) (73, 75). Mutant cells failed to exit the cell cycle at the appropriate time, proliferating up to 24 hours longer than their wild-type counterparts. This prolonged proliferation resulted in excessive tissue growth on imaginal disc-derived adult structures such as the eye and head. Furthermore, the programmed cell death involved in normal eye development was markedly impaired in these mutant cells (73-75).

The observation that loss-of-function mutations in these tumor suppressor genes increased Cyclin E and DIAP1 expression led to the idea that the Hippo pathway represses the transcription of these growth-promoting genes. However, the mechanism by which Hippo kinases regulate *cyclin E* and *diap1* transcription remained unclear. The connection between the core components of Hippo signaling and transcriptional control was elucidated by Huang and colleagues (80). They identified the *yorkie (yki)* gene which encoded a transcriptional co-activator that was negatively regulated by Wts phosphorylation. Wts interacts with Yki at its two WW-domains contained in the region between residues 229 to 418 (80, 81). Wts phosphorylates Yki at its serine-168 (Ser168) residue, which sequesters it in the cytoplasm by 14-3-3 proteins (82). Overexpressing the *yki* gene in wing and eye imaginal discs produced the same phenotypes seen in the loss-of-function mutations of *wts, sav, hpo,* and *mats:* elevated Cyclin E and DIAP1

expression, late cell-cycle exit, reduced apoptosis, and the resulting tissue overgrowth. Conversely, a *yki* loss-of-function mutation had the opposite phenotypic outcome whereby adult eyes that were composed mainly of *yki*-mutant cells, were significantly smaller than controls. Additionally, knock-down of *yki* resulted in the repression of *diap1* transcription. Altogether, Huang and colleagues (80) showed that Yki functions antagonistically to the Hippo kinases; Yki activates growth mechanisms whereby the Hippo pathway suppresses them. The activation of Hippo signaling leads to the growth-suppressive function of the pathway; Wts interacts with and phosphorylates Yki to deactivate it. A schematic of the *Dm* Hippo signaling pathway is shown below in Figure 6.

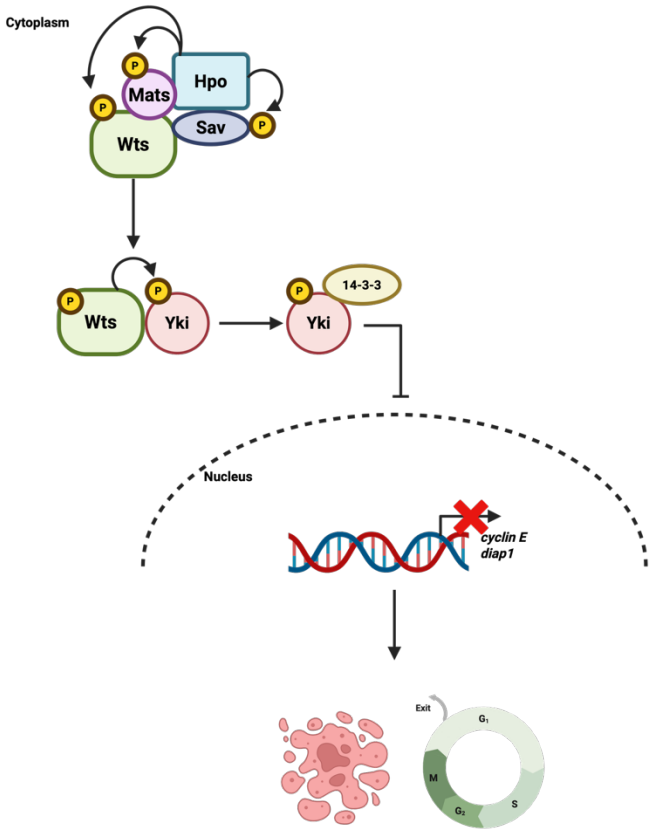

Figure 6. **Schematic of the Hippo signaling pathway in *Drosophila melanogaster*.** Independent research groups established the interactions among the core components of the Hippo kinase complex in *Drosophila melanogaster*. In this pathway, the Hpo-Sav-Wts module mediates the phosphorylation of Wts by Hpo, while the Hpo-Mats-Wts module facilitates the interaction and phosphorylation of Mats by Hpo to strengthen its affinity for Wts, stimulating Wts kinase activity. Once activated, Wts will bind to and phosphorylate the transcriptional co-activator, Yki, leading to its inhibition and preventing the transcription of growth-promoting genes. Together, these phosphorylation events establish a growth-suppressive signaling cascade that governs organ development and size. *Created in Biorender.com.*

As previously mentioned, Yki functions as an oncogene that stimulates the expression of proliferative and growth-inducing genes (83). As a transcriptional co-activator, it does not have its own DNA-binding domain and thus cannot bind DNA directly. Instead, it exerts its effects by interacting with DNA-binding transcription factors. Downstream of the Hippo pathway, Yki activity is repressed through phosphorylation by Wts. The transcription factor that binds to unphosphorylated, active Yki, to drive tissue growth was identified as Scalloped (Sd) (84). Sd binds Yki at its C-terminus (residues 226-440), while Yki interacts with Sd at its N-terminus, upstream of its first WW-domain. Sd binds to and recruits Yki to a Sd-binding motif with the consensus sequence CATTCCA, located within a 26 base-pair Hpo-responsive element in the *diap1* promoter. Through this interaction shown in Figure 7, Yki activates the transcription of *diap1* by Sd (84). Collectively, the identification of the core Hippo signaling components in *Dm* and the discovery of their downstream effector Yki, along with its DNA-binding partner Sd, revealed the mechanism by which the Hippo pathway regulates proliferation and apoptosis to ultimately suppress abnormal tissue growth.

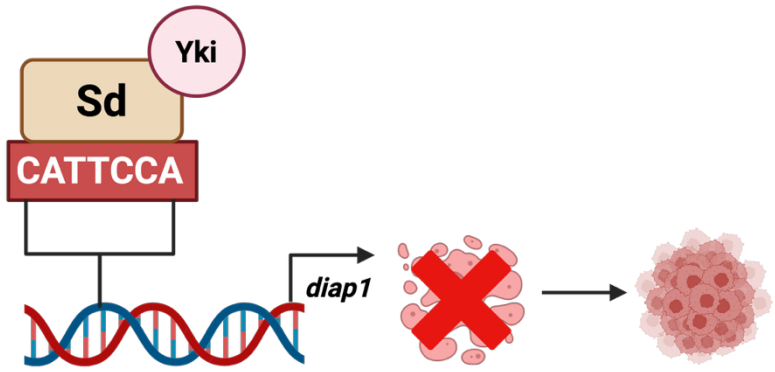

Figure 7. **Scalloped (Sd) recruits Yorkie (Yki) to the Hpo-responsive element upstream of the *diap1* gene, promoting *diap1* transcription and inhibiting apoptosis.** When Hippo signaling is inactive and Yki remains unphosphorylated, Sd recruits Yki to the Sd-binding motif within the Hpo-responsive element in the *diap1* promoter. Acting as a transcriptional co-activator, Yki drives *diap1* expression, resulting in reduced apoptosis and hyperproliferation. *Created in Biorender.com.*

The core components of the Hippo signaling pathway are highly conserved across evolution, dating back to pre-metazoan lineages. Comparative genomic analyses suggest that the Hippo signaling pathway originated prior to the emergence of multicellular organisms. Orthologs of Yki and Sd have been identified in unicellular organisms such as *Capsaspora owczarzaki* (a filasterean) and the choanoflagellates *Monosiga brevicollis* and *Salpingoeca rosetta* (85). The Yki orthologs in these species retain the conserved phosphorylation site for Yki inactivation, and the N-terminal region where Sd binds. Similarly, Sd orthologs possess conserved C-terminal domains responsible for the interaction with Yki. Along with the downstream transcriptional effectors, the discovery of conserved core Hippo kinases in these unicellular organisms underscores the view that the Hippo signaling pathway predates the evolution of multicellularity (85). The evolutionary conservation of Hippo signaling extends to mammals, where the orthologous pathway carries out the same functions to repress uncontrolled proliferation and initiate apoptosis, to ensure normal tissue growth in organ development.

b. Regulation of Yap/Taz by Hippo signaling

i. Active Hippo signaling represses YAP/TAZ transcriptional induction

Similar to *Dm*, the mammalian Hippo pathway consists of a cytoplasmic serine/threonine kinase cascade that regulates the phosphorylation, sub-cellular localization, and consequent activity of Yes-associated protein (Yap) and Transcriptional co-activator with PDZ-binding domain (Taz, also known as WW-domain containing transcription regulator protein 1 (WWTR1)), orthologous to Yki (80). Hippo signaling is initiated by the activation of mammalian Sterile20-like protein kinases 1 and 2 (Mst1/2; Hpo in *Dm*). These proteins belong to the germinal center kinase (GCKs) subfamily of Sterile 20 proteins, defined by an N-terminal kinase domain and a non-catalytic region that mediates interactions with signaling molecules and cytoskeletal proteins (86). Mst1/2 heterodimerize with and phosphorylate Salvador homolog 1 (Sav1; Sav in *Dm*) through their C-terminal Salvador/Ras-association domain family (SARAH) domains located within their coiled-coil regions (87-89), and this interaction stabilizes and promotes the accumulation of Sav1 (88). Co-immunoprecipitation experiments using Mst1/2 and Sav1 deletion constructs by Callus et al. (88) confirmed that these coiled-coil domains are required for the formation of the Mst1/2-Sav1 complex.

In contrast to the *Dm* Hippo module, where Sav acts as a scaffold to bring together Hpo and Wts for Wts phosphorylation and activation, activated Mst1/2 in mammals directly binds to the large tumour suppressor kinases 1 and 2 (Lats1/2; Wts in *Dm*) to phosphorylate them. Whether this phosphorylation event occurs in a Sav1-dependent manner remains unclear (87). Nonetheless, Mst1/2 phosphorylates Lats1/2 at their threonine-1079 (Thr1079) residues within their C-terminal hydrophobic motifs (87). Furthermore, Mst1/2 binds and phosphorylates Mps

one binder kinase activator 1 (Mob1α/β; Mats in *Dm*) at Thr12 and Thr35, promoting their association with Lats1/2 (90).

Phosphorylated Mob1α/β binds to a MOB1-binding motif at the N-terminus of Lats1/2 that is similar to the N-terminal S100B and MOB Association (SMA) domain in NDR, a kinase closely related to Lats1/2 (91, 92). The catalytic domain of NDR contains a basic autoinhibitory sequence that suppresses kinase activity. Bichsel and colleagues (91) demonstrated that Mob1 binding to the SMA domain relieves this inhibition and stimulates NDR catalytic function. This basic sequence likely corresponds to the activation loop within the catalytic domain of Lats1/2 described by Praskova et al (90). Accordingly, the interaction of phosphorylated Mob1α/β with the MOB1-binding motif of Lats1/2 may facilitate autophosphorylation at Ser909 within the activation loop, thereby alleviating autoinhibition (90). Phosphorylation at both Thr1079 and Ser909 residues are required for full Lats1/2 catalytic activity (87).

Once Lats1/2 is activated through the aforementioned phosphorylation events, the mechanism by which Lats1/2 regulates the sub-cellular localization and subsequent activation of Yap/Taz is conserved from *Dm* to mammals. Lats1/2 interacts with the WW-domains of Yap/Taz through its PPXY motif (81, 93). This interaction facilitates Lats1/2-mediated phosphorylation of Yap at Ser61, Ser109, Ser127, Ser164, and Ser381 (94). Phosphorylation of Taz occurs at Ser66, Ser89, Ser117, and Ser311 (95). Phosphorylation at Yap Ser127 and Taz Ser89, both of which are orthologous to Yki Ser168, promotes the recruitment of 14-3-3 proteins, sequestering Yap/Taz to the cytoplasm (96, 97). The cytoplasmic sub-cellular localization of Yap/Taz ultimately prevents their co-activating role in gene transcription.

A more permanent mechanism by which Hippo signaling regulates Yap/Taz co-activating properties is through additional phosphorylation by Lats1/2. Phosphorylation of Yap Ser381 and

Taz Ser311 by Lats1/2 primes them for subsequent phosphorylation by casein kinase 1 (CK1) at Ser384 and Ser314, respectively. Using Taz mutants in which individual Lats1/2-phosphorylation sites were substituted from serine to alanine, Liu and colleagues (95) demonstrated that phosphorylation of Taz at Ser311 is necessary for the formation of a C-terminal phosphodegron. This phosphodegron is recognized and bound by β-transducin repeat containing protein (β-TrCP), the substrate-binding subunit of the SKP1-CUL1-F-box ($SCF^{\beta\text{-}TrCP}$) E3 ubiquitin ligase. The interaction between Taz and β-TrCP drives β-TrCP-mediated polyubiquitination of Yap/Taz, targeting them for proteasomal degradation (95). Similar findings were reported for the requirement of Yap Ser381 phosphorylation by Lats1/2 (98). A schematic of the *active* mammalian Hippo signaling pathway is shown in Figure 8.

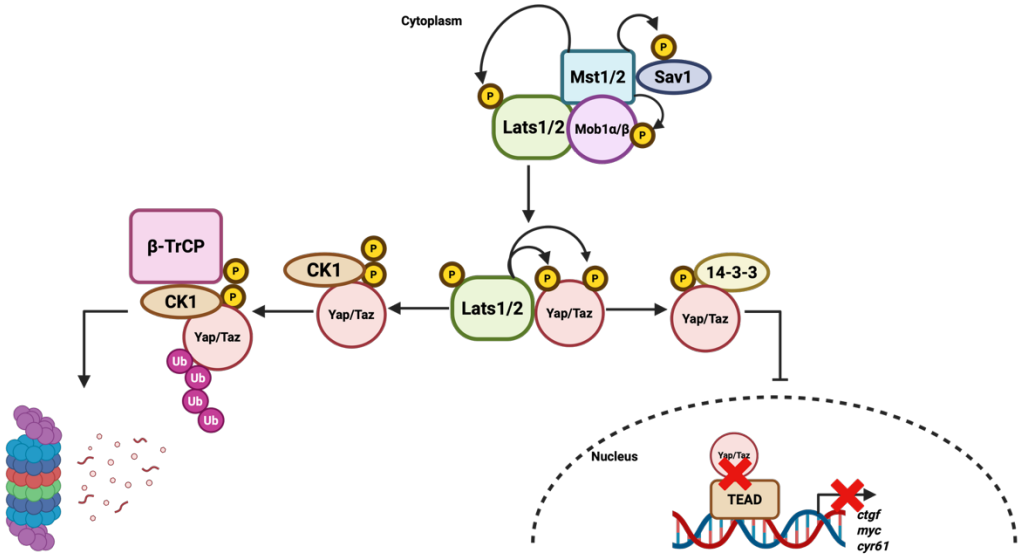

Figure 8. **Schematic of the *active* mammalian Hippo signaling pathway.** Independent research groups established the regulation of transcriptional co-activators Yap/Taz through the canonical Hippo signaling cascade. When this pathway is ON, activated Mst1/2 interacts with and phosphorylates Sav1, Lats1/2, and Mob1α/β. Phosphorylated Mob1α/β binds Lats1/2, promoting Lats1/2 activation. Activated Lats1/2 subsequently phosphorylate Yap/Taz at their Ser127 and Ser89, respectively. These phosphorylation events lead to 14-3-3 protein binding, resulting in cytoplasmic sequestration of Yap/Taz. A more permanent mechanism of Yap/Taz regulation involves the Lats1/2-mediated phosphorylation at Yap Ser381 and Taz Ser311, which primes them for additional phosphorylation by CK1 at Ser384 and Ser314, respectively. These sequential phosphorylation events generate a phosphodegron that is recognized by β-TrCP. This interaction promotes ubiquitination and subsequent proteasomal degradation of Yap/Taz. *Created in Biorender.com.*

ii. Inactive Hippo signaling allows YAP/TAZ transcriptional induction

It is well established that general transcription factors involved in the initiation and elongation of gene transcription cannot stably bind to promoter regions on DNA (99). Instead, they are recruited to cis-regulatory elements by sequence-specific transcription factors that contain both a DNA-binding domain and an effector domain. The effector domain enables the recruitment and interaction with regulatory molecules to promote the transcriptional activation of their specific target genes (99). TEA-domain containing transcription factors (Tead1-4; Sd in *Dm*) are a type of sequence-specific transcription factors that appear to require a co-regulator to activate transcription (100). Transient transfection experiments conducted by Xiao and colleagues showed that Tead1 expression alone was insufficient to activate Tead-dependent transcription in cells that do not endogenously express Tead (101).

When Hippo signaling is inactive, Tead1-4 recruit Yap/Taz to muscle CAT (MCAT) elements, CATTCC, located in the promoter regions of target genes in a variety of tissues, including striated and smooth muscle (102). As illustrated in Figure 9, this occurs because the Hippo core kinase cascade is *inactive*; therefore, Yap/Taz remains in an unphosphorylated state and accumulate in the nucleus where they function as robust transcriptional co-activators. As co-

activators, Yap/Taz cannot bind DNA directly and therefore, they must depend on interactions with DNA-binding transcription factors such as Tead1-4 to regulate gene expression.

Yap is categorized as a Class 1 Tead co-factor, characterized by its transactivation domain and its ability to activate MCAT promoter-driven gene expression through its interaction with Tead proteins (102). Given that Taz shares similar structural and functional properties, it is likely classified as a Class 1 Tead co-factor as well. Yap/Taz directly bind to the C-terminal transactivation domains of Tead1-4 through their N-terminal Tead-binding domains, and Tead1-4 will bind the MCAT motif through their N-terminal TEA-domains, to activate transcription of their target genes (102). Using crystallography and multi-angle light scattering, Kaan and colleagues (103) demonstrated that Taz binds to Tead in two distinct conformations: either as a heterodimer, in which one Taz binds one Tead similar to the Yap-Tead complex, or as a heterotetrameric complex, where two Taz molecules bind and bridge together two Teads. In both cases, the Yap/Taz-Tead complex functions as an activating transcriptional module that drives expression of genes, including *cellular myelocytomatosis (c-myc), connective tissue growth factor* (*ctgf), cysteine-rich angiogenic inducer 61 (cyr61), GLI family zinc finger 2 (gli2), baculoviral IAP repeat-containing 5 (birc5),* and *AXL receptor tyrosine kinase (axl)*, all of which are involved in cellular growth and proliferation (104-106).

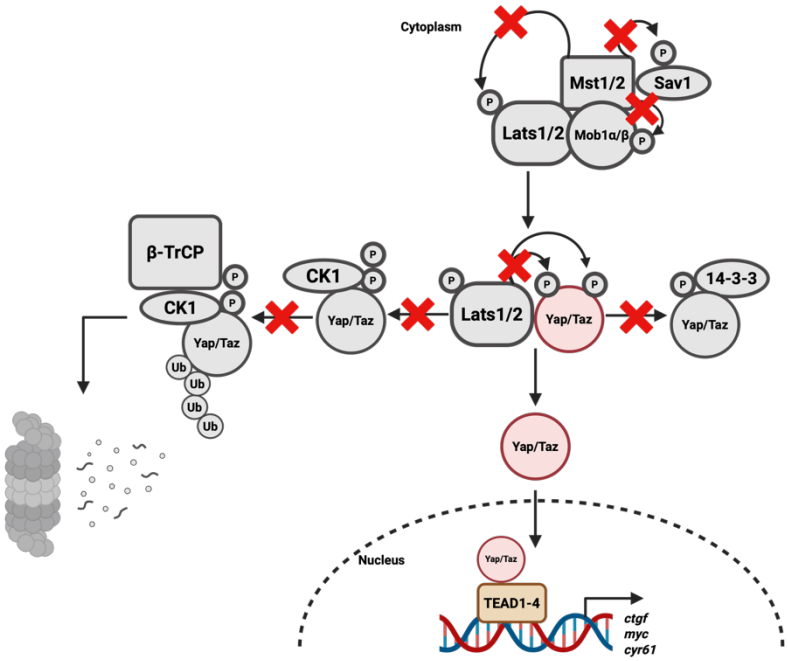

Figure 9. **Schematic of the *inactive* mammalian Hippo signaling pathway.** Independent research groups established the regulation of transcriptional co-activators Yap/Taz through the canonical Hippo signaling cascade. When this pathway is OFF, the core kinase module remains inactive and no downstream phosphorylation events occur. As a result, Yap/Taz are not phosphorylated by Lats1/2 and can translocate into the nucleus, where they bind Tead transcription factors. They are recruited to MCAT promoter elements by Teads, to activate transcription of genes involved in cellular growth and proliferation. *Created in Biorender.com.*

iii. Upstream activation of Hippo signaling and YAP/TAZ repression

The upstream signals that activate the Hippo pathway have recently begun to be elucidated. Hippo signaling is initiated by various mechanisms including cell-cell contact inhibition and ECM stiffness, to name a few (107, 108). These mechanisms are illustrated in Figure 10. The Hippo pathway transmits these external biophysical signals into intracellular regulation of gene expression, through a process known as mechano-transduction (109).

As cells proliferate, they become crowded and form cell-cell contacts and junctions (108). Cell-cell contact inhibition is among the upstream regulators of Hippo signaling, playing a central role in controlling the sub-cellular localization and activity of Yap/Taz (110).

Phosphorylation and localization assays performed by Zhao and colleagues (110) demonstrated that Hippo signaling becomes progressively activated with increasing cell density. Under high-density conditions, phosphorylation of Yap at Ser127 corresponding to enhanced Lats1/2 activation, markedly increased, as did sequestration of phosphorylated Yap in the cytoplasm. Conversely, when cells were lower in confluence, Hippo signaling remained inactive and Yap localized primarily to the nucleus (110).

Upstream activators of Hippo signaling include the Neurofibromatosis type 2 (Nf2) tumor suppressor (Merlin in *Dm)* and Expanded (Ex), both of which are members of the Ezrin/radixin/moesin (ERM) family of actin-binding proteins (111, 112). Nf2 and Ex appear to promote the cytoplasmic retention and repression of Yap by Mst1/2 and Lats1/2 kinases. This effect occurs under high density conditions, suggesting that Nf2 may act upstream of the Hippo core kinases to activate them and thereby suppress Yap activity through Lats1/2 phosphorylation-mediated cytoplasmic sequestration (110). Taz contains a corresponding phosphorylation site at Ser89; therefore, it is likely regulated through cell-cell contact inhibition in a manner similar to Yap.

Gene expression microarray and quantitative PCR (qPCR) analyses further revealed that Yap activity and cell density exert antagonistic regulation of gene transcription (110). Consistent with the role of nuclear Yap in promoting proliferation, cells expressing nuclear Yap were also positive for the proliferative marker Ki67. Moreover, stable expression of Yap maintained cells within the cell cycle even under high-density conditions, indicating that Yap hyperactivity can bypass contact inhibition, and the associated activation of Hippo signaling. These findings closely resemble those of Huang and colleagues (80) in *Dm,* wherein overexpression of Yki phenocopied loss-of-function mutations of genes encoding the core Hpo kinases. Together, these

results demonstrate that elevated Yap/Yki activity can circumvent the suppressive regulation of Hippo signaling, driving sustained proliferation irrespective of upstream activation of the pathway.

ECM stiffness represents another physical cue in which the Hippo pathway responds. Physical attachment to ECM *in vivo* is necessary for cell survival and proliferation. This attachment activates Ras homologous (Rho)-GTPases, such as RhoA, which promote the polymerization of globular actin (G-actin) into filamentous actin (F-actin) (113). Actin polymerization facilitates the translocation of Yap to the nucleus through cytoskeleton reorganization (113, 114). Hippo signaling appears to become activated at the level of Lats1/2 when cells become detached from the ECM. In this case, Yap becomes primarily cytoplasmic and therefore inactive, possibly due to Hippo-mediated apoptosis of unanchored cells that are no longer attached to the ECM. In this way, the Hippo pathway helps to ensure tissue integrity during development (114). Furthermore, when cells are attached to a soft ECM, Yap/Taz remain largely cytoplasmic because the cells experience low levels of mechanical signaling (109, 113). On the other hand, stiff ECM promotes their nuclear localization due to more mechanical stimulation and cytoskeletal tension (113).

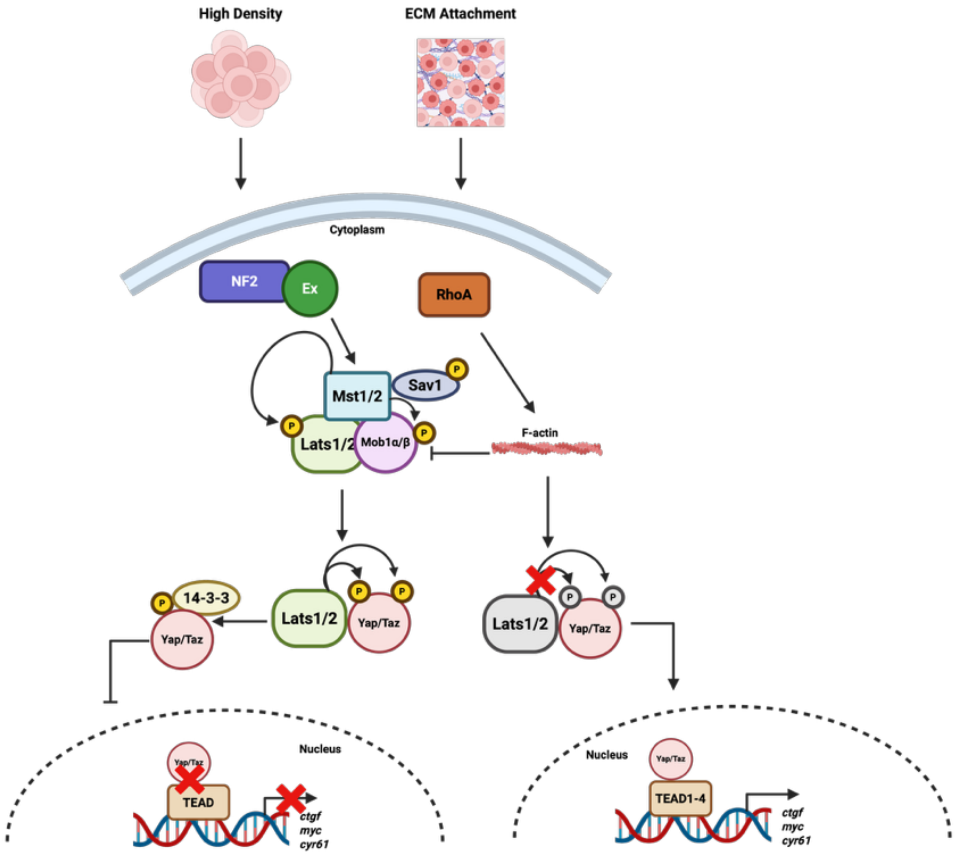

Figure 10. **Upstream mechano-regulation of the Hippo signaling pathway.** Hippo signaling is regulated by upstream signals from cell-cell contact and extracellular matrix (ECM) stiffness. The Hippo pathway transmits these signals into an intracellular cascade to ultimately regulate the co-activating function of Yap/Taz on gene transcription. When cells are at a high density, Lats1/2-mediated phosphorylation of Yap Ser127 is enhanced resulting in its cytoplasmic retention. Under these conditions, Nf2 and Ex activate Lats1/2 to regulate Yap sub-cellular localization and activity. Conversely, the attachment of cells to the ECM activates RhoA to promote F-actin polymerization and the translocation of Yap/Taz to the nucleus. In this case, Hippo signaling remains inactive unless cells become detached from the ECM. *Created in Biorender.com.*

iv. Regulation of Yap/Taz by Hippo-independent signaling

Aside from the Lats1/2 kinases, additional PPXY domain-containing proteins regulate Yap/Taz activity through Hippo-independent mechanisms; they do not require Lats1/2-mediated phosphorylation to sequester Yap/Taz in the cytoplasm. One such protein family are the Angiomotins (Amots), comprising of Angiomotin (Amot) and its related proteins Angiomotin-

like 1 (AmotL1) and Angiomotin-like 2 (AmotL2) (115). Amots associate with the actin cytoskeleton and localize to cell-cell junctions, where they interacts with tight-junction proteins such as zonula occludens-1 (ZO-1), a process that is enhanced in high-density conditions (115, 116).

As previously discussed, Yap/Taz accumulates in the cytoplasm through Hippo kinase-mediated phosphorylation under high-density conditions, when cell-cell contact is increased. However, Chan and colleagues (117) identified Amots as novel regulators of Yap/Taz sub-cellular localization, independent of Hippo kinase activity (117). Amots bind to the WW-domain of Yap/Taz through their PPXY motifs, and this interaction persists even with a Taz S89A mutant construct, in which the Lats1/2 phosphorylation site (Ser89) is mutated to alanine, and thus cannot be phosphorylated or sequestered to the cytoplasm by 14-3-3 proteins. This mutation results in a constitutively active, nuclear form of Taz. However, in the presence of Amot, Taz S89A was no longer retained in the nucleus; instead, it became localized to the cytoplasm.

Furthermore, ectopic expression of Taz S89A upregulated the canonical Taz-Tead target genes *ctgf* and *cyr61*. Conversely, these elevated levels were significantly attenuated with the co-expression with Amot or AmotL1 (117). Collectively, these findings that Amots negatively regulate Taz S89A, which is not regulated by Hippo kinases, supports a model in which Amot suppresses Taz activity in a Hippo-independent manner.

Although Amot was shown to repress Yap/Taz through direct interaction and sequestration, another research group identified a Hippo-dependent mechanism as well. Under high-density (low-serum) conditions, Amot was shown to function downstream of Hippo signaling, where it is phosphorylated by Lats1/2 at its Ser175. This phosphorylation event facilitated its interaction with 14-3-3 and atrophin-1 interacting (AIP4) proteins. Phosphorylated

Amot subsequently enabled Yap Ser127 phosphorylation, and subsequent ubiquitination and degradation, thereby suppressing *ctgf* expression (118). The discrepancy between these studies suggests that Amot may act as a negative regulator of Yap/Taz activity through multiple mechanisms, operating either in coordination with, or independently, of Hippo signaling.

Uncharacterized protein regulators of Yap/Taz were also identified in a proteomic screen conducted by Wang and colleagues (119). Using tandem affinity purification coupled with mass spectrometry analysis, the authors identified a previously unrecognized Yap-interacting protein called coiled-coil domain-containing protein 85C (CCDC85C). Similar to the Amot proteins, CCDC85C has been shown to co-localize with ZO-1 at cell-cell junctions (120). CCDC85C also binds Yap through its PPXY motif, located within the middle region of the protein. This motif directly interacts with both WW-domains of Yap. Formation of the CCDC85C-Yap complex promoted the translocation of Yap to the cytoplasm, and repressed Yap-dependent co-activation of Tead-mediated gene transcription (119).

Consistent with its localization to tight-junction complexes (120) and functional similarity to Amot-Taz complex (117), these findings suggest that CCDC85C interacts with Yap as a negative regulator to sequester it in the cytoplasm (119). These findings support a model of regulation (Figure 11) where Yap/Taz are recruited by Amots or CCDC85C to cell-cell junctions.

This retains Yap/Taz in the cytoplasm and represses their co-activating role of gene transcription, independent of canonical Hippo kinase regulation.

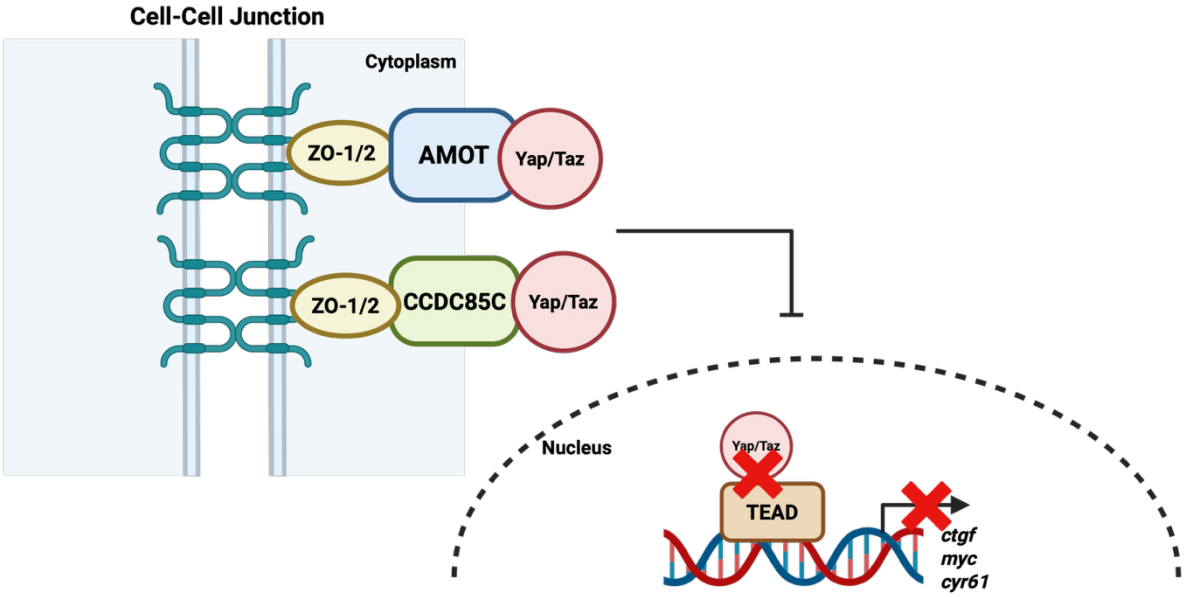

Figure 11. **Hippo-independent regulation of Yap/Taz by tight-junction proteins.** Amots and CCDC85C are Yap/Taz-binding proteins that regulate Yap/Taz activity through direct protein-protein interactions, independent of the canonical Hippo signaling cascade. Both Amots and CCDC85C promote cytoplasmic localization of Yap/Taz irrespective of Lats1/2-mediated phosphorylation(117, 119, 120). These proteins localize to cell-cell junctions at the plasma membrane; therefore, they may sequester Yap/Taz in the cytoplasm by recruiting them to tight-junction protein complexes. *Created in Biorender.com.*

IV. Structure of Yap/Taz/Yki

The mammalian transcriptional co-activators, Yap/Taz, closely resemble the *Dm* co-activator Yki in both function and structure. Yap shares approximately 31% amino acid sequence similarity with Yki (80), and 45% similarity with Taz (97). Yki and Yap/Taz exist in different species; therefore, they are orthologous to each other (105). In contrast, Yap and Taz are paralogous, as they exist within the same species and have similar, yet non-redundant functions.

As shown in Figure 12, Yap and Taz possess a C-terminal coiled-coil domain implicated in protein-protein interactions (121). This coiled-coil region appears absent in Yki (97, 105).

Downstream of this region is the unstructured trans-activation domain that is necessary for Yap/Taz transcriptional co-activating functions, enabling them to facilitate the transcriptional output of their interacting transcription factors (105, 121, 122). Yki, Yap, and Taz contain a conserved N-terminal binding domain that mediates interaction with Tead (in mammals) and Sd (in *Dm*). These N-terminal regions in Yap and Taz share approximately 77% sequence similarity (100, 102). This suggests that, similar to Yap which has been reported to interact with all four Tead transcription factors, Taz can also bind to Tead1-4 (102). In these transcription factor-binding domains, there are serine residues that serve as phosphorylation sites for Lats1/2 (or Wts in *Dm*), which promote subsequent 14-3-3 protein binding. The specific serine residues differ: Yki is phosphorylated at its Ser168, Yap at its Ser127, and Taz at its Ser89. These phosphorylation sites reside within the Tead-binding domain of Yap/Taz. Therefore, it has been proposed that 14-3-3 proteins and Tead transcription factors likely compete for Yap/Taz binding (100).

Despite the strong evolutionary conservation between Yki, Yap, and Taz, notable structural differences exist. Yap is the largest of the three proteins, with a molecular weight of approximately 65 kilodaltons (kDa) and a length of 488 amino acids. It contains additional regions that expand its capacity for protein-protein interactions, including a N-terminal proline-rich domain and a Src homology 3 (SH3)-binding domain that mediates its interaction with the SH3 domain of Yes kinase (97, 121). These regions are absent in Taz, which has a molecular weight of approximately 45 kDa and consists of 400 amino acids (97), and in Yki which is approximately 47 kDa with 418 amino acids (80).

Both Yap and Yki contain two WW-domains, whereas Taz has only one (80, 81, 93, 97). Yap isoforms with one WW-domain have also been reported (123). Each WW-domain is

approximately 38 amino acids long and is required for interactions with the PPXY motifs of Lats1/2, Amot, and other Yap/Taz-regulatory proteins and transcription factors (121, 124). The Yap/Taz WW-domains contain histidine-x-arginine-x-x-serine (HXRXXS) motifs; three are present in Yki, five in Yap, and four in Taz (95, 98, 110). These HXRXXS motifs serve as Lats1/2 phosphorylation sites that ultimately control Yap/Taz nucleocytoplasmic shuttling and thereby regulate their transcriptional activity (95, 98). Yap/Taz also contain a C-terminal Post-synaptic density, Discs large, ZO-1 (PDZ)-binding motif that mediates nuclear localization as well as additional interactions with PDZ-domain-containing proteins, including tight junction proteins such as zonula occludens-2 (ZO-2) (105).

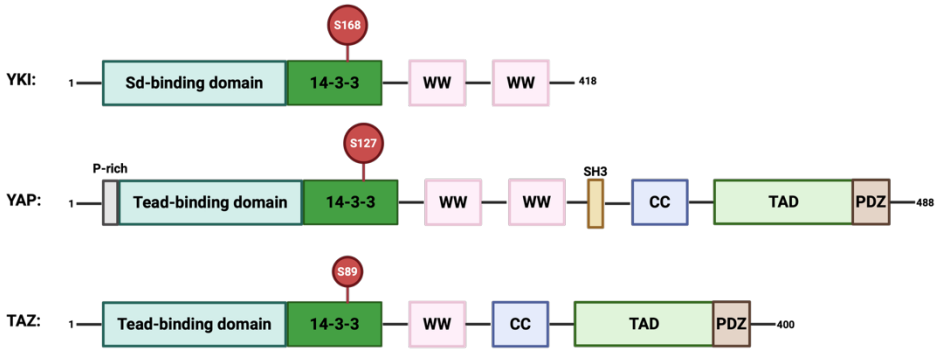

Figure 12. **Structural comparison between Yorkie, Yap, and Taz.** Yap is the largest of the three proteins consisting of additional protein-binding sites, including a N-terminal proline-rich domain and a SH3-binding motif. Both Yorkie (Yki) and Yap have two WW-domains, whereas Taz contains only one. These WW-domains are essential for binding to PPXY motif-containing proteins such as Lats1/2 (or Wts). All three co-activators share a Tead/Sd-binding domain that mediates the interaction with Tead/Sd transcription factors. Within this region, there is a serine residue that serves as a phosphorylation site for Lats1/2 or Wts. It acts as a docking site for 14-3-3 proteins, whose binding facilitates the cytoplasmic sequestration of Yki, Yap, and Taz. Yap/Taz share a PDZ-binding domain to interact with proteins that contain a PDZ domain. *Created in Biorender.com.*

V. Regulation of Yap/Taz by Hippo signaling in striated muscle development and regeneration

Hippo signaling plays a critical role in embryogenesis, beginning as early as the inception of the blastocyst stage at E3.5 in mouse and E5 in humans (13, 15, 125). As previously discussed, the morula comprises of small inner cells surrounded by larger outer cells, which ultimately give rise to the ICM and TE of the blastocyst. A 2009 study by Nishioka and colleagues (126) demonstrated that differential Hippo signaling between the inner and outer cells governs the first cellular fate specification in embryonic development, determining whether a cell contributes to the ICM or TE.

At the 8-cell stage, Yap is detectable in the nuclei of all blastomeres. As development proceeds, Yap remains nuclear in cells fated to form the TE but becomes cytoplasmic in cells destined for the ICM. This cytoplasmic sequestration of Yap is driven by Lats1/2-mediated phosphorylation. Nuclear localization of Yap in the outer cells restricts Tead4 activity to the nascent TE. The resulting Yap-Tead4 complex promotes the upregulation of TE-specific genes such as *cdx2* (126). Importantly, Taz can compensate for *yap* knockdown, supporting normal TE development, whereas a simultaneous knockdown of both *yap* and *taz* results in embryonic lethality before the morula stage, prior to the ICM/TE cell fate decision (126). Therefore, Hippo regulation of the Yap/Taz-Tead complex and its activation on downstream effector genes is essential for cell fate specification during early embryonic development.

Yap/Taz exhibit distinct expression patterns during embryonic development (127). The non-redundant functions of Yap and Taz are reflected in the specific embryonic tissues where each is upregulated. QPCR analysis in *Xenopus tropicalis* embryos revealed that Yap is highly expressed in the notochord, hindgut, and tailbud, whereas Taz expression is enriched in the

presomitic mesoderm and migrating hypaxial myoblasts. Notably, Taz mRNA was not detected in differentiated muscle cells, suggesting a role for Taz in myoblast proliferation (127). Furthermore, Tead1/3 expression has been detected in the somites and heart, among other tissues (128). Collectively, these findings indicate that Yap/Taz-Tead complexes are prominent in developing skeletal and cardiac muscle.

The co-activating functions of Yap/Taz are central to skeletal and cardiac muscle formation. Independent research groups investigated the developmental role of Yap through targeted disruption of the *yap* gene in *Danio rerio* (zebrafish) and mouse embryos (129-131). *Yap* knockdown resulted in embryonic lethality or delayed development, accompanied by increased apoptosis in the head and caudal regions, and reduced cellular proliferation compared to wild-type embryos (129, 131). Yap was found to be particularly important for somitogenesis, the early phase of skeletal muscle development, as *yap*-deficient embryos exhibited morphological deformities, including a shortened body axis and absence of tail formation (129, 130). The severity of these phenotypes was dependent on the extent of Yap ablation (129). Moreover, MyoD expression was elevated in *yap* mutants, and somitogenesis occurred at an accelerated rate, potentially explaining the premature body axis formation observed (129). In addition, *yap* mutants also displayed shallow primitive heart fields relative to the linear heart tube observed in the control embryos (129). Taken together, these cellular and structural abnormalities in *yap*-deficient zebrafish embryos highlight the essential role of Yap in coordinating cellular proliferation, apoptosis, and overall muscle formation, to ensure the proper development of skeletal and cardiac muscle.

These results further showcase the non-redundant roles of Yap and Taz, as Taz expression did not increase in response to *yap* deletion, in order to compensate for *yap* loss. *Yap* mutants

continued to exhibit defects in myogenesis and cardiogenesis, even with *taz* expression intact (129, 131). Therefore, Taz could not rescue these mutant phenotypes, further suggesting that while Yap and Taz share structural and functional similarities, they may not regulate later developmental processes in the same manner as observed during the pre-implantation stage.

To investigate Yap/Taz function in striated muscle differentiation and regeneration, studies have also examined their roles using the C2C12 myogenic model. During normal myogenic progression, myoblasts proliferate to confluence, withdraw from the cell cycle, differentiate, and fuse into multinucleated myotubes. This transition is recapitulated *in vitro* upon transfer to a low-serum differentiation medium, containing reduced levels of growth factors and mitogens (132). In C2C12 cells, both Hippo core kinases and the downstream effector Yap, were shown to be expressed in both proliferative skeletal myoblasts and differentiated myotubes (132).

In proliferative myoblasts, Yap cytoplasmic localization and Ser127 phosphorylation, hallmarks of active Hippo signaling, were found to be low, with Yap predominantly localized to the nucleus (132). This suggests that Yap remains in its active form, promoting proliferation and maintaining cells within the cell cycle. However, upon serum withdrawal and induction of differentiation, Yap Ser127 phosphorylation and cytoplasmic localization increased dramatically. Moreover, ectopic expression of constitutively active Yap S127A repressed myogenic differentiation and myotube formation. Expression of key myogenic transcription factors such as MyoG and Mef2, as well as myotube markers MyHC and muscle creatine kinase (MCK), were significantly decreased, indicating that differentiation had been impaired with activated Yap expression (132). Similar results were also observed in MuSCs (133).

These findings indicate the possibility that Hippo signaling is repressed during the proliferative phase of the myogenic differentiation program. This has important implications in

both skeletal muscle development and regeneration, whereby nuclear Yap acts to facilitate myoblast proliferation and drive tissue growth. Then, upon differentiation cues, active Hippo signaling phosphorylates and represses Yap, thereby preventing further proliferation to mediate cell cycle exit and eventually, terminal differentiation. In this manner, skeletal muscle development and regeneration may proceed to form multinucleated myofibers characteristic of mature muscle tissue.

Not only is Yap essential for skeletal muscle development and regeneration, but it also plays a critical role in cardiogenesis, where it promotes the proliferation of embryonic cardiomyocytes, thereby contributing to proper heart size. *Yap* deficiency in mice results in embryonic lethality around E10.5 due to insufficient cardiomyocyte proliferation and increased apoptosis (134-136). Mutant mice displayed severe cardiac defects, including ventricular wall thinning and dilated cardiomyopathy, ultimately leading to heart failure and death (134, 135). Importantly, simultaneous deletion of both *yap* and *taz* causes lethality within one day after birth, accompanied by severe cardiac abnormalities (134), indicating that Yap/Taz possess overlapping, and potentially redundant roles in regulating cardiomyocyte proliferation and heart growth during cardiac development.

Mechanistically, Yap appears to stimulate cardiomyocyte proliferation in part by modulating IGF and Wingless integration site (Wnt) signaling pathways. Yap has been shown to upregulate IGF1 receptor expression, activating phosphatidylinositol 3 (PI3K) and Akt kinases. This in turn inhibits glycogen synthase kinase 3β (GSK-3β), thereby stabilizing β-catenin to drive proliferation (134, 135). These findings highlight the complexity of Hippo signal transduction, which integrates cross-talk with many other regulatory pathways, like IGF and Wnt

signaling in cardiac development, to coordinate organogenesis and tissue homeostasis throughout the body.

Similar to Yap, Taz is expressed in both proliferative skeletal myoblasts and differentiated myotubes (132, 137), and its expression levels are higher than those of Yap in skeletal muscle (137). Unlike Yap, however, there is conflicting evidence regarding the role of Taz in myogenesis. One study reported that ectopic Taz expression accelerates myotube formation and increases the expression of myogenic markers, including MyHC. Additionally, Taz was demonstrated to promote myogenic differentiation through its interaction with MyoD, which enhances MyoG expression (138). Taz expression was upregulated *in vivo* following freeze-induced skeletal muscle injury, implicating Taz in skeletal muscle regeneration.

By contrast, work from our research group identified a repressive role for Taz in skeletal myogenesis. Tripathi et al. (137) found that Taz was primarily nuclear in proliferative myoblasts, where it functions as a co-activator with Tead transcription factors. This finding is consistent with the role of Taz in promoting myoblast proliferation, which may explain the post-injury increase in Taz observed in the earlier study, ultimately reflecting its pro-proliferative activity rather than a direct pro-differentiation function.

Importantly, Taz was found to negatively regulate myogenic differentiation through cross-talk with Wnt and transforming growth factor-beta (TGF-β) signaling pathways. We previously showed that the downstream effectors, Smad7 and β-catenin, promote myogenesis in cooperation with MyoD (139). However, Taz interacts with and inhibits Smad7, resulting in repression of MyoD, MyoG, and MCK (139), all of which were upregulated in the pro-myogenic study (138). Conversely, *taz* depletion enhanced the expression of these markers, in a Smad7-dependent manner (137). In line with this inhibitory role, Taz nuclear localization decreased

during differentiation, potentially relieving this repressive effect (137). Together, these findings suggest that Taz exerts context-dependent roles in skeletal myogenesis, promoting or inhibiting the differentiation program depending on its interacting partners and the surrounding transcriptional milieu. Nonetheless, Taz remains a key co-activator in proliferative myoblasts and a regulator of myogenic differentiation, both of which are essential for skeletal muscle development and regeneration.

Taz has been shown to modulate cellular proliferation, minimize cell-cell contact inhibition, and promote EMT. These cellular processes collectively contribute to skeletal myogenesis and cardiogenesis (96). Similarly, during skeletal muscle regeneration, activated MuSCs must migrate to the site of injury to initiate muscle repair. Ectopic expression of Taz was found to markedly alter epithelial cell morphology, resulting in disorganized cell-cell junctions and an increase in mesenchymal markers such as F-actin and N-cadherin, accompanied by a reduction in the epithelial marker E-cadherin (96). Importantly, Taz activation enhanced cell migration and motility during wound closure (96). Cumulatively, these findings indicate that Taz functions as a key regulator of skeletal muscle development and regeneration by promoting cellular proliferation, tissue growth, and EMT-dependent cell motility required for muscle growth and repair.

The specific role of Taz in cardiac muscle development has only recently begun to be defined and remains less well characterized than that of Yap. Taz regulation of EMT has been implicated in cardiogenesis. A 2018 study (140) demonstrated that Taz is required for cardiac trabeculation, a developmental process necessary for proper ventricular contractility and heart function (141). Cardiac trabeculation begins when a subset of compact layer-residing cardiomyocytes proliferate and migrate from the epithelial ventricular wall to form the trabecular

layer (141, 142). Impaired trabeculation results in embryonic lethality or adult cardiomyopathy (143).

Taz has been shown to be primarily localized to the nuclei of ventricular cardiomyocytes (140). *Taz*-deficient zebrafish hearts exhibited reduced trabeculation, less trabecular cardiomyocytes, and decreased cardiomyocyte proliferation. Notably, nuclear Taz levels were high in cardiomyocytes of the compact layer and lower in those present in the trabecular layer, suggesting that Taz may influence the fate decision to remain within the compact epithelial sheet or under EMT-driven delamination to form trabeculae (140). These findings suggest that Taz may regulate cardiomyocyte proliferation and EMT in cardiac muscle development and this is essential for proper heart wall and ventricle formation.

VI. Dysregulation of Yap/Taz in striated muscle and their potential use as therapeutic targets in striated muscle pathology

Dysregulated Yap/Taz activity is strongly linked to tumorigenesis and malignancy, reflecting their fundamental roles in promoting cellular proliferation, survival, growth, and motility (144). Accordingly, Yap/Taz have emerged as central therapeutic targets across multiple cancer types, including myogenic tumors such as rhabdomyosarcomas (144). Rhabdomyosarcoma is characterized as a soft tissue sarcoma associated with the skeletal muscle lineage, characterized by maintenance of an undifferentiated state, despite its expression of myogenic transcription factors such as MyoD (145, 146). Notably, nuclear Taz expression has been shown to be elevated in alveolar rhabdomyosarcoma. Moreover, Taz inhibition suppressed tumor proliferation and tumor growth, and promoted apoptosis (147). These findings underscore the oncogenic potential of sustained Yap/Taz activation when organ growth regulation by Hippo signaling becomes disrupted.

In addition to cancer, cardiovascular disease remains a leading cause of morbidity and mortality worldwide (134, 148). Unlike skeletal muscle, post-natal cardiomyocytes permanently exit the cell cycle shortly after birth, rendering the adult heart largely incapable of regeneration. Consequently, injury from ischemic heart disease or myocardial infarction leads to irreversible cardiomyocyte loss, followed by replacement with non-contractile fibrotic tissue, ultimately resulting in reduced contractility, and progression to heart failure (134, 149).

Regenerative strategies, therefore, focus on re-activating post-natal cardiomyocyte proliferation to restore heart function after injury. Yap/Taz are promising therapeutic targets, as their activation stimulates cardiomyocyte proliferation, enabling replacement of dead cells with functional muscle, rather than fibrotic scar tissue. Additionally, Yap/Taz activity is responsive to mechanical cues, including cell-cell contact and ECM stiffness, both of which change dramatically following cardiac injury (150).

Gain-of-function experiments support this approach. Expression of constitutively active Yap S112A (human S127A) in mice has been shown to increase cardiomyocyte proliferation and leads to myocardial wall thickening (134, 135). Moreover, following myocardial infarction, Yap activation reduced scarring and loss of myocardial tissue, indicating that Yap can promote regenerative repair in cardiac muscle (134). These findings suggest that pharmacological inhibitors of Hippo kinases, thereby releasing Yap from phosphorylation and repression, may enhance cardiac muscle regeneration (151).

However, the therapeutic activation of Yap requires caution. Excessive Yap activity is associated with pathological cardiac hypertrophy. Human hypertrophic cardiomyopathy tissue displays elevated Yap expression, increased levels of Yap/Taz target genes such as *ctgf*, and reduced Yap Ser127 phosphorylation, consistent with Hippo inactivation. Experimentally, Yap

overexpression has been found to increase cell size of primary murine cardiomyocytes *ex vivo*, whereas Yap depletion prevents phenylephrine-induced hypertrophy (152). This hypertrophic phenotype appeared to be mediated by Yap-dependent activation of the IGF pathway; accordingly, PI3K and Akt inhibition prevented Yap-induced hypertrophy (152).

Additionally, Yap/Taz broadly promote cellular proliferation and suppress apoptosis across multiple tissues, consistent with the established role of the Hippo pathway as a central regulator of organ size (70). Consequently, therapeutic strategies, such as TDI-011536, aimed at activating Yap/Taz by inhibiting Lats1/2-mediated phosphorylation (153), must be carefully targeted to the heart, as systemic activation could disrupt overall homeostasis in other organs. Thus, although Yap/Taz activation can drive cardiac muscle regeneration, dysregulated or chronic Yap/Taz signaling may promote pathological hypertrophy, underscoring the need for precise, tissue-specific, and temporally controlled modulation of Yap/Taz activity in regenerative therapies.

Although skeletal muscle possesses a far greater regenerative capacity than cardiac muscle, this ability declines with age, and many pathological conditions including cancer-associated cachexia, all of which lead to progressive skeletal muscle atrophy. Muscular degeneration contributes significantly to morbidity, mortality, and reduced quality of life (8). Unexpectedly, sustained Yap activation has been linked to skeletal muscle wasting. In transgenic mice expressing constitutively active Yap, prolonged Yap expression resulted in 20-25% loss of total body weight and 34-40% reduction in skeletal muscle mass within 5 to 7 weeks, compared to control mice (154). Consistent with these degenerative phenotypes, myogenic markers expressed in muscle regeneration, such as Myf5, MyoG, and Pax7 were upregulated. Importantly, suppression of Yap activity rescued the muscle and body mass in these mice (154).

These findings indicate that unlike cardiac muscle, sustained Yap activation promotes skeletal muscle atrophy rather than hypertrophy, highlighting the necessity for precise, tissue-specific regulation of Yap/Taz signaling. In the context of skeletal muscle degeneration, therapeutic inhibition of Yap/Taz activity or their nuclear accumulation such as through Verteporfin (155), may help prevent muscular atrophy, while simultaneously limiting Yap/Taz-driven metastatic or proliferative behaviour of tumor malignancy.

VII. Yap/Taz Biomolecular Phase Separation

Biomolecular condensates are dynamic, membraneless cellular compartments formed by liquid-liquid phase separation (LLPS) (156). LLPS occurs within the aqueous environment of the cytoplasm or nucleoplasm, analogous to the formation of oil droplets in water. These condensates arise from weak and reversible multivalent interactions among proteins and nucleic acids, allowing specific molecules to become locally concentrated within distinct microenvironments. LLPS is often mediated by intrinsically disordered regions (IDRs), coiled-coil domains, and other structural motifs that enable proteins to engage with multiple binding partners simultaneously. By enriching selected factors in close proximity, condensates enhance the efficiency of biochemical reactions, including transcriptional activation (157).

Both Yap/Taz contain IDRs and coiled-coil domains, suggesting they possess the structural capacity to under phase separation. However, accumulating evidence indicates that Taz, but not Yap, forms phase-separated biomolecular condensates to recruit and concentrate general transcriptional machinery and sequence-specific transcription factors (158). *In vitro,* Taz has been shown to spontaneously form condensates, and their size is dependent on protein concentration, ionic strength, and temperature, whereas Yap does not phase separate under the same conditions (158). Chimeric experiments revealed that the coiled-coil domain of Taz is

necessary for condensate formation. Taz proteins containing the Yap coiled-coil domain lost the ability to form nuclear puncta, while Yap containing the Taz coiled-coil domain exhibited robust puncta formation (158). Additionally, the PDZ-binding motif of Taz has also been implicated in nuclear puncta formation, as its deletion disrupts puncta assembly and reduces Taz-mediated transcriptional activation (97).

Two hallmark characteristics of LLPS-based condensates are spherical morphology and fusion (159, 160). Our research group demonstrated that Taz satisfies both criteria within a skeletal muscle context (137). Tripathi et al. showed that 1) endogenous Taz forms nuclear puncta in proliferative myoblasts, 2) ectopically expressed fluorescent Taz forms spherical condensates in these cells, and 3) these condensates fuse in real-time (137), all of which suggest that Taz exhibits phase separation properties in a skeletal muscle context. Moreover, Taz condensates correlate with transcriptional activation, as they recruit Tead transcription factors and transcriptional elongation machinery, including cyclin-dependent kinase 9 (CDK9) and active RNA polymerase II (158). To our knowledge, the ability of Taz to form biomolecular condensates in cardiac muscle is not currently known.

Statement of Purpose

Organogenesis and tissue regeneration are essential events that rely on the co-ordinated regulation of cellular proliferation, survival, and differentiation to ensure that organs develop to their proper form and size. The Hippo signaling pathway is a central regulator of these processes, functioning as a critical control system for tissue growth and homeostasis. Taz, a downstream effector of this evolutionarily conserved pathway, is regulated by the Hippo core kinase cascade. When Hippo signaling is active, it acts as a growth-suppressive pathway, promoting Taz phosphorylation and its cytoplasmic sequestration, thereby preventing its transcriptional activity. Conversely, when Hippo signaling is inactive, Taz remains unphosphorylated and translocates to the nucleus, where it functions as a transcriptional co-activator or co-repressor, depending on its interacting partners. Although Taz has previously been characterized as a pro-myogenic activator, our research demonstrates that Taz promotes myoblast proliferation while repressing myogenic differentiation. As Taz lacks a DNA-binding domain, it exerts its regulatory function through protein-protein interactions with DNA-binding transcription factors. Notably, these interactions can be further modulated by liquid-liquid phase separation, enabling Taz to form biomolecular condensates that concentrate transcriptional machinery at specific enhancer/promoter elements to enhance transcriptional output. Hyperactivation of Taz, and its paralog Yap, is highly associated with pathological muscle conditions, including cardiac hypertrophy and skeletal muscle atrophy and degeneration. Thus, elucidating the molecular mechanisms that govern Taz activity in striated muscle is essential for identifying therapeutic targets to treat life-threatening diseases such as cardiovascular disorders and heart failure. Since a foundational aspect of TAZ function is heterologous protein interactions, ***the purpose of this study was to identify and characterize the regulation of Taz by protein-protein interactions in striated muscle.***

Chapter II: Regulation of Taz (WWTR1) by protein-protein interactions in striated muscle

Stephanie Sansone, Tetsuaki Miyake, and John C. McDermott

Author contributions

Experimental Design

Stephanie Sansone, Tetsuaki Miyake, and John C. McDermott

Drafting manuscript

Stephanie Sansone

Editing manuscript

Stephanie Sansone, John C. McDermott

Conducting experiments

Stephanie Sansone:	Figure 1 A-D
	Figure 2 A-B
	Figure 3 A-E
	Figure 4 A-E
	Figure 5 A-D
	Figure 6 A-J
	Figure 7 A-D
	Figure 8 A-D
	Figure 9 A-I

Abstract

Tissue growth depends on cellular proliferation, survival, and differentiation. Hippo signaling controls these processes by regulating transcriptional co-activators Yap/Taz. Taz function is context-dependent, including repression of myogenic differentiation. Taz does not bind DNA; its activity is determined by interacting partners. To discover functional regulators of Taz, nuclear FLAG-affinity purification and LC-MS/MS were performed in HEK293T, identifying 57 interactors (33 unique; 24 ≥3-fold enriched). Among these, transcription factor Yin-Yang1 (YY1) was prioritized. Biochemical analyses revealed YY1 binds Taz at/near its Tead-binding domain, with Tead1 enhancing this interaction. YY1 repressed Taz-mediated transcription on a Tead-responsive reporter. In proliferating myoblasts, YY1 increased phospho-Taz (Ser89), its Hippo-inactivated form. Taz formed LLPS-driven nuclear condensates, during which YY1 was excluded from the nucleus. During differentiation, YY1-mediated stabilization of phospho-Taz (Ser89) was not observed, and Taz and YY1 co-operatively repressed myogenic gene expression. Collectively, these findings identify YY1 as a regulator of Taz function in striated muscle.

Introduction

Skeletal and cardiac muscle are fundamental to human physiology, each fulfilling distinct roles necessary for survival. Skeletal muscle, which enables posture, respiration, energy metabolism, and voluntary movement, also exhibits a remarkable capacity for regeneration (1, 5). Muscle satellite cells (MuSCs) mediate this repair process by activating, proliferating, and differentiating to replace damaged myofibers (7). In contrast, cardiac muscle serves a singular but vital function: the continuous pumping of blood to sustain oxygen and nutrient delivery to all tissues (1). Post-natal cardiomyocytes, however, possess only limited regenerative capacity; thus, cardiac injury leads to fibrosis and progressive loss of function (12). Disruption of striated muscle homeostasis contributes to pathologies including skeletal muscle atrophy and degeneration, hypertrophic cardiomyopathy, and rhabdomyosarcomas.

A major regulator of striated muscle growth, regeneration, and homeostasis is the Hippo signaling pathway, an evolutionarily conserved kinase cascade that governs cellular proliferation, survival, and differentiation to ensure proper organ size. The pathway was first defined in *Drosophila melanogaster* (*Dm*), where loss of the core kinases Hippo (Hpo), Warts (Wts), Salvador (Sav), and Mats, resulted in tissue overgrowth due to delayed cell cycle exit and impaired apoptosis (71, 72). In mammals, the orthologous kinases Mst1/2 and Lats1/2, together with adaptor proteins Sav1 and Mob1α/β, phosphorylate the transcriptional co-activators Yap and Taz (*Dm* Yki), leading to their cytoplasmic sequestration by 14-3-3 proteins or proteasomal degradation (81, 93). When Hippo signaling is inactive, unphosphorylated Yap/Taz translocate to the nucleus and promote gene expression by transcription factors, such as Tead1-4 (*Dm* Sd), driving transcriptional programs that control tissue growth (104-106).

The functional importance of Yap/Taz is evident in striated muscle development. *Yap* deficiency in zebrafish and mouse embryos results in increased apoptosis, reduced proliferation,

and severe morphological defects, including truncated body-axis formation, impaired somitogenesis, and ventricular wall thinning leading to heart failure (129-131). Conversely, activated Yap promotes cardiomyocyte proliferation and myocardial growth (134-136). Taz also influences striated muscle development, particularly through cell proliferation, migration, and EMT, processes critical for early skeletal myogenesis and cardiac trabeculation (96, 161).

However, Yap and Taz are not functionally redundant, despite often being considered interchangeable. During pre-implantation development, *taz* can compensate for *yap* loss in ICM/TE specification (126); yet during somitogenesis and cardiogenesis, *taz* cannot rescue *yap*-deficient phenotypes (129, 131), demonstrating context-dependent differences in their regulatory roles. Moreover, while Yap consistently promotes proliferation and inhibits myogenic differentiation (132), Taz displays dual regulatory capacity: acting either as a co-activator or co-repressor depending on its interacting partners and cellular environment (137, 138). Importantly, Taz, but not Yap, undergoes liquid-liquid phase separation to form nuclear condensates that spatially concentrate transcriptional machinery (137, 158).

Given these differences, grouping Yap and Taz together potentially obscures critical, muscle-specific regulatory roles of Taz. To address functional protein interactions with TAZ directly, we performed FLAG-affinity purification coupled with LC-MS/MS proteomic analysis to identify potential Taz-interacting partners. This interactome analysis revealed both known and previously unrecognized Taz-interacting proteins, including the transcription factor Yin-Yang1 (YY1), which has previously established roles in skeletal and cardiac muscle gene regulation. Here, we validate the Taz-YY1 interaction in striated muscle and investigate the role of this interaction on regulating Taz function in both skeletal and cardiac muscle. The characterization

of the Taz-YY1 interaction provides new insight into how protein interactions regulate TAZ transcriptional networks that modulate striated muscle development and regeneration.

Materials and Methods

Cell line culture

C2C12 mouse myoblasts and human embryonic kidney (HEK)-293T cells were acquired from the American Type Culture Collection (ATCC). Cells were cultured in growth media (GM) comprising of high-glucose Dulbecco's modified Eagle's medium (DMEM, Gibco), 10% fetal bovine serum (FBS) supplemented with 1% penicillin-streptomycin (Invitrogen, ThermoFisher Scientific). Myotube formation of C2C12 cells was induced by substituting GM with differentiation medium (DM), consisting of DMEM supplemented with 2% FBS and 1% penicillin-streptomycin. Cell cultures were maintained in an incubator set at 95% humidity, 5% carbon dioxide (CO_2), and 37°C. Cells were replenished with fresh medium every 48 hours.

Neonatal rat primary cardiomyocyte isolation

Primary neonatal rat cardiomyocytes (PCMs) were isolated from 1-3 days old Sprague Dawley rats using the Neonatal Cardiomyocyte Isolation System (Worthington Biochemical Corp). Pups were immediately euthanized by decapitation following cervical dislocation, in accordance with Animal Care Committee (ACC) guidelines. Whole hearts were extracted, ventricles isolated from atria and subsequently digested with trypsin (#LK003225) and collagenase (#LK003245). Cells were re-suspended in DMEM/F-12 GM (Gibco) supplemented with 10% FBS and 1% penicillin-streptomycin (Invitrogen, ThermoFisher Scientific). The isolated cells were then pre-plated for 1 hour in an incubator set at 95% humidity, 5% CO_2, and 37°C, to remove non-cardiomyocytes. Cardiomyocytes were seeded on 1% gelatin-coated plates overnight in DMEM/F12 GM. The following day, cells were replenished with fresh media for subsequent experimentation, unless transfected.

Transfections

To facilitate ectopic protein expression in HEK293T cells, polyethyleneimine (PEI) was utilized for transfection at a PEI:DNA ratio of three. For transient transfection of C2C12 and PCMs, Lipofectamine 2000 (Invitrogen) was used at a Lipofectamine 2000:DNA ratio of three, allowing efficient uptake of DNA plasmids by the cells. All cells were harvested 24 hours post-transfection, unless differentiated. In this case, C2C12 cells were replenished with fresh GM the following day after transfection. They were recovered for 24 hours, then transferred to DM to be harvested at various time points in the myogenic program.

Plasmids

Expression plasmid for FLAG-TAZ was gifted by Jeff Wrana (Addgene #24809). Kunliang Guan gifted the following plasmids: HA-TAZ (Addgene #32839), MYC-TEAD4 (Addgene #24638), MYC-TEAD1 (Addgene #33109), and MYC-TEAD1 (Y406A) (Addgene #33047). FLAG-YY1 (Addgene #104396) and HA-YY1 (Addgene #104395) were gifted by Richard Young. Additionally, pcDNA-FLAG was gifted by Michele Pagano (Addgene #210342). For functional reporter assays, HOP-Flash (Addgene #83467) and HIP-Flash (a mutant of HOP-Flash serving as a negative control) (Addgene #83466) were gifted by Barry Gumbiner. *Myogenin-promoter* luciferase plasmid was a gift from Michael Chin (Addgene # 134722). *Muscle creatine kinase-promoter* luciferase plasmid was described previously.(162) *Renilla luciferase* plasmid (pRL-Renilla) was purchased from Promega. As reported elsewhere,(163) an eYFP-TAZ construct was created by amplifying Taz open reading frame by PCR with EcoRI and XhoI incorporated primers and inserted into pcDNA3-eYFP. HA-TAZ deletion constructs were created by manually deleting increasing amounts of the N-terminus from the HA-TAZ plasmid (Addgene #32839)

obtained from Kunliang Guan. eYFP-TAZ and all HA-TAZ deletion constructs were cloned by Dr. Tetsuaki Miyake from the McDermott research group.

Cell Harvesting

All cells were harvested using NP-40 lysis buffer, unless designated for functional reporter assays. For these gene reporter assays, 1X reporter lysis buffer (Promega, #E4030) was utilized. Cells were washed three times with cold phosphate-buffered saline (PBS) before adding in lysis buffer. The collected lysates were then vortexed at 4°C for 20 to 30 minutes. Subsequently, lysates were centrifuged at 10 000 revolutions per minute (RPM) for 10 minutes at 4°C. The supernatant containing soluble protein was then collected.

Western Blot (WB) Analysis

Protein samples were denatured in 3X SDS loading buffer at 100°C for 10 minutes. Subsequently, these samples were loaded onto 10% SDS-PAGE gels and electrophoresed at approximately 100V for a duration ranging from one hour to one hour and 30 minutes. The gels were then transferred to a polyvinylidene fluoride (PVDF) membrane (Millipore) in 1X transfer buffer. Following the transfer, the membranes were blocked in 5% blocking buffer for one hour on an orbital shaker at room temperature. Primary antibody solutions were prepared by diluting the necessary antibody in 1% blocking buffer at an antibody:1% blocking buffer ratio suggested by the antibody manufacturer. In most cases, the ratio of antibody:1% blocking buffer was 1:1000. Membranes were incubated with primary antibody solutions overnight at 4°C on a rocker. For secondary antibody incubation, secondary antibody solutions were prepared by diluting the respective horseradish peroxidase (HRP)-conjugated secondary antibody in 1% blocking buffer at an antibody:1% blocking buffer ratio of 1:2000. After washing the membranes three times with TBS supplemented with 0.1% Tween® 20 (TBS-T) for 5 minutes each, the

membranes were incubated with the secondary antibody solution for 1 hour on an orbital shaker at room temperature. Following another round of washing with TBS-T, protein/antibody immune-complexes were detected by incubating membranes in HRP substrate (Bio-Rad or ThermoFisher Scientific) and exposing them to an iBright CL1500 Imaging System (ThermoFisher Scientific).

Antibodies

Antibodies for YAP/TAZ (rabbit, monoclonal, #D24E24), HA (rabbit, polyclonal, #C29F4), MYC (mouse, monoclonal, #9B11), α-tubulin (rabbit, polyclonal, #2144S), c-Myc (rabbit, monoclonal, #5605), and Histone H3 (rabbit, polyclonal, #9715S) were sourced from Cell Signaling Technology. Antibodies for β-actin (mouse, monoclonal, #SC-47778) and MCK (mouse, monoclonal, SC-365046) were purchased from Santa Cruz Biotechnology. FLAG antibody (mouse, monoclonal, #F3165) was purchased from Sigma-Aldrich. Antibodies for YY1 (rabbit, polyclonal, #22156-1-AP), YY1 (mouse, monoclonal, #66281-1-Ig), TAZ (mouse, monoclonal, #66500-1-Ig), FLAG (rabbit, polyclonal, #20543-1-AP), MYC (mouse, monoclonal, #60003-2-Ig), and cardiac troponin-T (mouse, monoclonal, #68300-1-Ig) were from Proteintech. Phospho-TAZ (Ser89) antibody (rabbit, polyclonal, #PA5-105066) was purchased through Invitrogen, ThermoFisher Scientific. HA (mouse, monoclonal, #anti-HA rMs-IgG1), MyoG (mouse, monoclonal, #F5D) and MyHC (mouse, monoclonal, #MF20) antibodies were purchased from Developmental Studies Hybridoma Bank (DSHB).

Immunoprecipitation (IP) Analysis

For FLAG immunoprecipitation (IP), anti-FLAG M2 magnetic beads (Sigma #M8823) underwent three washes with PBS prior to incubation with 500 to 1000 μg of HEK293T cell extracts on a rotator overnight at 4°C. On the following day, the beads were washed three times

with PBS to eliminate nonspecific protein binding. Immunoprecipitation samples were then eluted in 100 ug/mL 3X FLAG peptide solution (Sigma #4799) on a rotator at room temperature for one hour. Subsequently, eluates were subjected to WB analysis (refer to WB analysis protocol mentioned above). For endogenous IPs, Dynabeads Protein G (Invitrogen, #10003D) were washed three times with PBS before incubation with YY1 antibody (mouse, monoclonal, #66281-1-Ig), diluted to 1µg for 30 µL of beads in 500 µL of 1X PBS. Antibody-bead complexes were incubated on a rotator at 4°C overnight. Beads were washed three times with 1X PBS to remove unbound antibody. Dynabeads were then incubated with 3 to 5 mg of C2C12 myoblast, C2C12 differentiated for one day, and PCM extracts on a rotator at 4°C overnight. Beads were then washed with 1X PBS to remove nonspecific protein binding. Subsequently, samples were eluted with SDS Loading Buffer for 10 minutes at 100°C and analyzed by WB analysis (refer to WB analysis protocol).

Gene Reporter Assays

Transcriptional reporter assays were conducted using Firefly luciferase reporter plasmids in conjunction with expression constructs. *Renilla* luciferase plasmid (Promega, pRL-Renilla) was used as an internal control for transfection efficiency. Following washing with cold PBS, cells were harvested in 1X reporter lysis buffer (Promega #E4030) (refer to Cell Harvesting protocol mentioned above). *Firefly* luciferase enzymatic activity was measured using a luminometer (Berthold, Lumat LB) for each of the three technical replicates per experimental condition, using *Firefly* luciferase assay substrate (Promega #E1501) and *Renilla* luciferase assay substrate (Promega #E2820). *Firefly* luciferase activity values were normalized to *Renilla* luciferase activity for each of the technical replicates within an experimental condition. Finally, activity

from each technical replicate was expressed as fold activation relative to the control, with an average fold activation calculated for each experimental condition.

Live-cell Imaging

C2C12 cells were seeded on glass-bottom dishes (MatTek). After transfection with eYFP-TAZ and GFP constructs, cells were replenished with fresh GM for at least 3 hours. Cells were counterstained with 4',6-diamidino-2-phenylindole (DAPI) and imaged immediately using a Zeiss Observer Z1 confocal fluorescent microscope equipped with Yokogawa CSU-X1 spinning disk. Image acquisition was performed by AxioCam MRm camera (Zeiss), and the images were processed using Zen 2.5 (blue edition) software (Zeiss).

Immunofluorescence (IF)

C2C12 cells were seeded on glass-bottom dishes (MatTek). Cells underwent three consecutive 5-minute washes with cold PBS on an orbital shaker at room temperature. Following this, cells were fixed with 4% paraformaldehyde at room temperature for 10 minutes. Subsequently, cells were subjected to another three washes with PBS and permeabilized on ice with ice-cold 90% methanol for 10 minutes on orbital shaker at room temperature. The cells were then incubated with IF blocking buffer (5% FBS in PBS) for one hour at room temperature. Primary antibody solutions were prepared by diluting the necessary antibody in IF blocking buffer at an antibody: IF blocking buffer ratio of 1:200. Following incubation with IF blocking buffer, cells were washed with cold PBS for 2 minutes prior to incubation with primary antibody solution overnight at 4°C. The following day, cells were washed three times with cold PBS to eliminate unbound antibody. Secondary antibody solutions were prepared by diluting the respective Alexa Fluor-conjugated secondary antibody (Life Technologies) in IF blocking buffer at an antibody: IF blocking buffer ratio of 1:200. Cells were then incubated with secondary antibody solutions for

one hour at room temperature. After another three washes with PBS, cells were counter-stained with DAPI. Cells were imaged using a Zeiss Observer Z1 confocal fluorescent microscope equipped with Yokogawa CSU-X1 spinning disk. Image acquisition was performed by AxioCam MRm camera (Zeiss), and the images were processed using Zen 2.5 (blue edition) software (Zeiss).

Cell Fractionation

FLAG-TAZ (Addgene #24809) constructs were transfected in HEK293T cells, and the cells were harvested the following day using cold PBS (refer to Transfection and Cell Harvesting protocol mentioned above). Subsequently, nuclear and cytoplasmic-enriched fractions were isolated using the NE-PER kit (ThermoFisher Scientific #78833), following the manufacturer's instructions.

Mass Spectrometry (MS) Preparation

FLAG-TAZ (Addgene #24809) was transfected into HEK293T cells and fractionated the following day (refer to Transfection and Cell Fractionation protocols above). Anti-FLAG M2 magnetic beads (Sigma #M8823) were washed three times with PBS. For the experimental condition, 1000 μg of nuclear fraction was incubated with 25 μL of anti-FLAG M2 magnetic beads (Sigma #M8823) overnight in a rotator at 4°C. For the out-competition control, 1000 μg of nuclear fraction with 10 μL of 500 μg/mL 3X FLAG peptide was incubated with 25 μL of anti-FLAG M2 magnetic beads (Sigma #M8823) overnight in a rotator at 4°C. On the following day, the beads were washed with 500 μL of 0.1% acetic acid for one to two minutes in a rotator at 4°C. Subsequently, the beads were neutralized with 50 mM ammonium bicarbonate (NH_4HCO_3) and reduced by 1M Dithiothreitol (DTT) to a final concentration of 10 mM, followed by heating at 60°C for 30 minutes. The beads were then alkylated by iodoacetamide and incubated in the dark at room temperature for 15 minutes. Additional 1M DTT was added to a final concentration

of 40 mM. Proteins in the sample (pH = 7.5 to 8.5) were then digested off the beads by 1 mg/mL trypsin and incubated overnight at 37°C. On the subsequent day, supernatants were transferred into a new tube. The prepared samples underwent analysis using the TimsToF Pro 2 (Bruker) instrument with liquid chromatography-tandem mass spectrometry (LC-MS/MS), conducted by the MS Facility at YSci core at York University.

Results

Proteomic Taz interactome study conducted by FLAG-affinity purification coupled with LC-MS/MS

Taz is an important regulator of gene expression, despite its lack of direct DNA-binding activity. Thus, Taz function and target gene specificity are determined through protein-protein interactions with sequence-specific DNA-binding transcription factors and transcriptional complex components (164). The function of Taz is dynamic; it acts either as a co-activator or co-repressor depending on the composition of these transcriptional networks. Furthermore, Taz uniquely undergoes liquid-liquid phase separation, forming biomolecular condensates that spatially organize transcriptional machinery and modulate gene expression programs (137, 158). Therefore, we reasoned that defining the Taz interactome is necessary to understand its transcriptional regulation in the nucleus.

For this purpose, we aimed to characterize Taz-protein interactors in nuclear-enriched fractions of a human embryonic cell line (HEK293T). Utilizing a FLAG-affinity purification method developed by Valdez-Sinon and colleagues (165), we immobilized Taz as the bait protein on anti-FLAG magnetic beads. We competitively eluted the bait using excess 3X FLAG peptide as a corresponding control. FLAG-TAZ was ectopically expressed in HEK293T cells, and nuclear- and cytoplasmic-enriched fractions were prepared prior to affinity capture. Affinity

purification was performed only on the nuclear fractions. This approach eliminated the need to transfer the immobilized bait to a secondary target lysate, thereby reducing the potential for cross contamination between samples and streamlining the proteomic analysis. We then coupled this purification assay with on-bead trypsinization and LC-MS/MS. A schematic of our proteomic screen workflow is shown in Figure 1A. Efficient ectopic expression and subsequent nuclear/cytoplasmic fractionation was confirmed by immunoblotting, using Histone H3 as a nuclear marker and alpha-tubulin (α-tubulin) as a cytoplasmic marker (Figure 1B).

Datasets were processed by filtering out non-specific interactions with less than threefold enrichment (Intensity $Score_{FLAG\text{-}TAZ}$ / Intensity $Score_{Control}$). This threshold was selected based on: 1) a previously established interactome screen from our group (166), and 2) recovery of known, high-confidence TAZ interactors at ≥ threefold enrichment in the FLAG-TAZ sample. Proteins detected exclusively in the FLAG-TAZ precipitate (and thus having infinite enrichment) were classified as "unique", whereas proteins meeting the ≥ threefold enrichment cutoff were categorized as "enriched". This analysis yielded 57 candidate nuclear Taz interactors, consisting of 33 unique proteins and 24 enriched proteins (Figure 1C).

Network analysis was performed using Cytoscape to identify functional clusters (Figure 1D). Node colour intensity reflects enrichment values in the MS list, with red indicating unique or highly enriched interactors; asterisks (*) denote interactors detected exclusively in the FLAG-TAZ eluate. Only pertinent networks to our study are shown. Notably, the dataset contained established Taz-interacting proteins, including components of the Hippo pathway (Tead1/3), membrane-associated proteins (Amot, AmotL1, AmotL2, Mpdz, Patj, Mpp5/Pals1, and TJP2/ZO-2), nuclear pore complex components (Nup160, Nup62, Nup155, and Nup153), and NuRD chromatin remodeling complex subunits (Mta1). Additionally, the dataset included other

unique and highly enriched protein interactors not shown here, including Prmt5, a member of the same Protein-Arginine methyltransferase family as Prmt4/Carm1, which we recently identified as a novel Taz interactor (166), as well as proteasomal subunits Psma4 and Psmc4. Imperative to our study, the MS analysis identified a unique protein, Yin-Yang1 (YY1), found entirely in the FLAG-TAZ eluate. YY1 is a DNA-binding transcription factor with well-established functions in skeletal and cardiac muscle, and a recently identified binding partner of Taz (167). A full list of the 57 protein candidates is available in Appendix I.

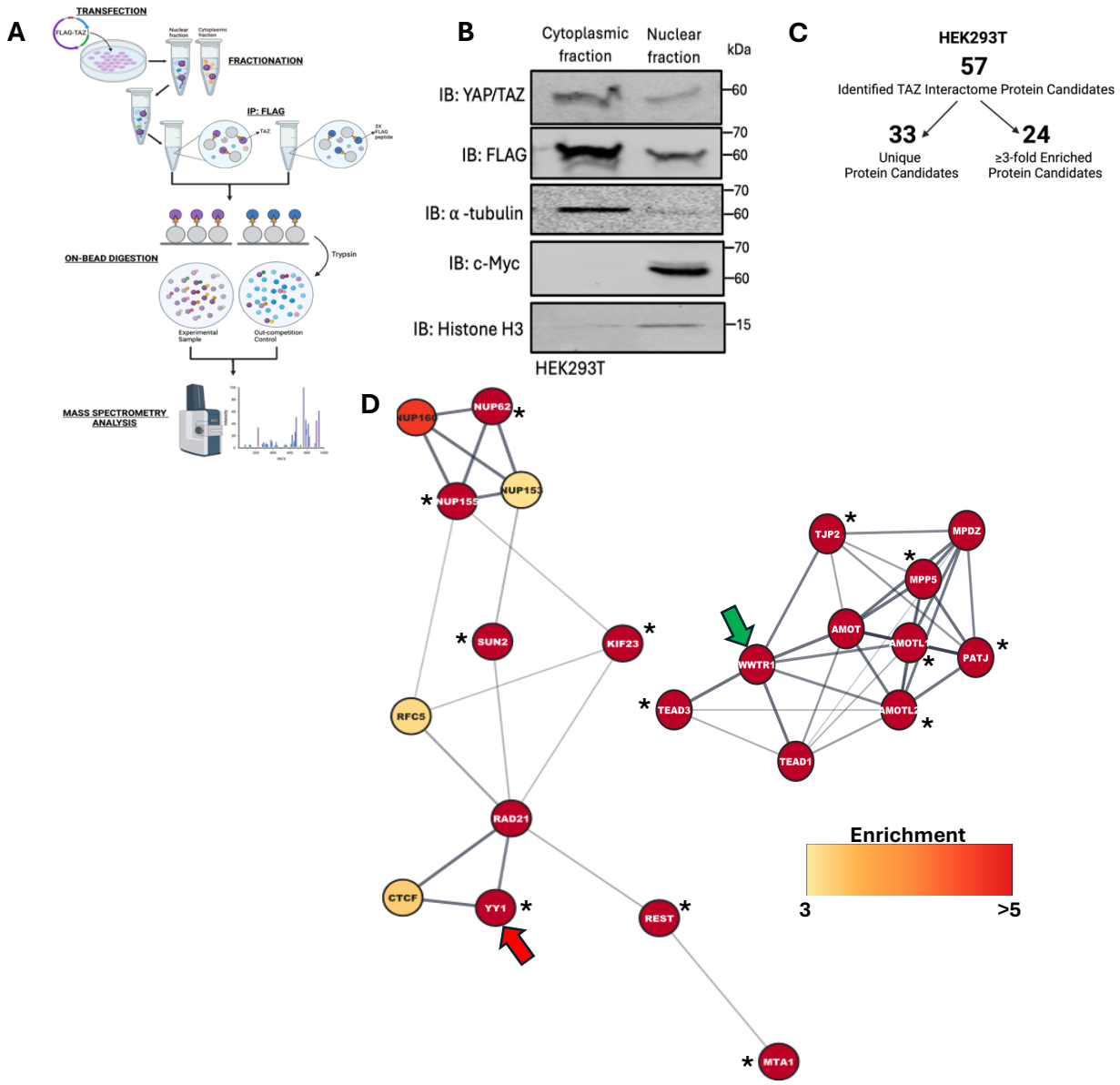

Figure 1. **Proteomic interactome study of potential Taz-interacting proteins in HEK293T cells. (A)** Schematic overview of FLAG-affinity purification method to identify potential interactors of Taz in a nuclear-enriched HEK293T extract. **(B)** Western blot analysis confirming the nuclear/cytoplasmic sub-cellular fractionation of HEK293T cells prior to FLAG-affinity purification. Protein levels of endogenous YAP/TAZ and FLAG-TAZ ectopic expression in cytoplasmic and nuclear-enriched fractions were assessed. α-Tubulin and Histone H3 were used as cytoplasmic and nuclear markers, respectively. **(C)** Flow chart indicating the number of total, unique, and ≥3-fold-enriched Taz protein partner candidates identified in the interactome screen. **(D)** Proteomic networks depicting Taz/WWTR1 (green arrow) with HIPPO signaling proteins, and YY1 (red arrow). Networks were created using Cytoscape software. Colour of nodes correspond to enrichment of protein candidates in the Taz interactome list based on intensity scores from the mass spectrometry analysis.
* Unique proteins to TAZ-immunoprecipitation condition.

Bioinformatic analysis of Taz interactome protein candidates

Bioinformatic analysis of the Taz interactome dataset was performed to identify biological processes and molecular functions associated with the protein candidates identified in the screen. Gene Ontology (GO) enrichment analysis was used to generate an enrichment score (-log(p-value)) for each significantly represented molecular function and biological process, reflecting the confidence that these proteins contribute to the corresponding category. Figure 2A presents a graphical summary of the molecular functions (orange) and biological processes (purple) relevant to transcriptional regulation, which is a central focus of this study.

Molecular functions enriched in the dataset included DNA binding, transcription cis-regulatory region binding, transcription regulatory region nucleic acid binding, sequence-specific double-stranded DNA binding, transcription factor binding, transcription regulator activity, protein-macromolecule adaptor activity, and DNA-binding transcription factor binding. Enriched biological processes included: Hippo signaling, protein localization, cell differentiation, gene expression, positive regulation of DNA-templated transcription, multicellular organism development, regulation of gene expression, cell cycle, regulation of apoptotic process, and negative regulation of DNA-templated transcription.

Figure 2B highlights specific Taz-interactors that are significantly associated with these GO terms. Node colour corresponds to the enrichment score, with yellow indicating lower significance and red indicating higher significance. Notably, Taz is associated with transcription regulator activity, Hippo signaling, positive and negative regulation of DNA-templated transcription, and cell differentiation, consistent with the established dual role of Taz as both a co-activator and co-repressor in transcriptional control.

Importantly, the bioinformatic analysis identified YY1 as a Taz-interacting protein significantly associated with transcription regulator activity, DNA-binding transcription factor binding, positive and negative regulation of DNA-templated transcription, and cell differentiation. This functional overlap, its exclusive presence in the FLAG-TAZ sample, and its well-established expression in striated muscle, together position YY1 as a biologically relevant candidate for further investigation into the mechanism by which it modulates Taz-dependent transcriptional programs in striated muscle.

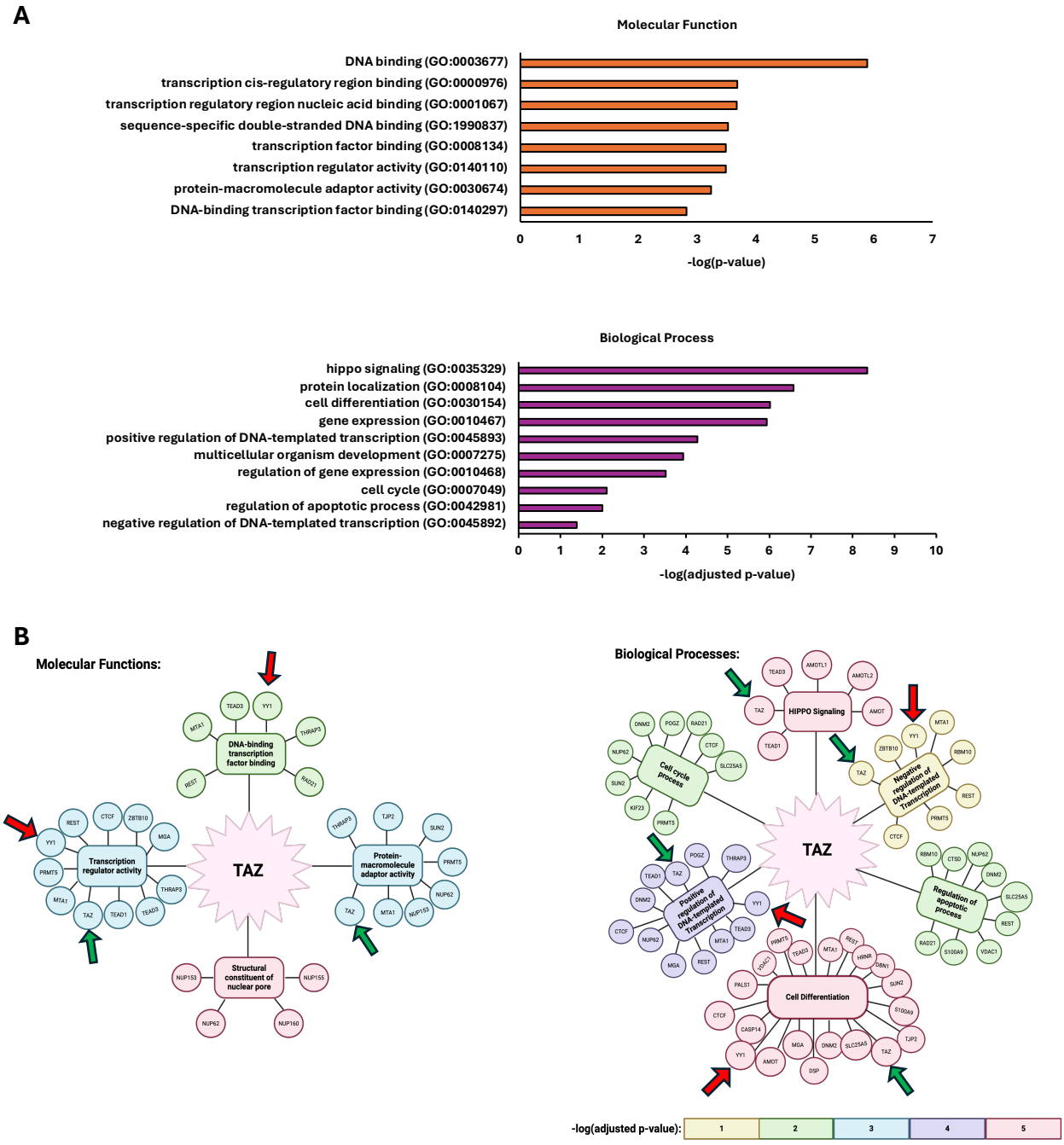

Figure 2. **Bioinformatic analysis of identified protein candidates from TAZ interactome screen. (A)** Bar graph depicting Gene Ontology (GO) terms of interest and corresponding enrichment scores (-log(p-values)). **(B)** Proteins identified in the Taz interactome categorized by GO molecular functions and biological processes, with enrichment scores indicated by colour (yellow = 1; red = 5). Taz (green arrow) and YY1 (red arrow) are depicted with their associated GO terms.

YY1 interacts with Taz and represses Taz-mediated transcriptional activation

To validate YY1 as a Taz-interacting partner, FLAG co-immunoprecipitation experiments were conducted in HEK293T cells. Positive controls were established using the known interaction between Taz and the transcription factors Tead1/4 (Figure 3A). We confirmed the interaction between Taz and YY1 biochemically, through co-immunoprecipitation analysis of ectopically expressed FLAG-TAZ and HA-YY1 (Figure 3B). The reciprocal co-immunoprecipitation, using FLAG-YY1 and HA-TAZ constructs, further validated this interaction (Figure 3C).

Subsequently, we investigated whether YY1 influences the transcriptional co-activator properties of Taz on a Tead-responsive HOP/HIP-Flash luciferase reporter gene assay. A schematic of the HOP/HIP-Flash luciferase reporter system is shown in Figure 3D. As expected, ectopic expression of Taz strongly activated the Tead-responsive reporter. We observed that co-expression of YY1 significantly decreased the potent Taz-driven transcriptional activation in this assay. Efficient ectopic expression of HA-TAZ and FLAG-YY1 was confirmed by immunoblot analysis (Figure 3E).

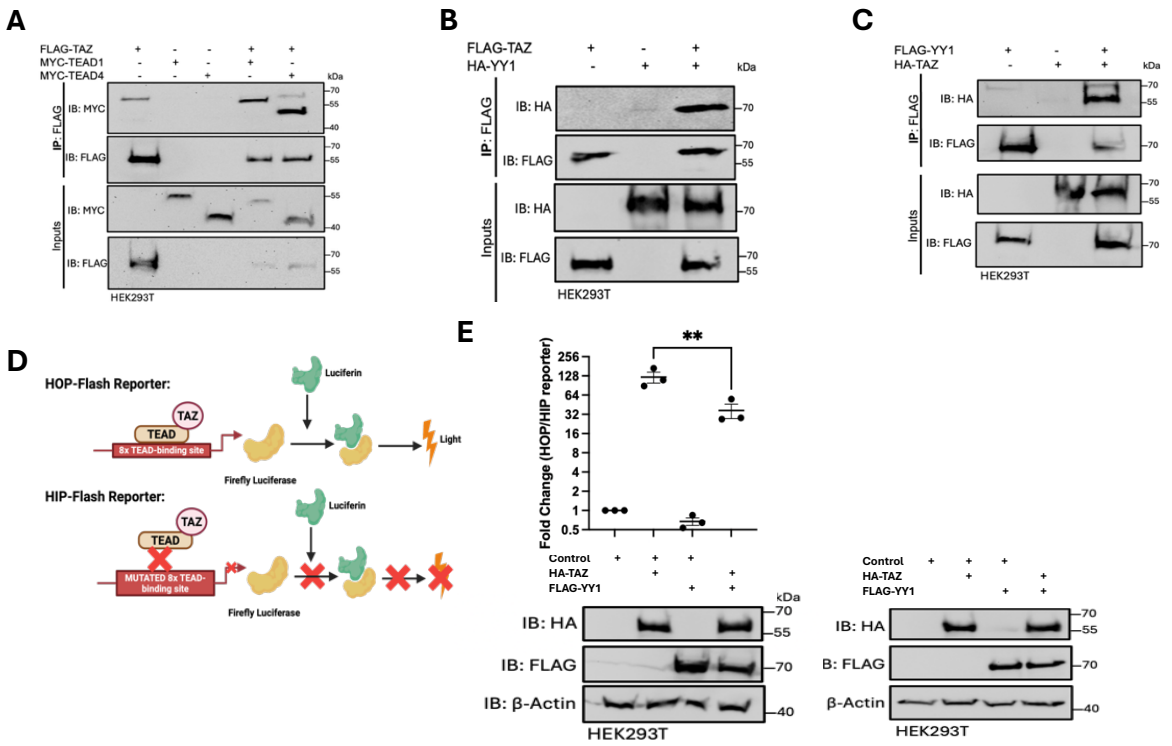

Figure 3. **Validation of biochemical and functional interaction between Taz and YY1. (A)** HEK293T cells were transfected with FLAG-TAZ with or without MYC-TEAD1/4, and MYC-TEAD1 or MYC-TEAD4 with or without FLAG-TAZ. Cells were harvested 24 hours post-transfection. Lysates were subjected to FLAG immunoprecipitation with anti-FLAG beads. Eluates were analyzed using immunoblotting for immunoprecipitated MYC-TEAD1/4 to serve as a positive control for subsequent co-immunoprecipitation analysis. **(B)** HEK293T cells were transfected with FLAG-YY1 with or without HA-TAZ, and HA-TAZ with or without FLAG-YY1. Cells were harvested 24 hours post-transfection. Lysates were subjected to FLAG immunoprecipitation with anti-FLAG beads. Eluates were analyzed using immunoblotting for immunoprecipitated HA-TAZ. **(C)** HEK293T cells were transfected with FLAG-TAZ with or without HA-YY1, and HA-YY1 with or without FLAG-TAZ. Cells were harvested 24 hours post-transfection. Lysates were subjected to FLAG immunoprecipitation with anti-FLAG beads. Eluates were analyzed using immunoblotting for immunoprecipitated HA-YY1. **(D)** Schematic of HOP-HIP-Flash luciferase gene reporter assay. **(E)** HA-TAZ alone and combined with FLAG-YY1 were ectopically expressed with the HOP-Flash *Firefly* luciferase reporter gene (normalized to Hip-Flash reporter as a negative control). *Renilla* luciferase served as a transfection control. An empty vector, pcDNA-FLAG, was used as a control for endogenous activity. Left panel: immunoblot showing ectopic expression of HA-TAZ and FLAG-YY1 in HOP-Flash system. Right panel: immunoblot showing ectopic expression of HA-TAZ and FLAG-YY1 in HIP-Flash system. Triplicate intra-experimental samples were analyzed, and the mean of these technical replicates constituted one biological replicate. This experiment was repeated three times and the data points on the graph indicate the biological replicates ($n=3$). Statistical analysis was conducted on PRISM from GraphPad 10.0. Using this software, a one-way ANOVA was conducted to test for statistical significance. Adjusted p-value ($^{**}P \leq 0.01$) is indicated for significance compared to the relevant control.

YY1 interacts with the Tead-binding domain of Taz, and this interaction is enhanced by Tead1

Having confirmed that YY1 interacts with Taz biochemically and represses TAZ function in a reporter gene system, we next sought to determine which region of Taz mediates this interaction. To this end, we performed FLAG co-immunoprecipitation assays using a series of N-terminal HA-TAZ deletion constructs. These deletion mutants were generated by progressively removing amino acids from the N-terminus of wild-type (WT) HA-TAZ (Figure 4A). Each HA-TAZ deletion construct was co-expressed with FLAG-YY1 in HEK293T cells and subjected to co-immunoprecipitation. Only HA-TAZ (WT) and HA-TAZ (Δ72-104) interacted with FLAG-YY1 (Figure 4B). These constructs share the Tead-binding domain, distinguishing them from the non-interacting deletion constructs. Thus, YY1 appears to bind Taz at or near its Tead-binding domain.

Tead transcription factors are well-characterized DNA-binding partners of Taz that recruit Taz to MCAT regulatory elements in the promoters of target genes in multiple tissues, including skeletal and cardiac muscle (102). Given that 1) YY1 represses Taz-mediated transcription on a Tead-responsive reporter, and 2) YY1 binds Taz at the Tead-binding domain, we hypothesized that the Taz-YY1 interaction may be facilitated by Tead proteins.

To test this possibility, FLAG-TAZ and HA-YY1 were co-expressed, and the eluate was probed for endogenous Tead1. Tead1 was detected in the Taz-YY1 immunoprecipitated complex (Figure 4C). Tead1 was selected based on its known expression in striated muscle and its established role in promoting Yap/Taz-dependent proliferation during muscle development and regeneration (168-170).

To further examine whether Tead1 mediates the interaction between Taz and YY1, co-immunoprecipitation experiments were performed with MYC-TEAD1 (WT) and a MYC-

TEAD1 (Y406A) mutant, in which a tyrosine 406 residue within the C-terminal Yap/Taz-binding domain is substituted with alanine, thereby disrupting Tead1-Taz binding (Figure 4D). As predicted, the MYC-TEAD1 (Y406A) mutation failed to interact with Taz (Supplementary Figure 1). Notably, YY1 associated with Taz to a greater extent in the presence of WT Tead1 compared to the Y406A mutant (Figure 4E). Quantification of YY1 enrichment (YY1/Taz ratio in the precipitate) is shown in Figure 4F. Together, these results indicate that the Tead-binding domain of Taz allows for YY1 binding, and Tead1 enhances this interaction.

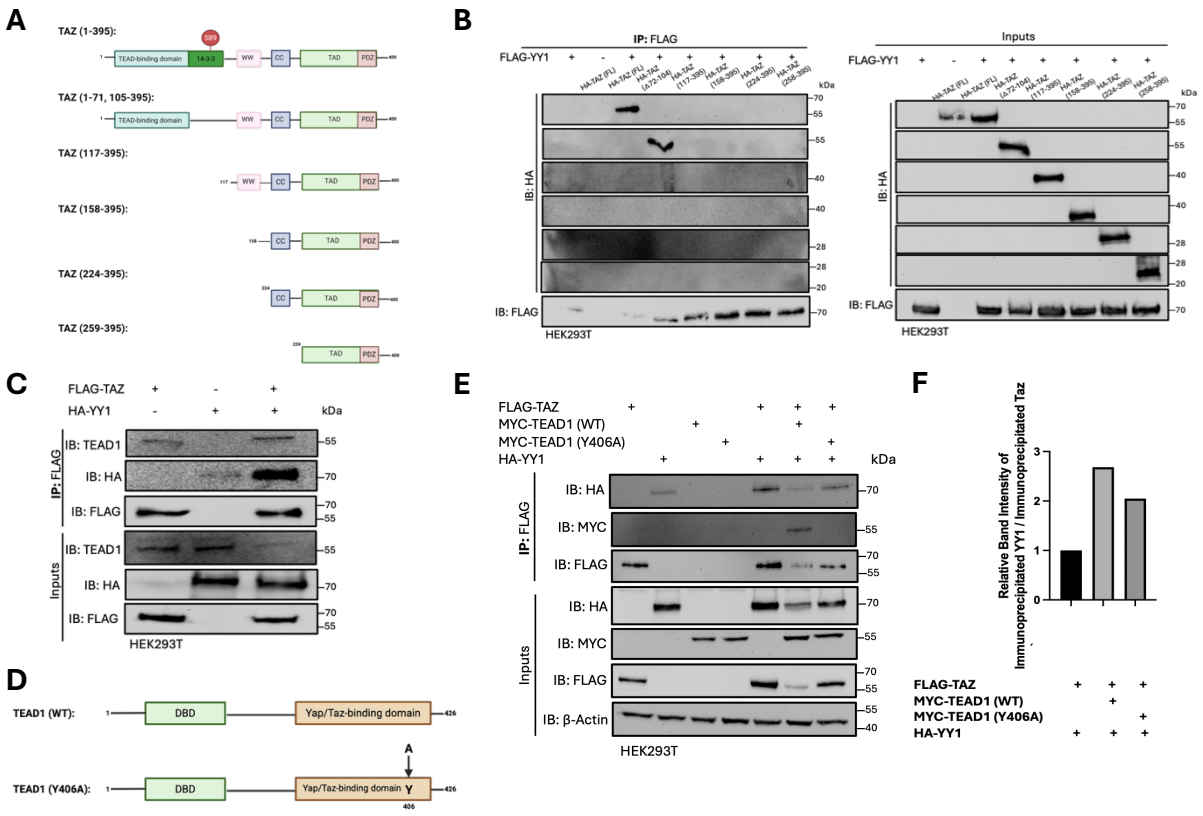

Figure 4. **YY1 binds to the TEAD-binding domain of Taz, and this interaction is enhanced by TEAD1. (A)** Schematic of Taz deletion constructs. Top panel: wild-type Taz, second panel: Taz (Δ72-104). **(B)** HEK293T cells were transfected with FLAG-YY1 with or without wild-type HA-TAZ, and HA-TAZ deletion constructs. Cells were harvested 24 hours post-transfection. Lysates were subjected to FLAG immunoprecipitation with anti-FLAG beads. Eluates were analyzed using immunoblotting for immunoprecipitated HA-TAZ constructs. This experiment was repeated for three biological replicates (*n=3*). **(C)** HEK293T cells were transfected with FLAG-TAZ with or without HA-YY1 alone, and HA-YY1 with or without FLAG-TAZ. Cells were then harvested 24 hours post-transfection. Lysates were subjected to FLAG immunoprecipitation with anti-FLAG beads. Eluates were analyzed using immunoblotting for immunoprecipitated TEAD1, HA-YY1, FLAG-TAZ. **(D)** Schematic of mutated TEAD1 (Y406A). DBD, DNA-binding domain. **(E)** HEK293T cells were transfected with FLAG-TAZ with or without HA-YY1 alone, and HA-YY1 with or without FLAG-TAZ. Cells were also transfected with MYC-TEAD1 (WT) or MYC-TEAD1 (Y406A) with or without FLAG-TAZ and HA-YY1. Cells were then harvested 24 hours post-transfection. Lysates were subjected to FLAG immunoprecipitation with anti-FLAG beads. Eluates were analyzed using immunoblotting for immunoprecipitated HA-YY1, MYC-TEAD1 (WT), MYC-TEAD1 (Y406A), and FLAG-TAZ. **(F)** Bar graph comparing the relative band intensity of HA-YY1 (HA-YY1/FLAG-TAZ) in FLAG-TAZ immunoprecipitated eluates, in the presence and absence of ectopically expressed MYC-TEAD1 (WT) or MYC-TEAD1 (Y406A). YY1 enrichment was normalized to the YY1-TAZ interaction observed without exogenous MYC-TEAD1 constructs. One biological replicate (*n=1*) was conducted for this experiment.

YY1 interacts and co-localizes with Taz in proliferating skeletal myoblasts

During skeletal muscle growth, Hippo signaling is repressed in proliferating myoblasts under high-serum conditions, allowing Taz to remain unphosphorylated and nuclear where it acts as a co-activator to promote cellular proliferation (137). Previously it was found that YY1 represses Taz-mediated transcriptional activation on a Tead-responsive HOP/HIP-Flash reporter in HEK293T cells, suggesting that YY1 can modulate Taz co-activator function. Therefore, whether YY1 also interacts with and regulates Taz activity in proliferative myoblasts was examined.

Initially, confirmation of the endogenous interaction between Taz and YY1 in C2C12 myoblast lysates using immunoprecipitation was carried out (Figure 5A). To determine whether Taz and YY1 localize to the same sub-cellular compartment, ectopically expressed FLAG-YY1 and eYFP-TAZ were visualized using immunofluorescence microscopy. Taz and YY1 co-localized in the nuclei of proliferating myoblasts (Figure 5B-C). Corresponding controls are displayed in Supplementary Figure 2A-B.

Finally, to assess whether YY1 influences Taz-mediated transcriptional activity in this cellular context, a HOP/HIP-Flash luciferase reporter assay was performed in C2C12 myoblasts. Co-expression of YY1 reduced Taz-driven reporter gene activation somewhat, although this decrease did not reach statistical significance under the conditions tested (Figure 5D).

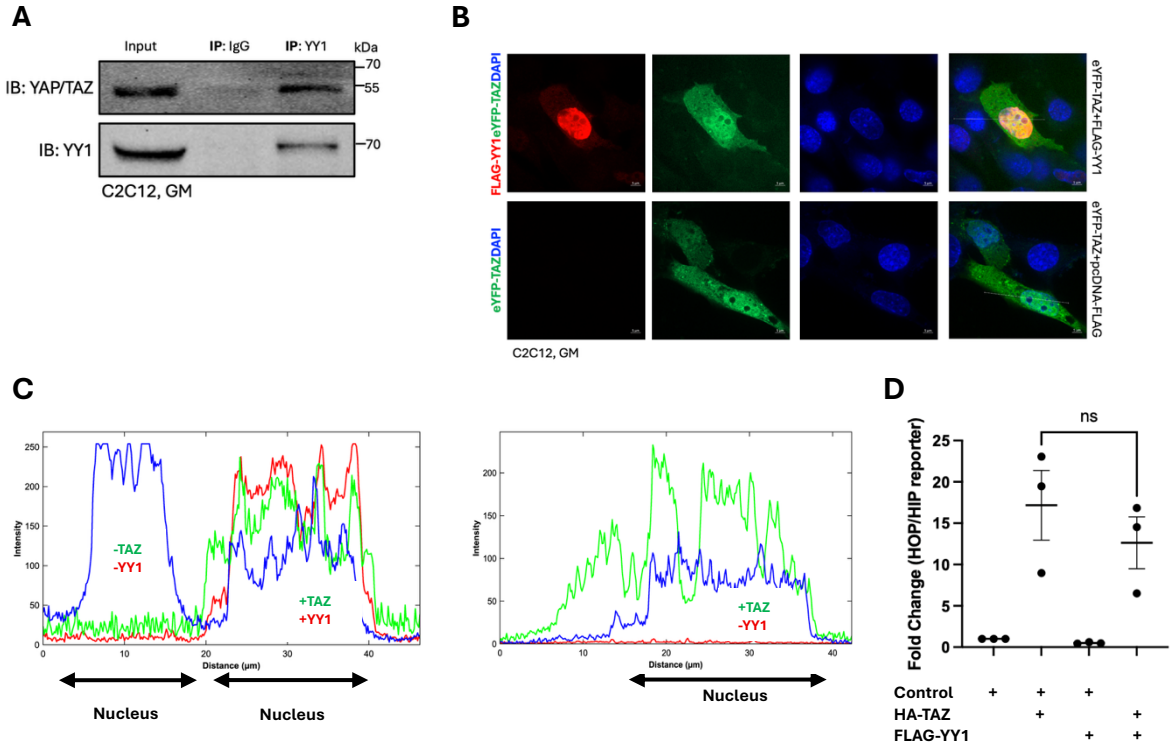

Figure 5. **YY1 interacts with and co-localizes with Taz in proliferating skeletal myoblasts.** **(A)** C2C12 myoblast extracts were subject to YY1 immunoprecipitation. Eluates were analyzed using immunoblotting for contents of immunoprecipitated Yap/Taz. **(B)** C2C12 myoblasts were transfected with eYFP-TAZ with or without FLAG-YY1 using an empty vector (pcDNA-FLAG) to equalize the amount of transfected DNA. Cells were fixed with 4% paraformaldehyde 24 hours post-transfection, and immunostained with anti-FLAG for FLAG-YY1 or pcDNA-FLAG (red), and counterstained with DAPI to indicate nuclei (blue). eYFP-TAZ fluorescence is shown in green. **(C)** Line scan analysis of fluorescence signal conducted using ImageJ. DAPI: blue, eYFP-TAZ: green, FLAG-YY1/pcDNA-FLAG: red. Left graph: eYFP-TAZ+FLAG-YY1 (top panel in (B)) and right graph: eYFP-TAZ+pcDNA-FLAG (bottom panel in (B)). **(D)** HA-TAZ alone and combined with FLAG-YY1 were ectopically expressed with the HOP-Flash *Firefly* luciferase reporter gene (normalized to Hip-Flash reporter as a negative control). *Renilla* luciferase served as a transfection control. An empty vector, pcDNA-FLAG, was used as a control for endogenous activity. Triplicate intra-experimental samples were analyzed, and the mean of these technical replicates constituted one biological replicate. This experiment was repeated three times and the data points on the graph indicate the biological replicates ($n=3$). Statistical analysis was conducted on PRISM from GraphPad 10.0. Using this software, a one-way ANOVA was conducted to test for statistical significance. ns, not significant.

YY1 interacts with Taz and represses the early myogenic program

When skeletal myoblasts reach confluence, they withdraw from the cell cycle and differentiate into multinucleated myotubes. This process is modeled *in vitro* by switching proliferating C2C12 myoblasts to low-serum differentiation medium. Under these conditions, cell-cell contact activates Hippo signaling, leading to phosphorylation of Taz at Ser89 and its cytoplasmic sequestration (110, 137). Our research group previously identified Taz as a co-repressor of myogenic differentiation, whereby it suppresses the transcription of myogenic-specific proteins such as MyoD, MyoG, and MCK (137). Based on this, the next objective was to determine the role of YY1 on Taz-mediated repression during myogenesis.

To establish the temporal relationship between Taz and YY1 during differentiation, we examined their protein expression patterns across a differentiation time course. Both YY1 and Taz were most highly expressed at the onset of differentiation (0 to 1 day), coinciding with increased phosphorylation of Taz Ser89 (Figure 6A). This suggests that Taz protein levels rise at the time when Hippo signaling becomes active, leading to its cytoplasmic retention and inactivation. Upregulation of MyoG and MyHC confirmed progression through the myogenic program.

Given that both proteins are expressed at the onset of differentiation, we tested whether YY1 and Taz interact under differentiation conditions using immunoprecipitation analysis. The endogenous interaction between YY1 and Taz at day 1 of differentiation was observed (Figure 6B). Next, an immunofluorescence analysis of C2C12 at different stages of differentiation was performed to determine the sub-cellular localization of YY1 and Taz during myogenesis. It was observed that YY1 and Yap/Taz appeared predominantly nuclear in proliferating myoblasts. Following the induction of MyoG protein expression, a well-characterized marker for the

initiation of myogenic differentiation, YY1 exhibited a progressive increase in its cytoplasmic localization in differentiating cells (Figure 6C-D). The localization of Taz, however, remained largely nuclear throughout differentiation, with a modest shift toward the cytoplasm observed on day 4 (Figure 6E-F; days 2 to 3 shown in Supplementary Figure 3A-D). Late differentiation (days 3 to 4) was marked by the expression of MyHC.

Next, whether YY1 functionally modulates Taz-mediated repression of myogenic gene expression was assessed using a *myog* promoter-driven gene reporter assay. Consistent with previous findings (137), we confirmed a trend toward Taz-dependent repression of a *myog* promoter-driven luciferase reporter at day 1 of differentiation (Figure 6G-H). YY1 expression significantly repressed the *myog* reporter activity, and co-expression of YY1 and Taz resulted in the greatest repression. Similar trends were observed using an *mck* promoter-driven reporter system (Supplementary Figure 4A-B).

To extend these findings to endogenous protein expression, we used immunofluorescence analysis to examine MyoG levels in differentiating C2C12 cells co-expressing eYFP-TAZ and FLAG-YY1. Both Taz and YY1 individually reduced the fraction of MyoG-positive cells, and co-expression produced the strongest decrease (Figure 6I). Quantification of the percentage of MyoG-positive transfected cells relative to total transfected cells is shown in Figure 6J. Collectively, these results support a model in which YY1 interacts with Taz during early differentiation to cooperatively repress the expression of myogenic transcription factors.

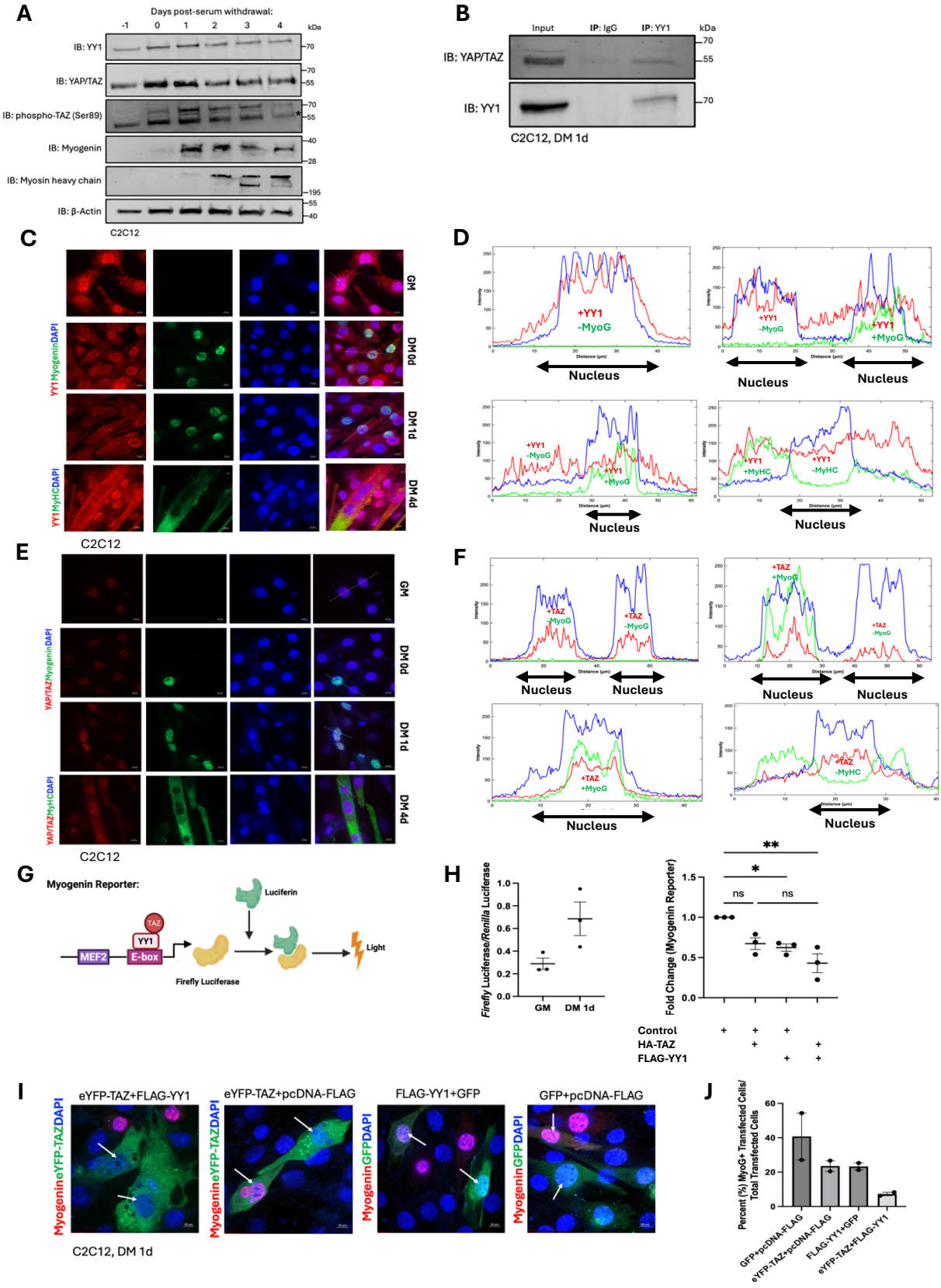
A
Days post-serum withdrawal:
-1 0 1 2 3 4 kDa
IB: YY1
IB: YAP/TAZ
IB: phospho-TAZ (Ser89)
IB: Myogenin
IB: Myosin heavy chain
IB: β-Actin
C2C12
B
Input IP: IgG IP: YY1 kDa
IB: YAP/TAZ
IB: YY1
C2C12, DM 1d
C
GM
DM 0d
DM 1d
DM 4d
YY1 MyogeninDAPI
YY1 MyHCDAPI
C2C12
D
+YY1 -MyoG
+YY1 +MyoG
+YY1 -MyHC
Nucleus
E
YAP/TAZ MyogeninDAPI
YAP/TAZ MyHCDAPI
C2C12
F
+TAZ -MyoG
+TAZ +MyoG
+TAZ -MyHC
Nucleus
G
Myogenin Reporter:
Luciferin
TAZ
YY1
MEF2
E-box
Light
Firefly Luciferase
H
Firefly Luciferase/Renilla Luciferase
GM DM 1d
Fold Change (Myogenin Reporter)
**
*
ns ns
Control
HA-TAZ
FLAG-YY1
I
eYFP-TAZ+FLAG-YY1
eYFP-TAZ+pcDNA-FLAG
FLAG-YY1+GFP
GFP+pcDNA-FLAG
MyogeninYFP-TAZDAPI
MyogeninGFPDAPI
C2C12, DM 1d
J
Percent (%) MyoG+ Transfected Cells/ Total Transfected Cells
GFP+pcDNA-FLAG
eYFP-TAZ+pcDNA-FLAG
FLAG-YY1+GFP
eYFP-TAZ+FLAG-YY1

Figure 6. **YY1 interacts with Taz and represses the early myogenic program. (A)** C2C12 myoblasts were cultured in growth media (GM) before transfer into differentiation media (DM). Lysates were collected at lower confluence (-1 day), right before media transfer at high confluence (0 day) and daily at four timepoints (1-4 days). Protein levels of Taz, phospho-Taz (Ser89), and YY1 were assessed using immunoblot analysis. Myogenin (MyoG) was used as an early-myogenic marker, and Myosin heavy chain (MyHC) was used as a late-myogenic marker. Beta-actin served as a loading control. **(B)** C2C12 myoblasts were grown to high confluence in GM and transferred to DM. Lysates were collected one day under differentiation conditions (DM 1d). Extracts were then subject to YY1 immunoprecipitation. Eluates were analyzed using immunoblotting for contents of immunoprecipitated Yap/Taz. **(C,E)** Individual immunofluorescence analysis of endogenous YY1 (red signal in (C)) and Yap/Taz (red signal in (E)) in C2C12 cells under growth conditions at low confluence (GM) and high confluence (DM 0d), as well as during early (DM 1d) and late (DM 4d) differentiation. Cells were immunostained for MyoG (green) during GM, DM 0d, and DM 1d to label cells entering myogenic differentiation. Cells were immunostained for MyHC (green) during DM 4d to label myotubes. Cells were also counterstained with DAPI to indicate nuclei (blue). Orthogonal projections were rendered from Z-stack images taken with confocal fluorescence microscopy. Images in C,E are representative of three independent experiments (*n=3*). **(D,F)** Line scan analysis of orthogonal projections depicting fluorescence signal conducted using ImageJ. DAPI: blue, MyoG/MyHC: green, YY1 (in (D))/Yap/Taz (in (F)): red. Top left graph: GM, top right graph: DM 0d, bottom left graph: DM 1d, and bottom right graph: DM 4d. **(G)** Schematic of *myogenin-promoter Firefly* luciferase gene reporter assay. **(H)** C2C12 cells were transfected with an empty vector (pcDNA-FLAG) and a *myogenin-promoter* reporter gene, then cultured in GM and DM for one day (DM 1d). Lysates served as a positive control for activation of endogenous machinery. HA-TAZ alone and combined with FLAG-YY1 were ectopically expressed with a *myogenin-promoter Firefly* reporter gene in C2C12 cells. These cells were cultured in GM and DM 1d. *Renilla* luciferase gene served as a transfection control. Differentiated lysates previously transfected with an empty vector (pcDNA-FLAG) served as a control for endogenous activity. Triplicate intra-experimental samples were analyzed, and the mean of these technical replicates constituted one biological replicate. This experiment was repeated three times and the data points on the graph indicate the biological replicates (*n=3*). Statistical analysis was conducted on PRISM from GraphPad 10.0. Using this software, a one-way ANOVA was conducted to test for statistical significance. Adjusted *p*-value (**P*≤0.05, ***P*≤0.01) is indicated for significance compared to the relevant control. ns, not significant. **(I)** C2C12 myoblasts were transfected with eYFP-TAZ or GFP with or without FLAG-YY1. Co-transfection of GFP with an empty vector (pcDNA-FLAG) served as a negative control. Next day, cells were recovered for 24 hours and then were transferred to DM for 1 day then fixed with 4% paraformaldehyde, and immunostained for MyoG (red) and counterstained with DAPI to indicate nuclei (blue). GFP/eYFP-TAZ fluorescence is shown in green. GFP/eYFP-TAZ positive cells were counted for two biological replicates (*n=2*). White arrows indicate nuclei in transfected cells. **(J)** Bar graph created on PRISM from GraphPad 10.0 to quantify fraction of MyoG positive cells. Datapoints represent two biological replicates constituting >10 technical replicates.

YY1 interacts with Taz, and both proteins localize in the nuclei of primary rat neonatal cardiomyocytes

Taz is expressed in pre-natal cardiomyocytes, where it promotes cardiomyocyte proliferation and heart growth during embryonic development (134, 140, 150). Unlike skeletal muscle, post-natal cardiomyocytes largely lose their regenerative capacity after birth; however, neonatal cardiomyocytes, such as those from mice or rats, retain transient regenerative potential for approximately one week post-natally (149).

Neonatal rat ventricular myocytes were thus used to assess whether the Taz-YY1 interaction also occurs in cardiac muscle. To this aim, endogenous protein levels of YY1, Taz, and deactivated Taz (phospho-Taz Ser89) were analyzed across several cell types including HEK293T, cardiac fibroblasts, C2C12 on days 0 and 4 in differentiation, and primary rat neonatal cardiomyocytes (PCMs). Immunoblot analysis revealed the presence of YY1, and both Taz and phospho-Taz (Ser89) in PCMs, indicating active Hippo signaling in these cells (Figure 7A). Cardiac troponin-T and MCK were used as markers to validate PCM enrichment and late C2C12 differentiation (DM 4d), respectively.

To determine whether YY1 interacts with Taz in PCMs, an immunoprecipitation was carried out, which confirmed an endogenous Taz-YY1 interaction in this cardiac muscle context (Figure 7B). Finally, immunofluorescence analysis indicated that both YY1 and TAZ localize predominantly to the nucleus in PCMs (Figure 7C-D). Cardiac troponin-T staining was used to identify PCMs within this primary culture.

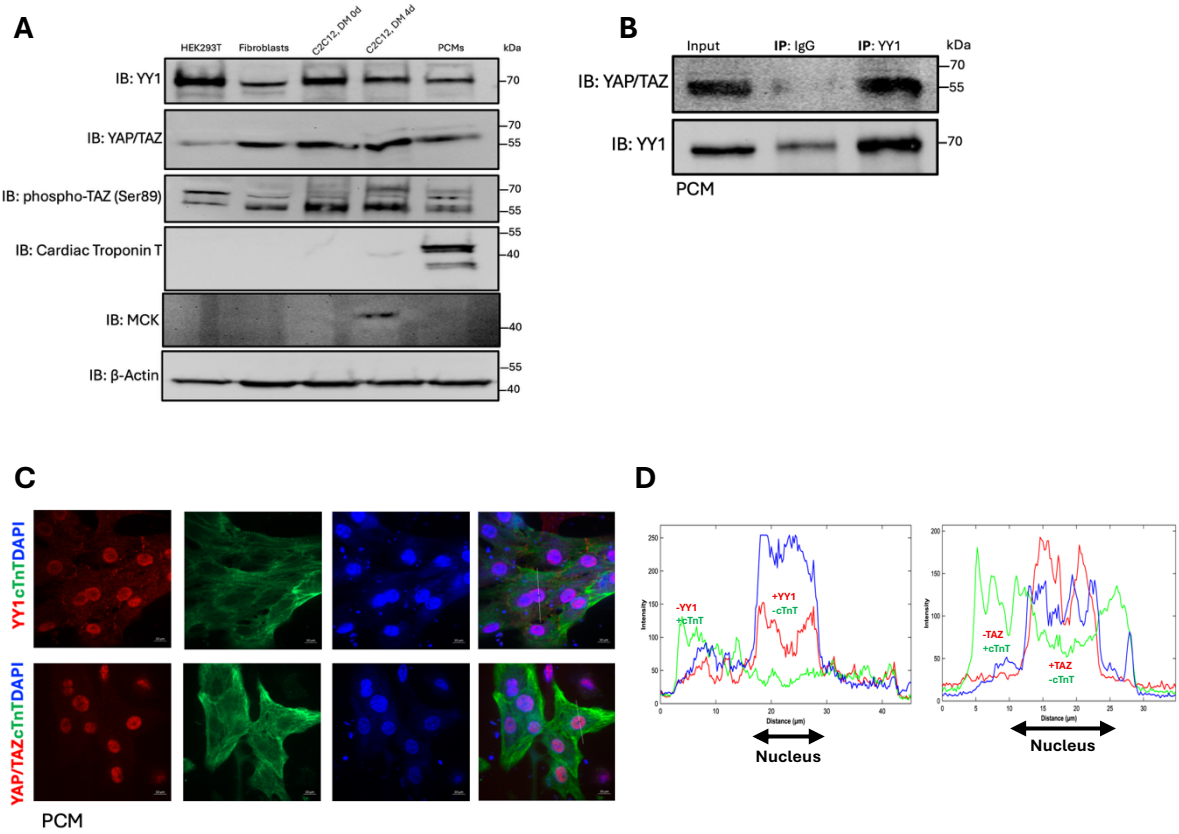

Figure 7. **YY1 interacts with Taz, and both proteins localize in the nuclei of rat neonatal cardiomyocytes. (A)** HEK293T cells and C2C12 cells were cultured in growth media (GM). C2C12 cells were then harvested at high confluence in GM (DM 0d) and after four days in DM (DM 4d). Primary rat neonatal cardiomyocytes (PCMs) were isolated from whole hearts and pre-plated to separate them from non-myocardial cells (cardiac fibroblasts). Cardiac fibroblasts and PCMs were cultured in DMEM/F-12 GM for one day before lysates were collected. Protein levels of Taz, phospho-Taz (Ser89), and YY1 were assessed using immunoblot analysis. Muscle creatine kinase (MCK) was used as a myogenic marker. Cardiac troponin-T (cTnT) was used as a cardiac muscle marker. Beta-actin served as a loading control. **(B)** PCMs were isolated from whole hearts and removed from any non-myocardial contamination. Cells were grown in DMEM/F-12 GM and harvested the next day. Extracts were then subject to YY1 immunoprecipitation. Eluates were analyzed using immunoblotting for contents of immunoprecipitated Yap/Taz. **(C)** Individual immunofluorescence analysis of endogenous YY1 (red, top panel) and Yap/Taz (red, bottom panel) in PCMs. Cells were immunostained for cTnT (green) to label PCMs. Cells were counterstained with DAPI to indicate nuclei (blue). **(D)** Line scan analysis of fluorescence signal was conducted using ImageJ. DAPI: blue, cTnT: green, YY1 (left panel)/Yap/Taz (right panel): red.

YY1 stabilizes phospho-Taz (Ser89) levels in proliferating myoblasts, and this effect is alleviated in differentiating skeletal muscle and rat neonatal cardiomyocytes

Based on our observations, the interaction of Taz and YY1 occurs in the nuclei of proliferating skeletal myoblasts, early differentiating C2C12 cells, and in rat neonatal cardiomyocytes (PCMs). In proliferating myoblasts, the Taz-YY1 interaction represses Taz-mediated transcription, whereas during early differentiation, YY1 and Taz act together to repress myogenic gene expression. To begin defining the mechanism by which the Taz-YY1 interaction regulates Taz, we examined the effect of YY1 expression on Taz protein levels.

In proliferating C2C12 cells, ectopic expression of HA-YY1 led to an increase in total Taz protein levels (Figure 8A). Importantly, phospho-Taz (Ser89), the Hippo-inactivated form of Taz, was similarly increased. These data are consistent with our model in which YY1 represses the co-activating role of Taz in this cellular context. The expression of c-Myc, a canonical proliferative Taz-target gene, remains unchanged, potentially reflecting compensatory Yap activity under these conditions. To further assess whether YY1 influences phospho-Taz (Ser89) stability, we titrated YY1 expression in HEK293T cells. Increasing YY1 expression resulted in a corresponding increase in both total and phospho-Taz (Ser89) protein levels (Figure 8B; quantification shown). Notably, this stabilizing effect was absent in differentiating C2C12 cells or in PCMs, where total and phospho-Taz (Ser89) levels remained unchanged upon ectopic YY1 expression (Figure 8C-D). These observations suggest that the YY1-dependent stabilization of phospho-Taz (Ser89) is context-dependent, occurring specifically in proliferating myoblasts and is alleviated in differentiating skeletal muscle and in PCMs.

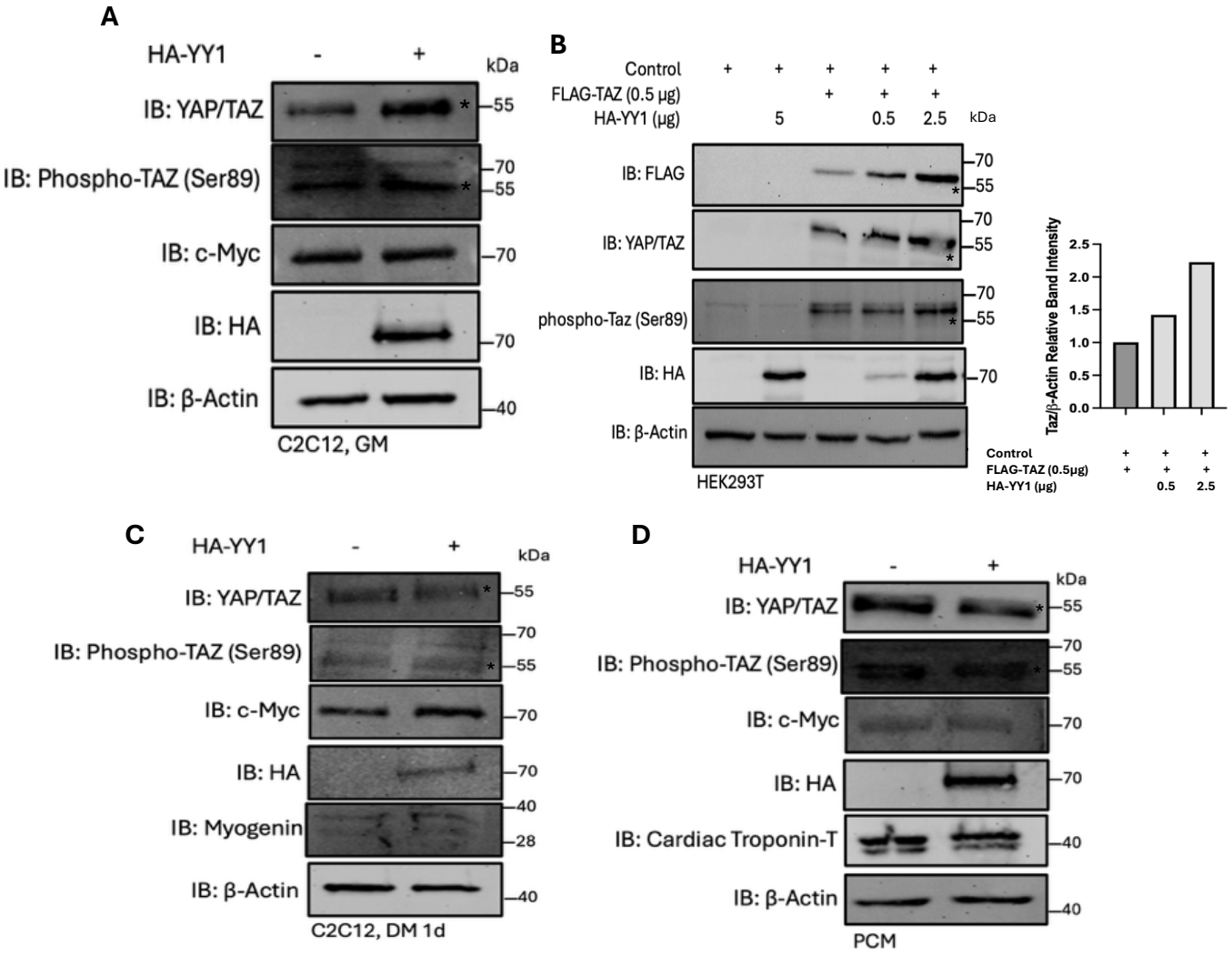
A
HA-YY1
-
+
kDa
IB: YAP/TAZ
55
IB: Phospho-TAZ (Ser89)
70
55
IB: c-Myc
70
IB: HA
70
IB: β-Actin
40
C2C12, GM
B
Control
FLAG-TAZ (0.5 μg)
HA-YY1 (μg)
5
0.5
2.5
kDa
IB: FLAG
IB: YAP/TAZ
phospho-Taz (Ser89)
IB: HA
IB: β-Actin
HEK293T
Taz/β-Actin Relative Band Intensity
2.5
2.0
1.5
1.0
0.5
0.0
Control
FLAG-TAZ (0.5μg)
HA-YY1 (μg)
0.5
2.5
C
HA-YY1
IB: YAP/TAZ
IB: Phospho-TAZ (Ser89)
IB: c-Myc
IB: HA
IB: Myogenin
28
IB: β-Actin
C2C12, DM 1d
D
HA-YY1
IB: YAP/TAZ
IB: Phospho-TAZ (Ser89)
IB: c-Myc
IB: HA
IB: Cardiac Troponin-T
IB: β-Actin
PCM

Figure 8. **YY1 stabilizes phospho-Taz (Ser89) in proliferating myoblasts, and this effect is alleviated in differentiating skeletal muscle and rat neonatal cardiomyocytes. (A)** C2C12 myoblasts were transfected with HA-YY1 or empty vector (to serve as a negative control). After 24 hours, cells were harvested and subjected to immunoblot analysis to assess Yap/Taz, phospho-Taz (Ser89), and c-Myc protein levels. Beta-actin served as a loading control. Two biological replicates (*n=2*) were conducted for this experiment. **(B)** HEK293T cells were transfected with 0.5 μg of FLAG-TAZ with or without varying amounts of HA-YY1 (0.5 or 2.5 μg). Cells were transfected with empty vector (pcDNA-FLAG) to either serve as a negative control or to equalize the amount of transfected DNA. Cells were harvested the next day and subjected to immunoblot analysis to assess protein levels of ectopically expressed FLAG-TAZ, total Yap/Taz and phospho-Taz (Ser89). Beta-actin served as a loading control. This experiment was conducted once (*n=1*). **(C)** C2C12 myoblasts were transfected with HA-YY1 or empty vector (to serve as a negative control). After one day of recovery in GM, the cells were transferred to differentiation media (DM) for 24 hours (DM 1d). Lysates were collected and Yap/Taz, phospho-Taz (Ser89) and c-Myc protein levels were assessed using immunoblot analysis. Myogenin was used as a marker for early differentiation. Beta-actin served as a loading control. Two biological replicates (*n=2*) were conducted for this experiment. **(D)** Rat neonatal primary cardiomyocytes (PCMs) were transfected with HA-YY1 or empty vector (to serve as a negative control). Cells were harvested 24 hours post-transfection. Lysates were analyzed using immunoblot analysis for Yap/Taz, phospho-Taz (Ser89), and c-Myc protein levels. Cardiac troponin-T served as a marker for PCM enrichment and beta-actin was used as a loading control. One biological replicate (*n=1*) was used for this experiment.

Taz forms biomolecular condensates in striated muscle, and YY1 localization becomes more cytoplasmic when Taz condensates are formed

Our research group previously demonstrated that Taz undergoes liquid-liquid phase separation (LLPS) to form biomolecular condensates in proliferating skeletal myoblasts, characterized by spherical morphology and dynamic fusion (137). Using live-cell imaging in C2C12 myoblasts, we confirmed these findings: ectopically expressed eYFP-TAZ formed discrete nuclear puncta that were absent in GFP controls (Figure 9A-C).

To our knowledge, whether Taz also forms phase-separated condensates in cardiac muscle has not previously been established. To address this, Taz localization in rat neonatal cardiomyocytes (PCMs) was examined using immunofluorescence analysis. Using Cardiac troponin-T as a cardiomyocyte marker, similar nuclear punctate structures were observed upon

eYFP-TAZ expression in PCMs (Figure 9D-F), indicating that Taz has the capacity to form biomolecular condensates in both skeletal and cardiac muscle contexts.

Given that Taz condensates are associated with transcriptional regulation and that YY1 functions as a repressor of Taz-mediated transcription, we next aimed to investigate whether YY1 remains nuclear when Taz forms condensates. Co-expression of FLAG-YY1 and eYFP-TAZ in proliferating C2C12 myoblasts revealed that YY1 was frequently excluded from the nucleus specifically in cells displaying Taz nuclear condensates (Figure 9G-H). Corresponding controls are shown in Supplementary Figure 5A-B. Quantification confirmed that the fraction of transfected cells exhibiting nuclear YY1 exclusion was highest in Taz nuclear condensate-positive cells compared to condensate-negative cells and GFP control (Figure 9I). Together, these observations suggest that Taz forms nuclear condensates through LLPS in both skeletal and cardiac muscle, and that condensate formation correlates with reduced YY1 nuclear localization

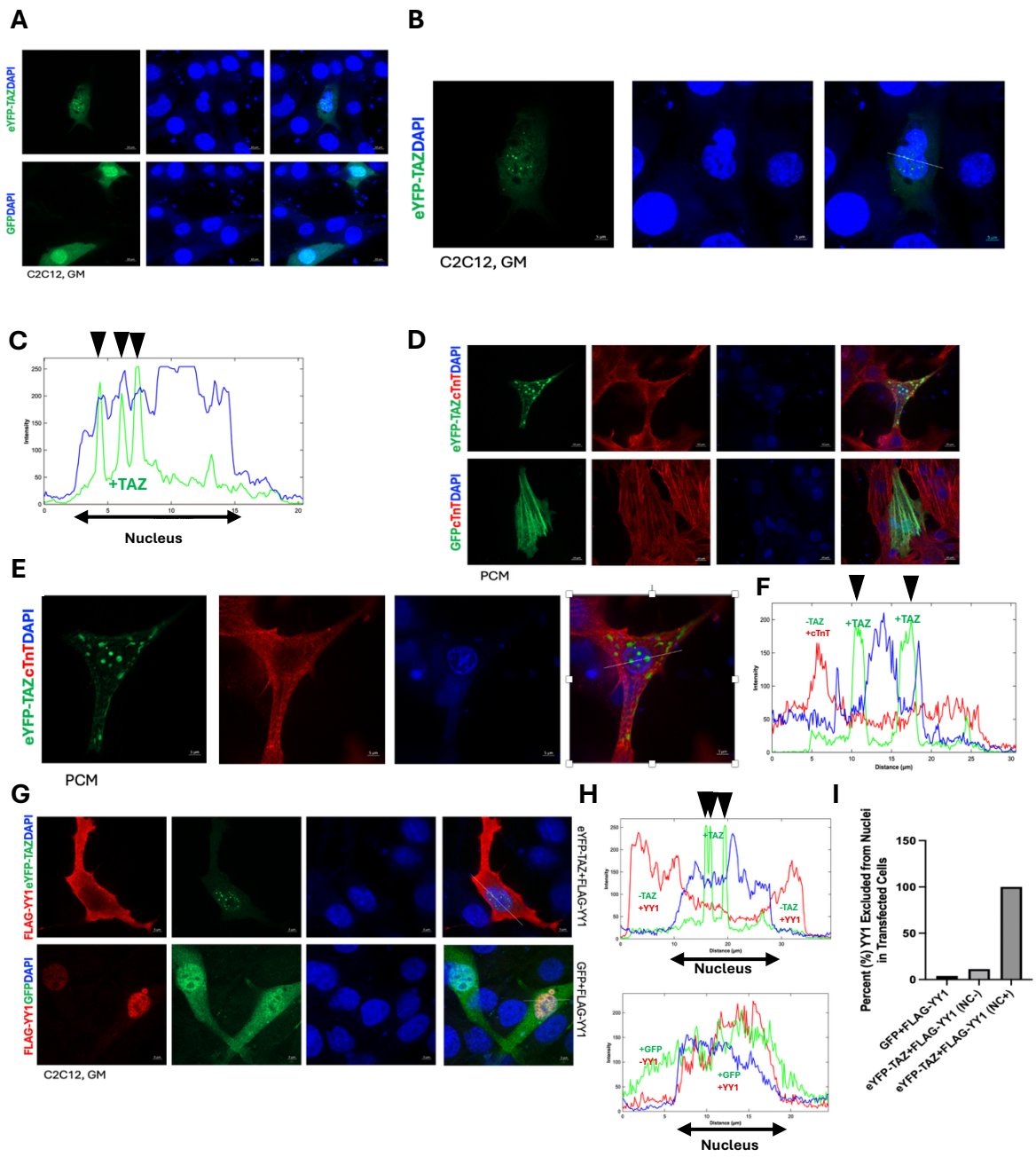
A
eYFP-TAZDAPI
GFPDAPI
C2C12, GM
B
eYFP-TAZDAPI
C2C12, GM
C
+TAZ
Nucleus
D
eYFP-TAZcTnTDAPI
GFPcTnTDAPI
PCM
E
eYFP-TAZcTnTDAPI
PCM
F
-TAZ
+cTnT
+TAZ
+TAZ
Distance (μm)
G
FLAG-YY1 eYFP-TAZDAPI
FLAG-YY1GFPDAPI
C2C12, GM
H
eYFP-TAZ+FLAG-YY1
+TAZ
-TAZ
+YY1
-TAZ
+YY1
Nucleus
GFP+FLAG-YY1
+GFP
-YY1
+GFP
+YY1
Nucleus
I
Percent (%) YY1 Excluded from Nuclei in Transfected Cells
150
100
50
0
GFP+FLAG-YY1
eYFP-TAZ+FLAG-YY1 (NC-)
eYFP-TAZ+FLAG-YY1 (NC+)

Figure 9. **Taz forms phase separated condensates in striated muscle, and YY1 localization becomes more cytoplasmic when Taz condensates are formed. (A)** C2C12 myoblasts were transfected with eYFP-TAZ or GFP (to serve as a negative control). Next day, cells were visualized using live-cell confocal microscopy. eYFP-TAZ/GFP fluorescence signal is shown in green and DAPI (blue) indicates nuclei. Scale bar: 10 μm. **(B)** Higher magnification live-cell confocal microscopy images of C2C12 myoblasts transfected with eYFP-TAZ. Scale bar: 5 μm. **(C)** Line scan analysis of fluorescence signal conducted using ImageJ. DAPI: blue, eYFP-TAZ: green. Black arrows point to eYFP-TAZ green fluorescence signal in nuclear phase separated condensates. **(D)** Rat neonatal primary cardiomyocytes (PCMs) were isolated from whole hearts, and any non-myocardial contamination was removed. Cells were transfected with eYFP-TAZ and GFP, and immunostained for Cardiac troponin-T (cTnT) to mark the PCMs. Cells were fixed with 4% paraformaldehyde 24 hours post-transfection and visualized using immunofluorescence confocal microscopy. Cells were counterstained with DAPI (blue) to indicate nuclei and eYFP-TAZ/GFP is shown in green. Scale bar: 10 μm. **(E)** Higher magnification immunofluorescence images of PCMs transfected with eYFP-TAZ. Scale bar: 5 μm. **(F)** Line scan analysis of fluorescence signal conducted using ImageJ. DAPI: blue, eYFP-TAZ: green, cTnT: red. Black arrows point to eYFP-TAZ green fluorescence signal in nuclear phase separated condensates. **(G)** C2C12 myoblasts were transfected with eYFP-TAZ with or without FLAG-YY1. Cells were fixed with 4% paraformaldehyde 24 hours post-transfection, and immunostained with anti-FLAG for FLAG-YY1 (red), and counterstained with DAPI to indicate nuclei (blue). GFP was used as a negative control. eYFP-TAZ (top panel)/GFP (bottom panel) fluorescence is shown in green. **(H)** Line scan analysis of fluorescence signal conducted using ImageJ. DAPI: blue, eYFP-TAZ (top panel)/GFP (bottom panel): green, FLAG-YY1: red. Black arrows point to eYFP-TAZ green fluorescence signal in nuclear phase separated condensates. **(I)** Bar graph created on PRISM from GraphPad 10.0 to quantify fraction of Taz-nuclear condensate positive cells exhibiting non-nuclear sub-cellular localization of YY1. One biological replicate ($n=1$) was analyzed consisting of >10 technical replicates. NC, nuclear condensates.

Discussion

The regulation of organ size during development and regeneration is a longstanding question in biology: how do cells know when to stop proliferating once the appropriate tissue size has been reached? The Hippo signaling pathway has emerged as a central regulator of this process (107). This evolutionarily conserved kinase cascade culminates in the phosphorylation and inhibition of the transcriptional co-activators Yap/Taz, which coordinate Hippo-dependent gene expression and integrate Hippo signaling with other developmental networks, including Wnt and IGF pathways (134, 135). Given that Taz lacks intrinsic DNA-binding capability, its

transcriptional output relies on its interaction with sequence-specific transcription factors, making its function highly dependent on its protein interaction network.

Using FLAG-affinity purification coupled with LC-MS/MS, we generated a nuclear Taz interactome in HEK293T cells and identified both known and previously uncharacterized Taz-interacting proteins. Among these, we focused on the transcription factor YY1, which plays prominent roles in skeletal and cardiac muscle gene regulation. Biochemical validation confirmed that YY1 interacts with Taz at or near its Tead-binding domain, and this interaction was enhanced with Tead1 binding. We found that YY1 modulates Taz function in proliferating myoblasts by increasing levels of phosphorylated Taz (Ser89), the Hippo-inactive form. Additionally, we demonstrated that Taz forms nuclear biomolecular condensates in striated muscle, and in proliferating myoblasts, YY1 was excluded from the nucleus when these condensates were present. Importantly, the YY1-mediated stabilization of phospho-Taz (Ser89) observed in proliferation was not present in differentiating skeletal muscle or PCMs. Instead, in differentiation, Taz and YY1 endogenously interact, and this complex significantly repressed *myog* promoter activity. Together, these findings suggest a model in which YY1 regulates Taz through distinct mechanisms during proliferation and differentiation (Figure 10), although the mechanism by which YY1 stabilizes the inactive form of Taz remains to be determined.

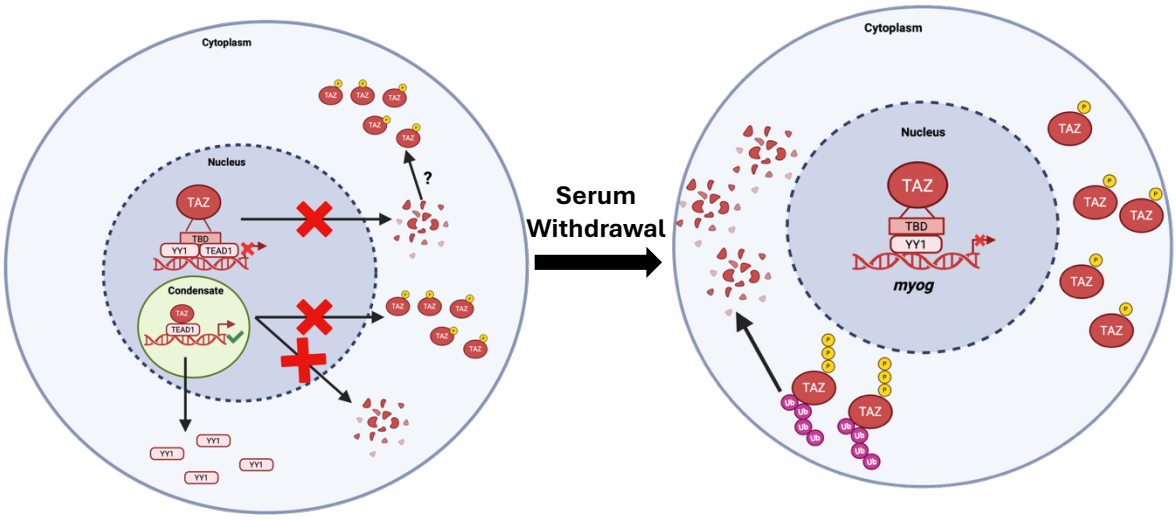

Figure 10. **Working model of YY1 regulation on Taz activity in proliferating and differentiating muscle.** In proliferating myoblasts, Hippo signaling is inactive and Taz is predominantly nuclear. YY1 interacts with Taz at its Tead-binding domain and reduces Taz-co-activating properties in a Hippo signaling context, corresponding with increased levels of phospho-Taz (Ser89). When Taz forms nuclear condensates in this context, YY1 is excluded from the nucleus, further supporting a repressive role of YY1 on Taz during proliferation. In contrast, during early differentiation, this repressive mechanism is alleviated. YY1 no longer increases phospho-Taz (Ser89) levels, and instead YY1 and Taz function cooperatively in a repressive complex that suppresses transcription of early myogenic genes such as *myogenin. Created in Biorender.com.*

Our research group previously developed a novel GFP-nanoTrap technology to purify potential Taz interacting proteins in striated muscle (for more details, see (166)). This affinity purification method is particularly useful in model systems with low transfection efficiency, where minimal bait expression often results in poor recovery of interacting partners. In this workflow, a highly transfectable cell line, such as HEK293T, is first used to yield high expression of the bait protein (in this case, Taz). The expressed bait and corresponding control protein is then immobilized on nano-trap beads and further incubated with lysates from a target cell line to ultimately purify interacting proteins of interest.

A potential limitation of this approach is the significant time investment required to ensure that purified interactors originate from the target model system rather than HEK293T

cells. Minimizing cross-contamination requires extensive and stringent washing between cell lines, which is technically demanding and time-intensive. Additionally, the subsequent data processing of the MS proteomic list is labour-intensive as well. When lysates are derived from different species, peptides can be searched against the target species database, and any human contaminants can be readily eliminated to ensure screened interactors are from the target lysate. This needs to be done in addition to filtering out any non-specific interactors. Lastly, any candidate interactors of interest identified in the proteomic screen need to be biochemically validated to confirm the interaction, adding another layer of complexity that requires experimental time and effort.

We employed a more streamlined approach to generate our Taz interactome list. Using a protocol adapted from Valdez-Sinon et al. (165), we transfected only one HEK293T sample with the bait construct (FLAG-TAZ), rather than transfecting two individual lysates with an expression and control construct. As a control, we used a 3X FLAG peptide to competitively elute FLAG-TAZ from the anti-FLAG beads, taking advantage of the higher affinity of the peptide. Unlike the previously described method (166) that required transferring the immobilized bait to a second cellular lysate, we performed LC-MS/MS analysis directly on the FLAG-TAZ-enriched HEK293T nuclear fraction. This strategy bypassed the need for extensive washing required to prevent cross-contamination when two different cell types are used. As a result, the experimental protocol as well as the data processing were simplified to removing non-specific interactors. Given that only one cell lysate was used, there was also no need for additional filtering of HEK293T background proteins. This expedited the workflow immensely and allowed us to proceed directly to biochemical validation of candidate interactors.

Comparison of the interactome identified in our study with the previously generated Taz interactome from our lab group (166) revealed several well-established Taz-interacting proteins. These included core Hippo components such as Tead1, as well as membrane-associated proteins such as Amot and ZO-2. All of these interactors were detected across multiple cellular contexts including HEK293T, C2C12 myoblasts, and PCMs, providing strong confidence for the reliability of our purification and proteomic workflow.

In addition to these well-known interactors, our dataset also revealed previously uncharacterized or less well-defined candidate interactors of Taz. We decided to focus our attention on YY1 because its co-expression with Taz produced a robust repressive effect of Taz-mediated transcription on a Tead-responsive promoter. YY1 is a 414 amino acid protein with the molecular weight of approximately 45 kDa. It belongs to the Gli-Krüppel class of zinc finger transcription factors. Its C-terminus contains four zinc finger domains that are essential to its DNA binding (171).

There are several notable similarities between YY1 and Taz. First, YY1, like Taz, can function as either a transcriptional repressor or activator depending on the cellular context and composition of its interacting protein network. Structurally, YY1 contains a transcriptional activation domain at its N-terminus and a central transcriptional repression domain (Figure 11), enabling this dual regulatory role. Second, YY1 also undergoes nucleocytoplasmic shuttling, and its localization and activity changes throughout different biological processes such as cell cycle progression and differentiation (171).

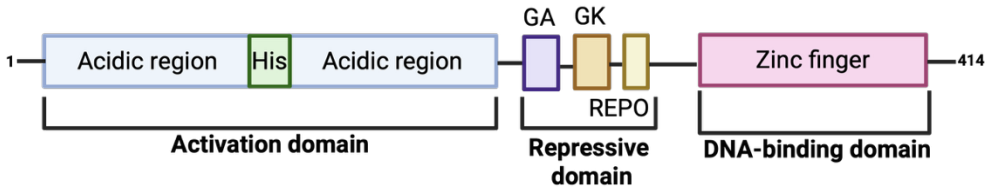

***Figure 11*. Structure of Yin-Yang 1 (YY1).** The N-terminal region of YY1 is intrinsically disordered and a transcriptional activation domain composed of two acidic regions separated by a histidine-rich motif. These acidic regions are comprised of glutamic and aspartic acid residues. The central part of its structure (amino acids 154 to 201), termed the transcriptional repressive domain, contains glycine-alanine (GA) and glycine-lysine (GK) motifs, as well as the Recruit POlycomb (REPO) domain to bind the Polycomb repressive complex. The C-terminal domain contains the four zinc fingers that mediate the binding of YY1 to DNA. *Created in Biorender.com.*

Relevant to our work, a study by Hoxha and colleagues (172) demonstrated that Yap recruits YY1 and Enhancer of zeste homolog 2 (Ezh2) from the Polycomb repressive complex to downregulate the expression of cell-cycle inhibitor p27, thereby promoting proliferation. In this context, Yap functions not only as a transcriptional co-activator of proliferative genes, but also as a transcriptional repressor by recruiting YY1 to inhibit genes that restrict proliferation. The authors reported similar findings for Taz (172). These observations suggest that in proliferative conditions, both Yap and Taz can form repressive transcriptional complexes with YY1 to maintain a proliferative state.

However, whether YY1 can also repress the co-activating function of Taz on Tead-dependent proliferative gene transcription, rather than Taz-mediated repression, was not addressed in the Hoxha et al. study (172), and remains unresolved. In our study, we demonstrate that YY1 interacts with Taz in proliferating myoblasts and represses its co-activating function on a Tead-responsive promoter. This repression is associated with increased levels of phospho-Taz (Ser89), the Hippo-inactive form of Taz. Therefore, these findings suggest that in proliferating cells, YY1 can act as a repressor in both contexts, when Taz functions as a co-repressor and when Taz functions as a co-activator.

In a similar way, Taz may exhibit a co-repressive role on myogenic differentiation by recruiting YY1 to inhibit muscle-specific gene expression. In striated muscle, YY1 is considered a repressor of myogenic differentiation, whereby it has been shown to inhibit the expression of

myogenic genes such as α-actin, MCK, and myosin heavy chain (173-176). Walowitz et al. (177) reported that YY1 protein levels, but not mRNA, decreased in differentiating skeletal and cardiac muscle from one to two days post-differentiation, suggesting YY1 is post-translationally regulated in this process. Consistent with these findings, our work shows a similar reduction in YY1 protein levels after one day of differentiation, as well as a shift from nuclear to diffuse cytoplasmic localization. These observations suggest that as myoblasts undergo the myogenic program, the cellular context changes to exclude repressors such as YY1 from the transcriptional milieu within the nucleus, thereby releasing repression to drive myogenic differentiation.

YY1 has also been reported to form LLPS-driven nuclear condensates, where it concentrates co-activators, RNA polymerase II, and other transcriptional elements to promote gene expression. Biomolecular condensate formation appears to be attributed to the histidine-rich region within its transcriptional activation domain at its N-terminus, which is likely an IDR (178). However, in our study, YY1 did not co-localize with Taz condensates in proliferating myoblasts and was instead excluded from the nucleus when Taz formed nuclear biomolecular condensates. This observation is consistent with our model in which YY1 functions as a repressor of Taz activity in proliferative conditions. Wang et al. (178) reported that YY1 condensates are associated with transcriptional activation, not repression. Therefore, the absence of YY1 within Taz condensates in our system may reflect that, as a repressor, YY1 remains excluded from the transcriptional machinery within the condensates.

Future Directions and Implications

Our MS analysis revealed many known and uncharacterized protein interactors of Taz. One protein that was identified in our proteomic study as well as our lab group's previously published C2C12 and PCM datasets, was Tead1 (166). The Tead family of transcription factors are well-established binding partners of Taz, with their interaction regulated by canonical Hippo signaling (102). Notably, Tead1 is the predominant Tead isoform expressed in cardiac muscle and is required for cardiac development (168). Tead1 has been shown to be essential for cardiomyocyte proliferation, whereby *tead1*-deficient cardiomyocytes exhibit markedly reduced proliferation, and *tead1*-deficient mice exhibit post-natal lethality due to dilated cardiomyopathy (168). These findings underscore the functional significance of Tead1 regulation in the heart. Further investigation into Taz-mediated regulation of Tead1 in cardiomyocytes may provide insight into the important role of Hippo signaling in cardiac development.

Another interesting, uncharacterized Taz-interacting protein that was identified in our interactome study was RE1-silencing transcription factor (Rest). Rest is an established transcriptional repressor of neuronal-specific genes, maintaining neural stem cells in an undifferentiated state (179). However, its role in myogenesis is still in its infancy, with one study (180) reporting that ectopic expression of Rest represses *myogenin* mRNA levels, and that Rest expression levels decline during myogenic differentiation. These findings are similar to our observations of Taz and YY1, which represses *myogenin*-promoter driven gene expression. Thus, Rest may function similarly to YY1 in supporting Taz-mediated repression of the early myogenic program. Biochemical and functional characterization of the Taz-Rest interaction is needed to determine the mechanism, if any, by which Rest modulates Taz-dependent repression of muscle-specific gene expression.

Our findings suggest that YY1 represses Taz through its interaction with its Tead-binding domain, and that this interaction is enhanced by Tead1 binding. An alternative model is that YY1 and Tead1 bind different pools of Taz rather than forming a tricomplex. In this case, YY1 may repress Taz-mediated transcription of a Tead-responsive promoter by sequestering Taz away from Tead, thereby reducing the number of Taz available to bind Tead and subsequently activate gene expression. Therefore, to further validate our model, a titration co-immunoprecipitation experiment could be performed to determine whether increasing levels of Tead1 proportionally increase the YY1 interaction with Taz. A corresponding titration using the Tead1 (Y406A) mutant, which is unable to bind Taz, should produce an opposing effect. If Tead1 facilitates the Taz-YY1 interaction, increasing wild-type Tead1 should enhance YY1 binding, whereas increasing mutant Tead1 should repress YY1 binding.

To evaluate this mechanism in a more physiological context, Tead1 knockdown assays using siRNA could be conducted in skeletal and cardiac muscle. If YY1 requires Tead1 to interact with Taz at its Tead-binding domain, *tead1* depletion should reduce or abolish the Taz-YY1 interaction. In cardiomyocytes, Tead1-targeted siRNA is sufficient to see an effect, if any, on the Taz-YY1 interaction, as Tead1 is the predominant Tead isoform in cardiac muscle (168). In skeletal muscle, however, siRNA knockdown should generally target the Tead1-4 isoforms to avoid compensation of the Taz-YY1 interaction by other Tead factors.

Our study demonstrated that YY1 represses Taz co-activation, in a Hippo signaling context, and that this repression may occur through the stabilization of phospho-Taz (Ser89), the Hippo-inactive form of Taz. The mechanism underlying this accumulation of phospho-Taz (Ser89) has yet to be determined. We also observe an increase in total Taz protein levels upon YY1 expression, suggesting that YY1 may reduce the proteasomal degradation of Taz.

Through the canonical Hippo signaling pathway, Taz is phosphorylated by Lats1/2 at multiple serine residues, most notably Ser89 and Ser311. Phosphorylation at Ser311 promotes recruitment of CK1, which subsequently phosphorylates Taz Ser314 to generate a phosphodegron that is recognized by β-TrCP, leading to ubiquitination and proteasomal degradation. Therefore, YY1 may stabilize Taz by interfering with Lats1/2 phosphorylation at Ser 311, CK1-mediated phosphorylation at Ser314, or β-TrCP recruitment. In this case, Hippo signaling may regulate Taz in an alternative way: through Ser89 phosphorylation, recruitment of 14-3-3 proteins, and subsequent cytoplasmic sequestration (Figure 12).

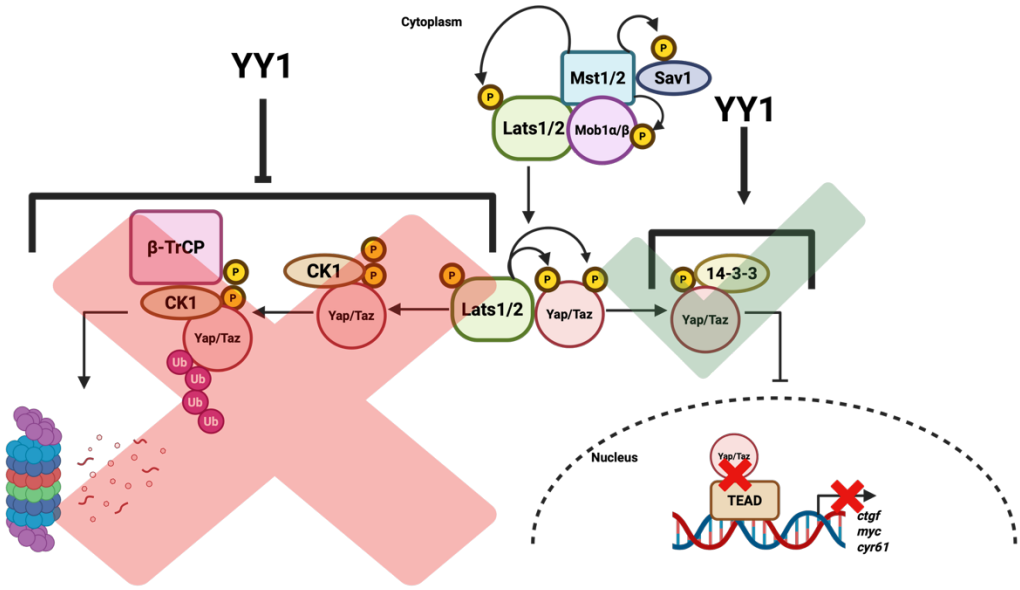

***Figure 12*. Possible mechanism of YY1 stabilization of Taz.** The observed increase in phospho-Taz (Ser89) and total Taz protein levels with YY1 expression may be due to YY1-mediated repression of Lats1/2 phosphorylation of Ser311, CK1 phosphorylation of Ser314, or recruitment of β-TRCP. In any case, Hippo signaling may compensate for this disruption in the pathway by enhancing Lats1/2-mediated phosphorylation of Ser89, and the subsequent binding of 14-3-3 proteins and cytoplasmic sequestration of Taz. *Created in Biorender.com.*

To determine the mechanism by which YY1 stabilizes Taz, several experiments are warranted. First, proteasomal inhibition with MG132 could be used to assess whether Taz accumulation observed with YY1 expression reflects decreased proteasomal degradation.

Increased Taz accumulation in the presence of YY1 and MG132, compared to MG132 alone, would support our stabilization mechanism. Second, immunoblot analysis with an antibody specific to phospho-Taz (Ser311) could determine whether YY1 alters phosphorylation at this key regulatory residue. Finally, co-immunoprecipitation assays could assess whether YY1 expression disrupts CK1 or β-TRCP recruitment, providing evidence for YY1-mediated disruption of the Hippo signaling-degradation pathway.

As discussed earlier, numerous studies have demonstrated the essential roles of Yap/Taz in striated muscle development (see Chapter I for details). Yap/Taz are required for the proliferation of skeletal and cardiac muscle cells to ensure that these tissues develop to their proper size. The importance of these effector proteins in striated muscle development is highlighted by the severe phenotypes associated with depletion of *yap/taz* genes. *Yap/taz*-deficiency has been shown to result in structural deformities and embryonic lethality (134-136, 140). Taz, the focus of our study, has been reported to regulate proliferation and EMT progression, processes that are critical for both embryonic development and post-natal muscle regeneration.

Similar to Yap/Taz, YY1 is also essential for normal cardiac development, whereby it regulates cardiomyocyte proliferation and survival. One study (181) reported that *yy1*-knockdown in mice resulted in embryonic lethality, with underdeveloped cardiac structures arising from reduced proliferation and increased apoptosis. Notably, EMT progression within the endocardial cushions of the atrio-ventricular canal and outflow tract was impaired (181), highlighting that, similar to Taz, YY1 is required to support cardiomyocyte proliferation and EMT to ensure proper cardiac development.

However, YY1 hyperactivation can contribute to cardiovascular diseases. Whereas Yap activation has been shown to promote cardiomyocyte proliferation and reduced fibrosis following myocardial infarction, YY1 overexpression has been associated with increased fibrosis. For example, YY1 appears to promote the expression pro-fibrotic factors such as soluble suppression of tumorigenicity 2 (sST2), whereas pharmacological reduction of YY1 levels, such as with metformin, decreased fibrosis and improved remodeling post-myocardial infarction (182). Conversely, other studies suggest that YY1 can exert protective effects against myocardial infarction, by enhancing Akt signaling to suppress apoptosis. According to a study conducted by Huang and colleagues (183), YY1 expression increased after myocardial infarction. YY1 overexpression decreased the formation of fibrotic scar tissue, and enhanced migratory ability of endothelial cells as well as overall cardiac function (183).

Cardiovascular disease remains a leading cause of morbidity and mortality, worldwide. Therefore, the demonstrated roles of Yap/Taz and YY1 in cardiac development and remodeling highlight the need for deeper characterization of the Taz-YY1 interaction, to uncover the regulatory mechanism of this complex that could be a potential target for cardiac regeneration and therapeutic intervention in heart failure.

Appendix I: Mass Spectrometry Data

Table 1. **Complete filtered list of HEK293T proteins identified in FLAG-affinity purification coupled with LC-MS/MS.** Proteomic interactome list was processed using a threshold of ≥ 3-fold enrichment when calculating the following ratio: (Intensity $Score_{FLAG\text{-}TAZ}$ / Intensity $Score_{Control}$). For proteins unique to the FLAG-TAZ sample, the enrichment score corresponded to their intensity value in the FLAG-TAZ condition, as no signal was detected in the control sample.
*Unique proteins

Proteins	**Uniprot Accession Number**	**Enrichment Score (Intensity $Score_{FLAG\text{-}TAZ}$ / Intensity $Score_{Control}$)**
InaD-like protein*	Q8NI35	491896.215
Protein PALS1*	Q8N3R9	386763.56
SUN domain-containing protein 2*	Q9UH99	314967.595
RNA-binding protein 10*	P98175	119475.565
Angiomotin-like protein 1*	Q8IY63	112698.232
Caspase-14*	P31944	64902.4765
Nuclear pore complex protein Nup155*	O75694	29098.882
Suppressor of SWI4 1 homolog*	Q9NQ55	27970.241
Cathepsin D*	P07339	18992.2115
MAX gene-associated protein*	Q8IWI9	15503.235
Nuclear pore glycoprotein p62*	P37198	15172.4725
Calmodulin-like protein 5*	Q9NZT1	15070.0325
Dynamin-2*	P50570	14959.407
Ribosome biogenesis protein BMS1 homolog*	Q14692	14953.665
Methionine aminopeptidase 2*	P50579	14095.7945
Proteasome subunit alpha type-4*	P25789	13890.269
Angiomotin-like protein 2*	Q9Y2J4	13856.1625
ADP/ATP translocase 2*	P05141	13446.4295
RE1-silencing transcription factor*	Q13127	11995.24775
Voltage-dependent anion-selective channel protein 1*	P21796	11392.1395
Calcyclin-binding protein*	Q9HB71	10385.259
Cytochrome b5 type B*	O43169	10312.283
26S proteasome regulatory subunit 6B*	P43686	10241.589
Dolichyl-diphosphooligosaccharide--protein glycosyltransferase subunit STT3A*	P46977	10185.5205
Drebrin*	Q16643	9628.71475
Tight junction protein ZO-2*	Q9UDY2	9081.05

Metastasis-associated protein MTA1*	Q13330	8947.1035
Kinesin-like protein KIF23*	Q02241	8650.185
Transcriptional enhancer factor TEF-5*	Q99594	7731.7135
Zinc finger RNA-binding protein*	Q96KR1	7226.5485
U2 snRNP-associated SURP motif-containing protein*	O15042	6946.2725
Copine-3*	O75131	5680.617
Transcriptional repressor protein YY1*	P25490	5169.225
Multiple PDZ domain protein	O75970	962.6775068
Angiomotin	Q4VCS5	109.9374155
Transcriptional enhancer factor TEF-1	P28347	71.38742696
WW domain-containing transcription regulator protein 1	Q9GZV5	63.16618609
Protein arginine N-methyltransferase 5	O14744	27.16548312
Pogo transposable element with ZNF domain	Q7Z3K3	7.785749165
Protein S100-A9	P06702	5.334336666
Desmoplakin	P15924	5.28444599
Double-strand-break repair protein rad21 homolog	O60216	5.050012413
Nucleolar protein of 40 kDa	Q9NP64	4.993937983
Filaggrin-2	Q5D862	4.808271925
Nuclear pore complex protein Nup160	Q12769	4.709817519
Thyroid hormone receptor-associated protein 3	Q9Y2W1	4.641809692
Hornerin	Q86YZ3	4.519275085
BolA-like protein 2	Q9H3K6	4.500217327

Appendix II: Supplementary Figures

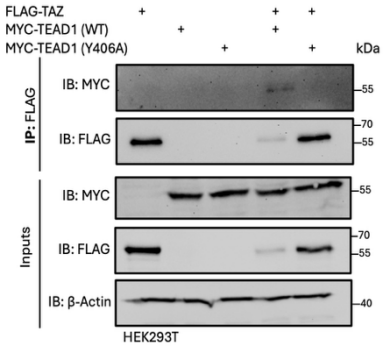

Supplementary Figure 1. **MYC-TEAD1 (Y406A) does not interact with Taz.** HEK293T cells were transfected with FLAG-TAZ with or without MYC-TEAD1 (Y406A), and MYC-TEAD1 (Y406A) with or without FLAG-TAZ. Cells were also transfected with FLAG-TAZ in the presence or absence of MYC-TEAD1 (WT) to serve as a positive control. Cells were harvested 24 hours post-transfection. Lysates were subjected to FLAG immunoprecipitation with anti-FLAG beads. Eluates were analyzed using immunoblotting for immunoprecipitated MYC-TEAD1 (WT) and MYC-TEAD1 (Y406A).

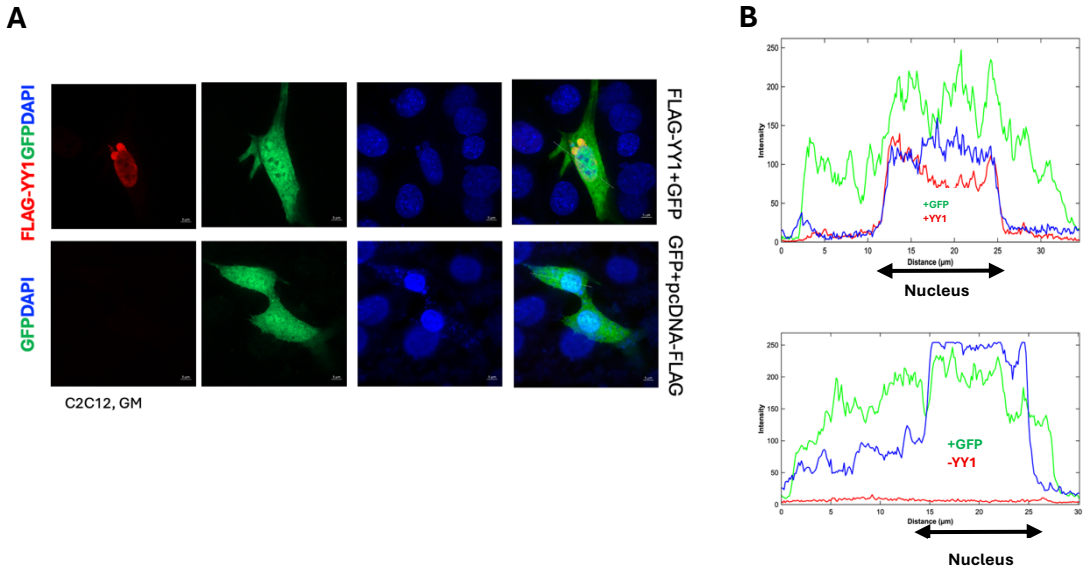

Supplementary Figure 2. **Relevant controls for immunofluorescence analysis of YY1 co-localization with Taz in skeletal myoblasts. (A)** C2C12 myoblasts were transfected with FLAG-YY1 and GFP, and GFP with pcDNA-FLAG empty vector to serve as negative controls. Cells were fixed with 4% paraformaldehyde 24 hours post-transfection, and immunostained with anti-FLAG for FLAG-YY1 (red) and pcDNA-FLAG (negative signal), and counterstained with DAPI to indicate nuclei (blue). GFP fluorescence is shown in green. **(C)** Line scan analysis of fluorescence signal conducted using ImageJ. DAPI: blue, GFP: green, FLAG-YY1/pcDNA-FLAG: red. Top graph: FLAG-YY1+GFP (top panel in (A)) and bottom graph: GFP+pcDNA-FLAG (bottom panel in (A)).

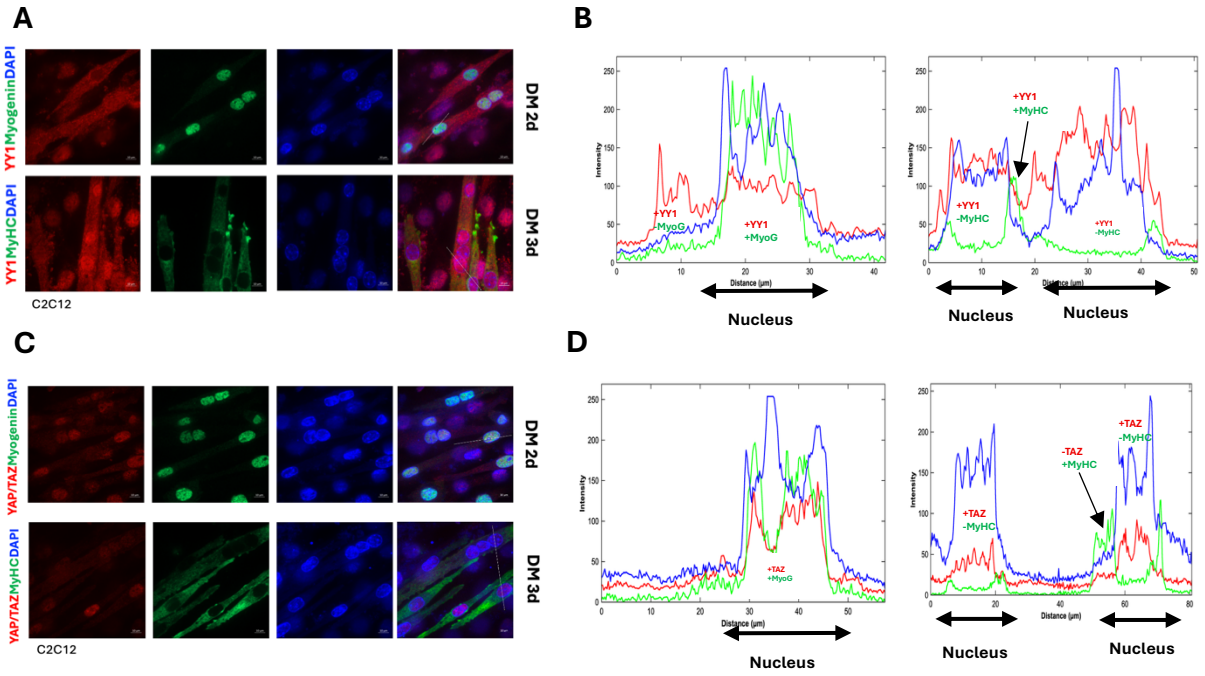

Supplementary Figure 3. **Individual immunofluorescence analysis of YY1 and Yap/Taz in differentiation conditions for two and three days. (A,C)** Endogenous YY1 (red signal in (A)) and Yap/Taz (red signal in (C)) in C2C12 cells under differentiation conditions for 2 and 3 days (DM 2d and DM 3d). Cells were immunostained for MyoG (green) during DM 2d to label cells entering myogenesis, and MyHC (green) during DM 3d to label myotubes. Cells were counterstained with DAPI to indicate nuclei (blue). Orthogonal projections were rendered from Z-stack images taken with confocal fluorescence microscopy. Images in A,C are representative of three independent experiments (*n=3*). **(B,D)** Line scan analysis of orthogonal projections depicting nuclear fluorescence signal conducted using ImageJ. DAPI: blue, MyoG/MyHC: green, YY1 (in (B))/Yap/Taz (in (D)): red. Left graph: DM 2d, right graph: DM 3d.

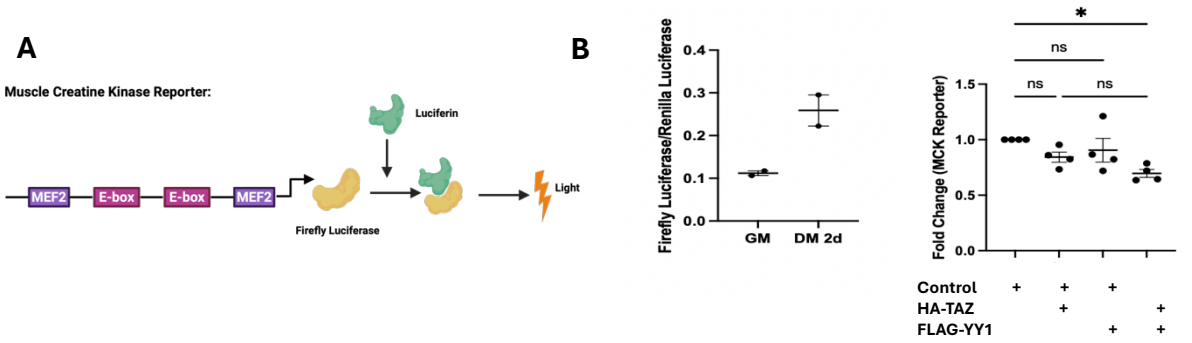

Supplementary Figure 4. **Dual luciferase reporter assay investigating the effect of YY1 and Taz on a *muscle creatine kinase-promoter.*** **(A)** Schematic of *muscle creatine kinase (MCK)-promoter Firefly* luciferase gene reporter assay. **(B)** C2C12 cells were transfected with an empty vector (pcDNA-FLAG) and a *MCK-promoter* reporter gene, then cultured in GM and DM for two days (DM 2d). Lysates served as a positive control for activation of endogenous machinery. HA-TAZ alone and combined with FLAG-YY1 were ectopically expressed with a *MCK-promoter Firefly* reporter gene in C2C12 cells. These cells were cultured in GM and DM 2d. *Renilla* luciferase gene served as a transfection control. Differentiated lysates previously transfected with an empty vector (pcDNA-FLAG) served as a control for endogenous activity. Triplicate intra-experimental samples were analyzed, and the mean of these technical replicates constituted one biological replicate. This experiment was repeated four times and the data points on the graph indicate the biological replicates (*n=4*). No statistical test was performed due to low sample size.

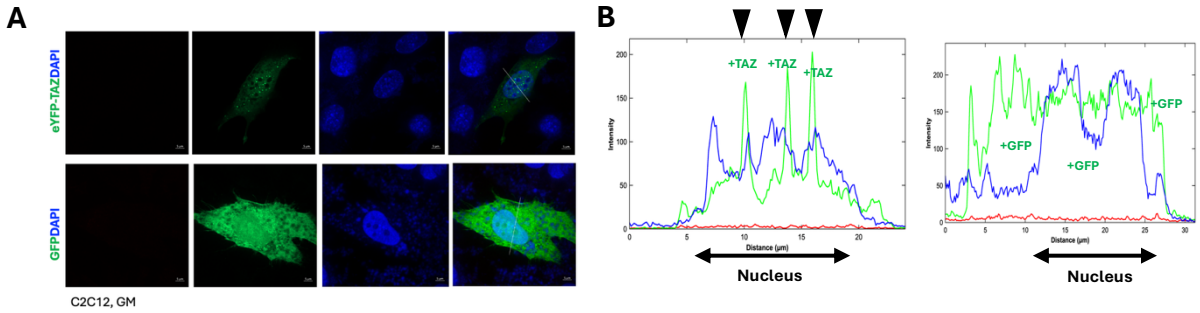

Supplementary Figure 5. **Relevant controls for immunofluorescence analysis of YY1 sub-cellular localization in Taz-phase condensate positive skeletal myoblasts. (A)** C2C12 myoblasts were transfected with empty vector (pcDNA-FLAG) with eYFP-TAZ or GFP to serve as negative controls. Cells were fixed with 4% paraformaldehyde 24 hours post-transfection, and immunostained with anti-FLAG for FLAG-YY1 (red) and pcDNA-FLAG (negative signal), and counterstained with DAPI to indicate nuclei (blue). eYFP-TAZ (top panel)/GFP (bottom panel) fluorescence is shown in green. **(C)** Line scan analysis of fluorescence signal conducted using ImageJ. DAPI: blue, eYFP-TAZ (right panel)/GFP (left panel): green, pcDNA-FLAG: red. Black arrows point to eYFP-TAZ green fluorescence signal in nuclear phase separated condensates.

Appendix III: Reagents

Table 1. **List of Reagents**

Reagents	**Ingredients**
NP-40 Lysis Buffer	0.5% NP-40 50mM Tris-HCl pH 7.6 150mM NaCl 100mM NaF 10mM Sodium Pyrophosphate 2mM EDTA 1mM Na_3VO_4 1mM PMSF ddH_2O
3X SDS Loading Buffer	1M Tris-HCl pH 6.8 Glycerol 10% SDS β-mercaptoethanol Bromophenol blue ddH_2O
1X Transfer Buffer	10% 10X Transfer Buffer 30.3g Tris-HCl 144.2g Glycine Equilibrated to 1L with ddH_2O 80% ddH_2O 10% methanol
5% Blocking Buffer	5% non-fat dry milk in 1X TBS 0.1% Tween ® 20
1% Blocking Buffer	1% non-fat dry milk in 1X TBS 0.1% Tween ® 20

Mass Spectrometry	50mM NH_4HCO_3 1M DTT (Sigma, 3483-12-3) Iodoacetamide (ThermoFisher Scientific) 1mg/ml trypsin (ThermoFisher Scientific (20µg trypsin + 50mM acetic acid)
SDS-PAGE gels	<u>10% Resolving Gel:</u> 20 mL ddH_2O 16.6mL acrylamide 12.5mL Tris pH 8.8 500µL 10% SDS 500µL 10% APS 20µL TEMED ® <u>Stacking Gel:</u> 6.8mL ddH_2O 1.7mL acrylamide 1.25mL Tris pH 6.8 100µL 10% SDS 100µL 10% APS 10µL TEMED ®
1X Reporter Lysis Buffer	800µL ddH_2O 200µL 5X Reporter Lysis Buffer (Promega, #E4030)
IF Blocking Buffer	5% FBS 1X PBS

Table 2. **List of Antibodies**

Antibodies	**Source**
Yap/Taz	Cell Signaling (#D24E24)
MYC	Cell Signaling (#9B11) Proteintech (#60003-2-Ig)
α-tubulin	Cell Signaling (#2144S)
c-Myc	Cell Signaling (#5605)
Histone H3	Cell Signaling (#9715S)
β-actin	Santa Cruz Biotechnology (#SC-47778)
MCK	Santa Cruz Biotechnology (#SC-365046)
FLAG	Sigma-Aldrich (#F3165) Proteintech (#20543-1-AP)
YY1	Proteintech (#6621-1-Ig, #22156-1-AP)
Cardiac troponin-T	Proteintech (#68300-1-Ig)
HA	DSHB (#anti-HA-rMs-IgG1)
MyHC	DSHB (#MF20)
MyoG	DSHB (#F5D)
Phospho-Taz (Ser89)	ThermoFisher Scientific (#PA5-105066)
Taz	Proteintech (#66500-1-Ig)

References

1. Shadrin IY, Khodabukus A, Bursac N. Striated muscle function, regeneration, and repair. Cellular and Molecular Life Sciences. 2016;73(22):4175-202.
2. Hanson J, Huxley HE. Structural Basis of the Cross-Striations in Muscle. Nature. 1953;172(4377):530-2.
3. Huxley HE. Electron microscope studies of the organisation of the filaments in striated muscle. Biochimica et Biophysica Acta. 1953;12(1):387-94.
4. Webb RC. SMOOTH MUSCLE CONTRACTION AND RELAXATION. Advances in Physiology Education. 2003;27(4):201-6.
5. Frontera WR, Ochala J. Skeletal Muscle: A Brief Review of Structure and Function. Calcified Tissue International. 2015;96(3):183-95.
6. Janssen I, Heymsfield SB, Wang Z, Ross R. Skeletal muscle mass and distribution in 468 men and women aged 18–88 yr. Journal of Applied Physiology. 2000;89(1):81-8.
7. Dumont NA, Wang YX, Rudnicki MA. Intrinsic and extrinsic mechanisms regulating satellite cell function. Development. 2015;142(9):1572-81.
8. Powers SK, Lynch GS, Murphy KT, Reid MB, Zijdewind I. Disease-Induced Skeletal Muscle Atrophy and Fatigue. Medicine & Science in Sports & Exercise. 2016;48(11).
9. Mann CJ, Perdiguero E, Kharraz Y, Aguilar S, Pessina P, Serrano AL, et al. Aberrant repair and fibrosis development in skeletal muscle. Skeletal Muscle. 2011;1(1):21.
10. Arnold HD. WEIGHT OF THE "NORMAL" HEART IN ADULTS. J Boston Soc Med Sci. 1899;3(6):174-84.
11. Mollova M, Bersell K, Walsh S, Savla J, Das LT, Park S-Y, et al. Cardiomyocyte proliferation contributes to heart growth in young humans. Proceedings of the National Academy of Sciences. 2013;110(4):1446-51.
12. Uygur A, Lee Richard T. Mechanisms of Cardiac Regeneration. Developmental Cell. 2016;36(4):362-74.
13. Biondic S, Canizo J, Vandal K, Zhao C, Petropoulos S. Cross-species comparison of mouse and human preimplantation development with an emphasis on lineage specification. Reproduction. 2023;165(4):R103-R16.
14. Niwa H, Toyooka Y, Shimosato D, Strumpf D, Takahashi K, Yagi R, et al. Interaction between Oct3/4 and Cdx2 Determines Trophectoderm Differentiation. Cell. 2005;123(5):917-29.
15. Arnold SJ, Robertson EJ. Making a commitment: cell lineage allocation and axis patterning in the early mouse embryo. Nature Reviews Molecular Cell Biology. 2009;10(2):91-103.
16. Mitsui K, Tokuzawa Y, Itoh H, Segawa K, Murakami M, Takahashi K, et al. The Homeoprotein Nanog Is Required for Maintenance of Pluripotency in Mouse Epiblast and ES Cells. Cell. 2003;113(5):631-42.
17. Fujikura J, Yamato E, Yonemura S, Hosoda K, Masui S, Nakao K, et al. Differentiation of embryonic stem cells is induced by GATA factors. Genes & Development. 2002;16(7):784-9.
18. Zhai J, Xiao Z, Wang Y, Wang H. Human embryonic development: from peri-implantation to gastrulation. Trends in Cell Biology. 2022;32(1):18-29.
19. Tam PPL, Beddington RSP. The formation of mesodermal tissues in the mouse embryo during gastrulation and early organogenesis. Development. 1987;99(1):109-26.

20. Mishina Y, Suzuki A, Ueno N, Behringer RR. Bmpr encodes a type I bone morphogenetic protein receptor that is essential for gastrulation during mouse embryogenesis. Genes & Development. 1995;9(24):3027-37.
21. Conlon FL, Lyons KM, Takaesu N, Barth KS, Kispert A, Herrmann B, et al. A primary requirement for nodal in the formation and maintenance of the primitive streak in the mouse. Development. 1994;120(7):1919-28.
22. Dunn NR, Vincent SpD, Oxburgh L, Robertson EJ, Bikoff EK. Combinatorial activities of Smad2 and Smad3 regulate mesoderm formation and patterning in the mouse embryo. Development. 2004;131(8):1717-28.
23. Amadei G, Handford CE, Qiu C, De Jonghe J, Greenfeld H, Tran M, et al. Embryo model completes gastrulation to neurulation and organogenesis. Nature. 2022;610(7930):143-53.
24. Massari ME, Murre C. Helix-Loop-Helix Proteins: Regulators of Transcription in Eucaryotic Organisms. Molecular and Cellular Biology. 2000;20(2):429-40.
25. Bentzinger CF, Wang YX, Rudnicki MA. Building Muscle: Molecular Regulation of Myogenesis. Cold Spring Harbor Perspectives in Biology. 2012;4(2):a008342.
26. Buckingham ME. Muscle: the regulation of myogenesis. Current Opinion in Genetics & Development. 1994;4(5):745-51.
27. Davis RL, Weintraub H, Lassar AB. Expression of a single transfected cDNA converts fibroblasts to myoblasts. Cell. 1987;51(6):987-1000.
28. Rhodes SJ, Konieczny SF. Identification of MRF4: a new member of the muscle regulatory factor gene family. Genes & Development. 1989;3(12b):2050-61.
29. Braun T, Bober E, Winter B, Rosenthal N, Arnold HH. Myf-6, a new member of the human gene family of myogenic determination factors: evidence for a gene cluster on chromosome 12. The EMBO Journal. 1990;9(3):821-31-31.
30. Edmondson DG, Olson EN. A gene with homology to the myc similarity region of MyoD1 is expressed during myogenesis and is sufficient to activate the muscle differentiation program. Genes & Development. 1989;3(5):628-40.
31. Rudnicki MA, Jaenisch R. The MyoD family of transcription factors and skeletal myogenesis. BioEssays. 1995;17(3):203-9.
32. Thayer MJ, Tapscott SJ, Davis RL, Wright WE, Lassar AB, Weintraub H. Positive autoregulation of the myogenic determination gene MyoD1. Cell. 1989;58(2):241-8.
33. Molkentin JD, Black BL, Martin JF, Olson EN. Cooperative activation of muscle gene expression by MEF2 and myogenic bHLH proteins. Cell. 1995;83(7):1125-36.
34. Musumeci G, Castrogiovanni P, Coleman R, Szychlinska MA, Salvatorelli L, Parenti R, et al. Somitogenesis: From somite to skeletal muscle. Acta Histochemica. 2015;117(4):313-28.
35. Parker MH, Seale P, Rudnicki MA. Looking back to the embryo: defining transcriptional networks in adult myogenesis. Nature Reviews Genetics. 2003;4(7):497-507.
36. Pownall ME, Gustafsson MK, Emerson CP. Myogenic Regulatory Factors and the Specification of Muscle Progenitors in Vertebrate Embryos. Annual Review of Cell and Developmental Biology. 2002;18(Volume 18, 2002):747-83.
37. Buckingham M, Relaix F. PAX3 and PAX7 as upstream regulators of myogenesis. Seminars in Cell & Developmental Biology. 2015;44:115-25.
38. Ott M-O, Bober E, Lyons G, Arnold H, Buckingham M. Early expression of the myogenic regulatory gene, myf-5, in precursor cells of skeletal muscle in the mouse embryo. Development. 1991;111(4):1097-107.

39. Hirsinger E, Duprez D, Jouve C, Malapert P, Cooke J, Pourquié O. Noggin acts downstream of Wnt and Sonic Hedgehog to antagonize BMP4 in avian somite patterning. Development. 1997;124(22):4605-14.
40. Marcelle C, Stark MR, Bronner-Fraser M. Coordinate actions of BMPs, Wnts, Shh and Noggin mediate patterning of the dorsal somite. Development. 1997;124(20):3955-63.
41. McMahon JA, Takada S, Zimmerman LB, Fan C-M, Harland RM, McMahon AP. Noggin-mediated antagonism of BMP signaling is required for growth and patterning of the neural tube and somite. Genes & Development. 1998;12(10):1438-52.
42. Braun T, Rudnicki MA, Arnold H-H, Jaenisch R. Targeted inactivation of the muscle regulatory gene Myf-5 results in abnormal rib development and perinatal death. Cell. 1992;71(3):369-82.
43. Rudnicki MA, Braun T, Hinuma S, Jaenisch R. Inactivation of MyoD in mice leads to up-regulation of the myogenic HLH gene Myf-5 and results in apparently normal muscle development. Cell. 1992;71(3):383-90.
44. Rudnicki MA, Schnegelsberg PNJ, Stead RH, Braun T, Arnold H-H, Jaenisch R. MyoD or Myf-5 is required for the formation of skeletal muscle. Cell. 1993;75(7):1351-9.
45. Denetclaw WF, Berdougo E, Venters SJ, Ordahl CP. Morphogenetic cell movements in the middle region of the dermomyotome dorsomedial lip associated with patterning and growth of the primary epaxial myotome. Development. 2001;128(10):1745-55.
46. Dietrich S, Abou-Rebyeh F, Brohmann H, Bladt F, Sonnenberg-Riethmacher E, Yamaai T, et al. The role of SF/HGF and c-Met in the development of skeletal muscle. Development. 1999;126(8):1621-9.
47. Buckingham M, Bajard L, Chang T, Daubas P, Hadchouel J, Meilhac S, et al. The formation of skeletal muscle: from somite to limb. Journal of Anatomy. 2003;202(1):59-68.
48. Birchmeier C, Brohmann H. Genes that control the development of migrating muscle precursor cells. Current Opinion in Cell Biology. 2000;12(6):725-30.
49. Zammit PS. Function of the myogenic regulatory factors Myf5, MyoD, Myogenin and MRF4 in skeletal muscle, satellite cells and regenerative myogenesis. Seminars in Cell & Developmental Biology. 2017;72:19-32.
50. Seale P, Sabourin LA, Girgis-Gabardo A, Mansouri A, Gruss P, Rudnicki MA. Pax7 is required for the specification of myogenic satellite cells. Cell. 2000;102(6):777-86.
51. Mauro A. Satellite cell of skeletal muscle fibers. The Journal of biophysical and biochemical cytology. 1961;9(2):493.
52. Fukada S-i, Yamaguchi M, Kokubo H, Ogawa R, Uezumi A, Yoneda T, et al. Hesr1 and Hesr3 are essential to generate undifferentiated quiescent satellite cells and to maintain satellite cell numbers. Development. 2011;138(21):4609-19.
53. Kuang S, Gillespie MA, Rudnicki MA. Niche regulation of muscle satellite cell self-renewal and differentiation. Cell stem cell. 2008;2(1):22-31.
54. Kuang S, Kuroda K, Le Grand F, Rudnicki MA. Asymmetric self-renewal and commitment of satellite stem cells in muscle. Cell. 2007;129(5):999-1010.
55. Dumont NA, Bentzinger CF, Sincennes MC, Rudnicki MA. Satellite cells and skeletal muscle regeneration. Comprehensive Physiology. 2015;5(3):1027-59.
56. Rodgers JT, King KY, Brett JO, Cromie MJ, Charville GW, Maguire KK, et al. mTORC1 controls the adaptive transition of quiescent stem cells from G0 to GAlert. Nature. 2014;510(7505):393-6.

57. Chakravarthy MV, Davis BS, Booth FW. IGF-I restores satellite cell proliferative potential in immobilized old skeletal muscle. Journal of Applied Physiology. 2000;89(4):1365-79.
58. Chakkalakal JV, Christensen J, Xiang W, Tierney MT, Boscolo FS, Sacco A, et al. Early forming label-retaining muscle stem cells require p27kip1 for maintenance of the primitive state. Development. 2014;141(8):1649-59.
59. Zhang H, Wen J, Bigot A, Chen J, Shang R, Mouly V, et al. Human myotube formation is determined by MyoD–Myomixer/Myomaker axis. Science Advances. 2020;6(51):eabc4062.
60. Park I-H, Chen J. Mammalian target of rapamycin (mTOR) signaling is required for a late-stage fusion process during skeletal myotube maturation. Journal of Biological Chemistry. 2005;280(36):32009-17.
61. Martinsen BJ, Lohr JL. Cardiac development. Handbook of cardiac anatomy, physiology, and devices: Springer; 2024. p. 79-89.
62. Srivastava D, Olson EN. A genetic blueprint for cardiac development. Nature. 2000;407(6801):221-6.
63. Schultheiss TM, Xydas S, Lassar AB. Induction of avian cardiac myogenesis by anterior endoderm. Development. 1995;121(12):4203-14.
64. Harvey RP. Nk-2homeobox genes and heart development. Developmental biology. 1996;178(2):203-16.
65. Durocher D, Charron F, Warren R, Schwartz RJ, Nemer M. The cardiac transcription factors Nkx2-5 and GATA-4 are mutual cofactors. The EMBO journal. 1997.
66. Kirby ML, Waldo wibKL. Molecular embryogenesis of the heart. Pediatric and Developmental Pathology. 2002;5(6):516-43.
67. Tanaka M, Chen Z, Bartunkova S, Yamasaki N, Izumo S. The cardiac homeobox gene Csx/Nkx2. 5 lies genetically upstream of multiple genes essential for heart development. Development. 1999;126(6):1269-80.
68. Biben C, Harvey RP. Homeodomain factor Nkx2-5 controls left/right asymmetric expression of bHLH gene eHand during murine heart development. Genes & development. 1997;11(11):1357-69.
69. Lin Q, Schwarz J, Bucana C, N. Olson E. Control of mouse cardiac morphogenesis and myogenesis by transcription factor MEF2C. Science. 1997;276(5317):1404-7.
70. Kim W, Jho E-h. The history and regulatory mechanism of the Hippo pathway. BMB Reports. 2018;51(3):106-18.
71. Justice RW, Zilian O, Woods DF, Noll M, Bryant PJ. The Drosophila tumor suppressor gene warts encodes a homolog of human myotonic dystrophy kinase and is required for the control of cell shape and proliferation. Genes & Development. 1995;9(5):534-46.
72. Xu T, Wang W, Zhang S, Stewart RA, Yu W. Identifying tumor suppressors in genetic mosaics: the Drosophila lats gene encodes a putative protein kinase. Development. 1995;121(4):1053-63.
73. Tapon N, Harvey KF, Bell DW, Wahrer DCR, Schiripo TA, Haber DA, et al. salvador Promotes Both Cell Cycle Exit and Apoptosis in Drosophila and Is Mutated in Human Cancer Cell Lines. Cell. 2002;110(4):467-78.
74. Kango-Singh M, Nolo R, Tao C, Verstreken P, Hiesinger PR, Bellen HJ, et al. Shar-pei mediates cell proliferation arrest during imaginal disc growth in Drosophila. Development. 2002;129(24):5719-30.

75. Wu S, Huang J, Dong J, Pan D. hippo Encodes a Ste-20 Family Protein Kinase that Restricts Cell Proliferation and Promotes Apoptosis in Conjunction with salvador and warts. Cell. 2003;114(4):445-56.
76. Udan RS, Kango-Singh M, Nolo R, Tao C, Halder G. Hippo promotes proliferation arrest and apoptosis in the Salvador/Warts pathway. Nature Cell Biology. 2003;5(10):914-20.
77. Harvey KF, Pfleger CM, Hariharan IK. The Drosophila Mst Ortholog, hippo, Restricts Growth and Cell Proliferation and Promotes Apoptosis. Cell. 2003;114(4):457-67.
78. Lai Z-C, Wei X, Shimizu T, Ramos E, Rohrbaugh M, Nikolaidis N, et al. Control of Cell Proliferation and Apoptosis by Mob as Tumor Suppressor, Mats. Cell. 2005;120(5):675-85.
79. Wei X, Shimizu T, Lai ZC. Mob as tumor suppressor is activated by Hippo kinase for growth inhibition in Drosophila. The EMBO Journal. 2007;26(7):1772-81-81.
80. Huang J, Wu S, Barrera J, Matthews K, Pan D. The Hippo Signaling Pathway Coordinately Regulates Cell Proliferation and Apoptosis by Inactivating Yorkie, the Drosophila Homolog of YAP. Cell. 2005;122(3):421-34.
81. Zhang X, Milton CC, Humbert PO, Harvey KF. Transcriptional Output of the Salvador/Warts/Hippo Pathway Is Controlled in Distinct Fashions in Drosophila melanogaster and Mammalian Cell Lines. Cancer Research. 2009;69(15):6033-41.
82. Oh H, Irvine KD. In vivo regulation of Yorkie phosphorylation and localization. Development. 2008;135(6):1081-8.
83. Staley BK, Irvine KD. Hippo signaling in Drosophila: Recent advances and insights. Developmental Dynamics. 2012;241(1):3-15.
84. Wu S, Liu Y, Zheng Y, Dong J, Pan D. Developmental Cell. 2008;14(3):388-98.
85. Sebé-Pedrós A, Zheng Y, Ruiz-Trillo I, Pan D. Premetazoan Origin of the Hippo Signaling Pathway. Cell Reports. 2012;1(1):13-20.
86. Dan I, Watanabe NM, Kusumi A. The Ste20 group kinases as regulators of MAP kinase cascades. Trends in Cell Biology. 2001;11(5):220-30.
87. Chan EHY, Nousiainen M, Chalamalasetty RB, Schäfer A, Nigg EA, Silljé HHW. The Ste20-like kinase Mst2 activates the human large tumor suppressor kinase Lats1. Oncogene. 2005;24(12):2076-86.
88. Callus BA, Verhagen AM, Vaux DL. Association of mammalian sterile twenty kinases, Mst1 and Mst2, with hSalvador via C-terminal coiled-coil domains, leads to its stabilization and phosphorylation. The FEBS Journal. 2006;273(18):4264-76.
89. Bae Sung J, Luo X. Activation mechanisms of the Hippo kinase signaling cascade. Bioscience Reports. 2018;38(4):BSR20171469.
90. Praskova M, Xia F, Avruch J. MOBKL1A/MOBKL1B Phosphorylation by MST1 and MST2 Inhibits Cell Proliferation. Current Biology. 2008;18(5):311-21.
91. Bichsel SJ, Tamaskovic R, Stegert MR, Hemmings BA. Mechanism of Activation of NDR (Nuclear Dbf2-related) Protein Kinase by the hMOB1 Protein*. Journal of Biological Chemistry. 2004;279(34):35228-35.
92. Hergovich A, Schmitz D, Hemmings BA. The human tumour suppressor LATS1 is activated by human MOB1 at the membrane. Biochemical and Biophysical Research Communications. 2006;345(1):50-8.
93. Oka T, Mazack V, Sudol M. Mst2 and Lats Kinases Regulate Apoptotic Function of Yes Kinase-associated Protein (YAP)*. Journal of Biological Chemistry. 2008;283(41):27534-46.

94. Hao Y, Chun A, Cheung K, Rashidi B, Yang X. Tumor Suppressor LATS1 Is a Negative Regulator of Oncogene YAP*. Journal of Biological Chemistry. 2008;283(9):5496-509.
95. Liu C-Y, Zha Z-Y, Zhou X, Zhang H, Huang W, Zhao D, et al. The Hippo Tumor Pathway Promotes TAZ Degradation by Phosphorylating a Phosphodegron and Recruiting the SCF^{β-TrCP} E3 Ligase *. Journal of Biological Chemistry. 2010;285(48):37159-69.
96. Lei Q-Y, Zhang H, Zhao B, Zha Z-Y, Bai F, Pei X-H, et al. TAZ Promotes Cell Proliferation and Epithelial-Mesenchymal Transition and Is Inhibited by the Hippo Pathway. Molecular and Cellular Biology. 2008;28(7):2426-36.
97. Kanai F, Marignani PA, Sarbassova D, Yagi R, Hall RA, Donowitz M, et al. TAZ: a novel transcriptional co-activator regulated by interactions with 14-3-3 and PDZ domain proteins. The EMBO Journal. 2000;19(24):6778-91-91.
98. Zhao B, Li L, Tumaneng K, Wang C-Y, Guan K-L. A coordinated phosphorylation by Lats and CK1 regulates YAP stability through SCFβ-TRCP. Genes & Development. 2010;24(1):72-85.
99. Frietze S, Farnham PJ. Transcription Factor Effector Domains. In: Hughes TR, editor. A Handbook of Transcription Factors. Dordrecht: Springer Netherlands; 2011. p. 261-77.
100. Vassilev A, Kaneko KJ, Shu H, Zhao Y, DePamphilis ML. TEAD/TEF transcription factors utilize the activation domain of YAP65, a Src/Yes-associated protein localized in the cytoplasm. Genes & Development. 2001;15(10):1229-41.
101. Xiao JH, Davidson I, Matthes H, Garnier J-M, Chambon P. Cloning, expression, and transcriptional properties of the human enhancer factor TEF-1. Cell. 1991;65(4):551-68.
102. Mahoney William M, Jr., Hong J-H, Yaffe Michael B, Farrance Iain KG. The transcriptional co-activator TAZ interacts differentially with transcriptional enhancer factor-1 (TEF-1) family members. Biochemical Journal. 2005;388(1):217-25.
103. Kaan HYK, Chan SW, Tan SKJ, Guo F, Lim CJ, Hong W, et al. Crystal structure of TAZ-TEAD complex reveals a distinct interaction mode from that of YAP-TEAD complex. Scientific Reports. 2017;7(1):2035.
104. Zhao B, Ye X, Yu J, Li L, Li W, Li S, et al. TEAD mediates YAP-dependent gene induction and growth control. Genes & Development. 2008;22(14):1962-71.
105. Hong W, Guan K-L. The YAP and TAZ transcription co-activators: Key downstream effectors of the mammalian Hippo pathway. Seminars in Cell & Developmental Biology. 2012;23(7):785-93.
106. Zender L, Spector MS, Xue W, Flemming P, Cordon-Cardo C, Silke J, et al. Identification and Validation of Oncogenes in Liver Cancer Using an Integrative Oncogenomic Approach. Cell. 2006;125(7):1253-67.
107. Halder G, Johnson RL. Hippo signaling: growth control and beyond. Development. 2011;138(1):9-22.
108. van Soldt BJ, Cardoso WV. Hippo-Yap/Taz signaling: Complex network interactions and impact in epithelial cell behavior. WIREs Developmental Biology. 2020;9(3):e371.
109. Panciera T, Azzolin L, Cordenonsi M, Piccolo S. Mechanobiology of YAP and TAZ in physiology and disease. Nature Reviews Molecular Cell Biology. 2017;18(12):758-70.
110. Zhao B, Wei X, Li W, Udan RS, Yang Q, Kim J, et al. Inactivation of YAP oncoprotein by the Hippo pathway is involved in cell contact inhibition and tissue growth control. Genes & Development. 2007;21(21):2747-61.

111. McClatchey AI, Giovannini M. Membrane organization and tumorigenesis—the NF2 tumor suppressor, Merlin. Genes & Development. 2005;19(19):2265-77.
112. Hamaratoglu F, Willecke M, Kango-Singh M, Nolo R, Hyun E, Tao C, et al. The tumour-suppressor genes NF2/Merlin and Expanded act through Hippo signalling to regulate cell proliferation and apoptosis. Nature Cell Biology. 2006;8(1):27-36.
113. Dupont S, Morsut L, Aragona M, Enzo E, Giulitti S, Cordenonsi M, et al. Role of YAP/TAZ in mechanotransduction. Nature. 2011;474(7350):179-83.
114. Zhao B, Li L, Wang L, Wang C-Y, Yu J, Guan K-L. Cell detachment activates the Hippo pathway via cytoskeleton reorganization to induce anoikis. Genes & Development. 2012;26(1):54-68.
115. Ernkvist M, Aase K, Ukomadu C, Wohlschlegel J, Blackman R, Veitonmäki N, et al. p130-Angiomotin associates to actin and controls endothelial cell shape. The FEBS Journal. 2006;273(9):2000-11.
116. Bratt A, Birot O, Sinha I, Veitonmäki N, Aase K, Ernkvist M, et al. Angiomotin Regulates Endothelial Cell-Cell Junctions and Cell Motility*. Journal of Biological Chemistry. 2005;280(41):34859-69.
117. Chan SW, Lim CJ, Chong YF, Pobbati AV, Huang C, Hong W. Hippo Pathway-independent Restriction of TAZ and YAP by Angiomotin*. Journal of Biological Chemistry. 2011;286(9):7018-26.
118. Adler JJ, Johnson DE, Heller BL, Bringman LR, Ranahan WP, Conwell MD, et al. Serum deprivation inhibits the transcriptional co-activator YAP and cell growth via phosphorylation of the 130-kDa isoform of Angiomotin by the LATS1/2 protein kinases. Proceedings of the National Academy of Sciences. 2013;110(43):17368-73.
119. Wang W, Li X, Huang J, Feng L, Dolinta KG, Chen J. Defining the Protein–Protein Interaction Network of the Human Hippo Pathway*. Molecular & Cellular Proteomics. 2014;13(1):119-31.
120. Mori N, Kuwamura M, Tanaka N, Hirano R, Nabe M, Ibuki M, et al. Ccdc85c Encoding a Protein at Apical Junctions of Radial Glia Is Disrupted in Hemorrhagic Hydrocephalus (hhy) Mice. The American Journal of Pathology. 2012;180(1):314-27.
121. Reggiani F, Gobbi G, Ciarrocchi A, Sancisi V. YAP and TAZ Are Not Identical Twins. Trends in Biochemical Sciences. 2021;46(2):154-68.
122. Yagi R, Chen LF, Shigesada K, Murakami Y, Ito Y. A WW domain-containing Yes-associated protein (YAP) is a novel transcriptional co-activator. The EMBO Journal. 1999;18(9):2551-62-62.
123. Gaffney CJ, Oka T, Mazack V, Hilman D, Gat U, Muramatsu T, et al. Identification, basic characterization and evolutionary analysis of differentially spliced mRNA isoforms of human YAP1 gene. Gene. 2012;509(2):215-22.
124. Chen HI, Sudol M. The WW domain of Yes-associated protein binds a proline-rich ligand that differs from the consensus established for Src homology 3-binding modules. Proceedings of the National Academy of Sciences. 1995;92(17):7819-23.
125. Niakan KK, Eggan K. Analysis of human embryos from zygote to blastocyst reveals distinct gene expression patterns relative to the mouse. Developmental Biology. 2013;375(1):54-64.
126. Nishioka N, Inoue K-i, Adachi K, Kiyonari H, Ota M, Ralston A, et al. The Hippo Signaling Pathway Components Lats and Yap Pattern Tead4 Activity to Distinguish Mouse Trophectoderm from Inner Cell Mass. Developmental Cell. 2009;16(3):398-410.

127. Nejigane S, Haramoto Y, Okuno M, Takahashi S, Asashima M. The transcriptional coactivators <I>Yap</I> and <I>TAZ</I> are expressed during early <I>Xenopus</I> development. The International Journal of Developmental Biology. 2011;55(1):121-6.
128. Naye F, Tréguer K, Soulet F, Faucheux C, Fédou S, Thézé N, et al. Differential expression of two <I>TEF-1 (TEAD)</I> genes during <I>Xenopus laevis</I> development and in response to inducing factors. The International Journal of Developmental Biology. 2007;51(8):745-52.
129. Hu J, Sun S, Jiang Q, Sun S, Wang W, Gui Y, et al. Yes-Associated Protein (Yap) Is Required for Early Embryonic Development in Zebrafish (Danio Rerio). International Journal of Biological Sciences. 2013;9(3):267-78.
130. Jiang Q, Liu D, Gong Y, Wang Y, Sun S, Gui Y, et al. yap is required for the development of brain, eyes, and neural crest in zebrafish. Biochemical and Biophysical Research Communications. 2009;384(1):114-9.
131. Morin-Kensicki EM, Boone BN, Howell M, Stonebraker JR, Teed J, Alb JG, et al. Defects in Yolk Sac Vasculogenesis, Chorioallantoic Fusion, and Embryonic Axis Elongation in Mice with Targeted Disruption of Yap65. Molecular and Cellular Biology. 2006;26(1):77-87.
132. Watt KI, Judson R, Medlow P, Reid K, Kurth TB, Burniston JG, et al. Yap is a novel regulator of C2C12 myogenesis. Biochemical and Biophysical Research Communications. 2010;393(4):619-24.
133. Judson RN, Tremblay AM, Knopp P, White RB, Urcia R, De Bari C, et al. The Hippo pathway member Yap plays a key role in influencing fate decisions in muscle satellite cells. Journal of Cell Science. 2012;125(24):6009-19.
134. Xin M, Kim Y, Sutherland LB, Murakami M, Qi X, McAnally J, et al. Hippo pathway effector Yap promotes cardiac regeneration. Proceedings of the National Academy of Sciences. 2013;110(34):13839-44.
135. Xin M, Kim Y, Sutherland LB, Qi X, McAnally J, Schwartz RJ, et al. Regulation of Insulin-Like Growth Factor Signaling by Yap Governs Cardiomyocyte Proliferation and Embryonic Heart Size. Science Signaling. 2011;4(196):ra70-ra.
136. Del Re DP, Yang Y, Nakano N, Cho J, Zhai P, Yamamoto T, et al. Yes-associated Protein Isoform 1 (Yap1) Promotes Cardiomyocyte Survival and Growth to Protect against Myocardial Ischemic Injury *. Journal of Biological Chemistry. 2013;288(6):3977-88.
137. Tripathi S, Miyake T, Kelebeev J, McDermott JC. TAZ exhibits phase separation properties and interacts with Smad7 and β-catenin to repress skeletal myogenesis. Journal of Cell Science. 2022;135(1):jcs259097.
138. Jeong H, Bae S, An SY, Byun MR, Hwang J-H, Yaffe MB, et al. TAZ as a novel enhancer of MyoD-mediated myogenic differentiation. The FASEB Journal. 2010;24(9):3310-20.
139. Tripathi S, Miyake T, McDermott JC. Smad7:β-catenin complex regulates myogenic gene transcription. Cell Death & Disease. 2019;10(6):387.
140. Lai JKH, Collins MM, Uribe V, Jiménez-Amilburu V, Günther S, Maischein H-M, et al. The Hippo pathway effector Wwtr1 regulates cardiac wall maturation in zebrafish. Development. 2018;145(10):dev159210.
141. Liu J, Bressan M, Hassel D, Huisken J, Staudt D, Kikuchi K, et al. A dual role for ErbB2 signaling in cardiac trabeculation. Development. 2010;137(22):3867-75.
142. Chen H, Shi S, Acosta L, Li W, Lu J, Bao S, et al. BMP10 is essential for maintaining cardiac growth during murine cardiogenesis. Development. 2004;131(9):2219-31.

143. Weiford BC, Subbarao VD, Mulhern KM. Noncompaction of the Ventricular Myocardium. Circulation. 2004;109(24):2965-71.
144. Piccolo S, Panciera T, Contessotto P, Cordenonsi M. YAP/TAZ as master regulators in cancer: modulation, function and therapeutic approaches. Nature Cancer. 2023;4(1):9-26.
145. Gustafson AL, Durbin AD, Artinger KB, Ford HL. Myogenesis gone awry: the role of developmental pathways in rhabdomyosarcoma. Frontiers in Cell and Developmental Biology. 2025;Volume 12 - 2024.
146. Yu PY, Guttridge DC. Chapter Nine - Dysregulated Myogenesis in Rhabdomyosarcoma. In: Sassoon D, editor. Current Topics in Developmental Biology. 126: Academic Press; 2018. p. 285-97.
147. Deel MD, Slemmons KK, Hinson AR, Genadry KC, Burgess BA, Crose LES, et al. The Transcriptional Coactivator TAZ Is a Potent Mediator of Alveolar Rhabdomyosarcoma Tumorigenesis. Clinical Cancer Research. 2018;24(11):2616-30.
148. Velagaleti RS, Pencina MJ, Murabito JM, Wang TJ, Parikh NI, D'Agostino RB, et al. Long-Term Trends in the Incidence of Heart Failure After Myocardial Infarction. Circulation. 2008;118(20):2057-62.
149. Porrello ER, Mahmoud AI, Simpson E, Hill JA, Richardson JA, Olson EN, et al. Transient Regenerative Potential of the Neonatal Mouse Heart. Science. 2011;331(6020):1078-80.
150. Misra JR, Irvine KDYR. The Hippo Signaling Network and Its Biological Functions. Annual Review of Genetics.52(Volume 52, 2018):65.
151. Heallen T, Morikawa Y, Leach J, Tao G, Willerson JT, Johnson RL, et al. Hippo signaling impedes adult heart regeneration. Development. 2013;140(23):4683-90.
152. Wang P, Mao B, Luo W, Wei B, Jiang W, Liu D, et al. The alteration of Hippo/YAP signaling in the development of hypertrophic cardiomyopathy. Basic Research in Cardiology. 2014;109(5):435.
153. Kastan NR, Oak S, Liang R, Baxt L, Myers RW, Ginn J, et al. Development of an improved inhibitor of Lats kinases to promote regeneration of mammalian organs. Proceedings of the National Academy of Sciences. 2022;119(28):e2206113119.
154. Judson RN, Gray SR, Walker C, Carroll AM, Itzstein C, Lionikas A, et al. Constitutive Expression of Yes-Associated Protein (Yap) in Adult Skeletal Muscle Fibres Induces Muscle Atrophy and Myopathy. PLOS ONE. 2013;8(3):e59622.
155. Wang C, Zhu X, Feng W, Yu Y, Jeong K, Guo W, et al. Verteporfin inhibits YAP function through up-regulating 14-3-3σ sequestering YAP in the cytoplasm. Am J Cancer Res. 2016;6(1):27-37.
156. Kiang KM, Ahad L, Zhong X, Lu QR. Biomolecular condensates: hubs of Hippo-YAP/TAZ signaling in cancer. Trends in Cell Biology. 2024;34(7):566-77.
157. Shin Y, Brangwynne CP. Liquid phase condensation in cell physiology and disease. Science. 2017;357(6357):eaaf4382.
158. Lu Y, Wu T, Gutman O, Lu H, Zhou Q, Henis YI, et al. Phase separation of TAZ compartmentalizes the transcription machinery to promote gene expression. Nature Cell Biology. 2020;22(4):453-64.
159. Hyman AA, Weber CA, Jülicher F. Liquid-Liquid Phase Separation in Biology. Annual Review of Cell and Developmental Biology. 2014;30(Volume 30, 2014):39-58.
160. Boeynaems S, Alberti S, Fawzi NL, Mittag T, Polymenidou M, Rousseau F, et al. Protein Phase Separation: A New Phase in Cell Biology. Trends in Cell Biology. 2018;28(6):420-35.

161. Murakami M, Nakagawa M, Olson EN, Nakagawa O. A WW domain protein TAZ is a critical coactivator for TBX5, a transcription factor implicated in Holt–Oram syndrome. Proceedings of the National Academy of Sciences. 2005;102(50):18034-9.
162. B. Donoviel D, A. Shield M, N. Buskin J, S. Haugen H, H. Clegg C, D. Hauschka S. Analysis of Muscle Creatine Kinase Gene Regulatory Elements in Skeletal and Cardiac Muscles of Transgenic Mice. Molecular and Cellular Biology. 1996;16(4):1649-58.
163. Pagiatakis C, Sun D, Tobin SW, Miyake T, McDermott JC. TGFβ-TAZ/SRF signalling regulates vascular smooth muscle cell differentiation. The FEBS Journal. 2017;284(11):1644-56.
164. Kim M-K, Jang J-W, Bae S-C. DNA binding partners of YAP/TAZ. BMB Reports. 2018;51(3):126-33.
165. Valdez-Sinon AN, Gokhale A, Faundez V, Bassell GJ. Protocol for Immuno-Enrichment of FLAG-Tagged Protein Complexes. STAR Protocols. 2020;1(2):100083.
166. Kelebeev J, MacKeracher A, Miyake T, McDermott JC. TAZ interactome analysis using nanotrap-based affinity purification–mass spectrometry. Journal of Cell Science. 2025;138(4):jcs263527.
167. Shao A, Kissil JL, Fan C-M. The L27 domain of MPP7 enhances TAZ-YY1 cooperation to renew muscle stem cells. EMBO reports. 2024;25(12):5667-86-86.
168. Liu R, Jagannathan R, Li F, Lee J, Balasubramanyam N, Kim BS, et al. Tead1 is required for perinatal cardiomyocyte proliferation. PLOS ONE. 2019;14(2):e0212017.
169. Sun C, De Mello V, Mohamed A, Ortuste Quiroga HP, Garcia-Munoz A, Al Bloshi A, et al. Common and Distinctive Functions of the Hippo Effectors Taz and Yap in Skeletal Muscle Stem Cell Function. Stem Cells. 2017;35(8):1958-72.
170. Tremblay Annie M, Missiaglia E, Galli Giorgio G, Hettmer S, Urcia R, Carrara M, et al. The Hippo Transducer YAP1 Transforms Activated Satellite Cells and Is a Potent Effector of Embryonal Rhabdomyosarcoma Formation. Cancer Cell. 2014;26(2):273-87.
171. Rodríguez-Campuzano AG, Castelán F, Hernández-Kelly LC, Felder-Schmittbuhl M-P, Ortega A. Yin Yang 1: Function, Mechanisms, and Glia. Neurochemical Research. 2025;50(2):96.
172. Hoxha S, Shepard A, Troutman S, Diao H, Doherty JR, Janiszewska M, et al. YAP-mediated recruitment of YY1 and EZH2 represses transcription of key cell-cycle regulators. Cancer research. 2020;80(12):2512-22.
173. Lee T-C, Shi Y, Schwartz RJ. Displacement of BrdUrd-induced YY1 by serum response factor activates skeletal alpha-actin transcription in embryonic myoblasts. Proceedings of the National Academy of Sciences. 1992;89(20):9814-8.
174. Vincent CK, Gualberto A, Patel CV, Walsh K. Different regulatory sequences control creatine kinase-M gene expression in directly injected skeletal and cardiac muscle. Molecular and cellular biology. 1993;13(2):1264-72.
175. Shrivastava A, Calame K. An analysis of genes regulated by the multi-functional transcriptional regulator Yin Yang-1. Nucleic acids research. 1994;22(24):5151.
176. Caretti G, Di Padova M, Micales B, Lyons GE, Sartorelli V. The Polycomb Ezh2 methyltransferase regulates muscle gene expression and skeletal muscle differentiation. Genes & development. 2004;18(21):2627-38.
177. Walowitz JL, Bradley ME, Chen S, Lee T. Proteolytic regulation of the zinc finger transcription factor YY1, a repressor of muscle-restricted gene expression. Journal of Biological Chemistry. 1998;273(12):6656-61.

178. Wang W, Qiao S, Li G, Cheng J, Yang C, Zhong C, et al. A histidine cluster determines YY1-compartmentalized coactivators and chromatin elements in phase-separated enhancer clusters. Nucleic acids research. 2022;50(9):4917-37.
179. Kim HJ, Denli AM, Wright R, Baul TD, Clemenson GD, Morcos AS, et al. REST Regulates Non-Cell-Autonomous Neuronal Differentiation and Maturation of Neural Progenitor Cells via Secretogranin II. J Neurosci. 2015;35(44):14872-84.
180. Iannotti FA, Barrese V, Formisano L, Miceli F, Taglialatela M. Specification of skeletal muscle differentiation by repressor element-1 silencing transcription factor (REST)-regulated Kv7.4 potassium channels. Molecular Biology of the Cell. 2012;24(3):274-84.
181. Beketaev I, Zhang Y, Kim EY, Yu W, Qian L, Wang J. Critical role of YY1 in cardiac morphogenesis. Developmental Dynamics. 2015;244(5):669-80.
182. Asensio-Lopez MC, Lax A, Fernandez del Palacio MJ, Sassi Y, Hajjar RJ, Januzzi JL, et al. Yin-Yang 1 transcription factor modulates ST2 expression during adverse cardiac remodeling post-myocardial infarction. Journal of Molecular and Cellular Cardiology. 2019;130:216-33.
183. Huang Y, Li L, Chen H, Liao Q, Yang X, Yang D, et al. The Protective Role of Yin-Yang 1 in Cardiac Injury and Remodeling After Myocardial Infarction. Journal of the American Heart Association. 2021;10(21):e021895.